EDITORIAL STAFF

Cecil V. King, Editor
Norman Hackerman, Technical Editor
Ruth G. Sterns, Managing Editor
U. B. Thomas, News Editor
Natalie Michalski, Assistant Editor
Eleanor Blair, Assistant Editor

DIVISIONAL EDITORS

W. C. Vosburgh, Battery
J. E. Draley, Corrosion
John J. Chapman, Electric Insulation
Abner Brenner, Electrodeposition
H. C. Froelich, Electronics
D. H. Baird, Electronics—Semiconductors
Sherlock Swann, Jr., Electro-Organic
John M. Blocher, Jr., Electrothermics and Metallurgy, I
A. U. Seybolt, Electrothermics and Metallurgy, II
W. C. Gardiner, Industrial Electrolytic
C. W. Tobias, Theoretical Electrochemistry

REGIONAL EDITORS

Howard T. Francis, Chicago
Joseph Schulein, Pacific Northwest
J. C. Schumacher, Los Angeles
G. W. Heise, Cleveland
G. H. Fetterley, Niagara Falls
Oliver Osborn, Houston
Earl A. Gulbransen, Pittsburgh
A. C. Holm, Canada
J. W. Cuthbertson, Great Britain
T. L. Rama Char, India

ADVERTISING OFFICE

Jack Bain, Advertising Manager
545 Fifth Avenue, New York 17, N. Y.

ECS OFFICERS

Hans Thurnauer, President
Minnesota Mining & Mfg. Co., St. Paul, Minn.

Norman Hackerman, Vice-President
University of Texas, Austin, Texas

Sherlock Swann, Jr., Vice-President
University of Illinois, Urbana, Ill.

W. C. Gardiner, Vice-President
Olin Mathieson Chemical Corp., Niagara Falls, N. Y.

Lyle I. Gilbertson, Treasurer
Air Reduction Co., Murray Hill, N. J.

Henry B. Linford, Secretary
Columbia University, New York, N. Y.

Journal of the Electrochemical Society

MAY 1957 **VOL. 104 • NO. 5**

CONTENTS

Editorial

Publication Problems 109C

Technical Papers

Effect of Pre-Oxidation in Oxygen on the Steam Corrosion Behavior of Zircaloy-2. *D. E. Thomas and S. Kass* 261

A Hydrogen Effusion Method for the Determination of Corrosion Rates in Aqueous Systems at Elevated Temperature and Pressure. *M. C. Bloom and M. Krulfeld* 264

Galvanic Corrosion, I. Current Flow and Polarization Characteristics of the Aluminum-Steel and Zinc-Steel Couples in Sodium Chloride Solution. *M. J. Pryor and D. S. Keir* 269

Inclusion of Fuchsin in Bright Nickel Deposits. *J. L. Dye and O. J. Klingenmaier* 275

Throwing Index. A New Graphical Method for Expressing Results of Throwing-Power Measurements. *R. V. Jelinek and H. F. David* 279

Tin Plating from the Pyrophosphate Bath. *J. Vaid and T. L. Rama Char* 282

A Simplified Procedure and Apparatus for Measuring Surface Area of Fine Powders by Gas Adsorption. *F. M. Starkweather and D. T. Palumbo* 287

Temperature Dependence of Electroluminescence. *C. H. Haake* 291

Transport Numbers and Structures in Fused $AgNO_3$-$NaNO_3$ Mixtures. *F. R. Duke, R. W. Laity, and B. Owens* 299

The Mechanism of Titanium Production by Electrolysis of Fused Halide Baths Containing Titanium Salts. *J. G. Wurm, L. Gravel, and R. J. A. Potvin* 301

Galvanic Cells for the Determination of the Standard Molar Free Energy of Formation of Metal Halides, Oxides, and Sulfides at Elevated Temperatures. *K. Kiukkola and C. Wagner* 308

Technical Notes

Growth of Silicon Crystals by a Vapor Phase Pyrolytic Deposition Method. *R. C. Sangster, E. F. Maverick, and M. L. Croutch* 317

Notes on Hydrogen Overvoltage, I. Maximum Concentration of Atomic Hydrogen on the Surface of a Working Cathode. *H. W. Salzberg and S. Schuldiner* 319

Technical Review

Electrical Conduction in Silicon Carbide. *G. H. Fetterley* 322

Current Affairs

News Notes in the Electrochemical Field 111C

Division News 112C
Section News 113C
New Members 114C
Book Reviews 115C
Announcements from Publishers 117C
Meetings of Other Organizations 118C
Employment Situation 118C

Published monthly by The Electrochemical Society, Inc., Manchester, N. H., combining the JOURNAL and TRANSACTIONS OF THE ELECTROCHEMICAL SOCIETY. Editorial offices: 216 West 102nd Street, New York 25, N. Y. Statements and opinions given in articles and papers in the JOURNAL OF THE ELECTROCHEMICAL SOCIETY are those of the contributors, and The Electrochemical Society assumes no responsibility for them. Nondeductible subscription to members $5:00; subscription to nonmembers $18.00. Single copies $1.25 to members, $1.75 to nonmembers.

Copyright 1957 by The Electrochemical Society, Inc.

Entered as second-class matter at the Post Office at Manchester, N. H., under the act of August 24, 1912.

ANOTHER STEP AHEAD IN ANODES

Recently developed grades of Stackpole graphite anodes for chlorine cells are showing rather startling cost savings for leading users.

Your own test can offer convincing proof of their ability to help *you* get more for *your* anode dollars.

STACKPOLE CARBON COMPANY, ***St. Marys, Pa.***

STACKPOLE

"Everything in Carbon but Diamonds"

BRUSHES for all rotating electrical equipment • ELECTRICAL CONTACTS • TUBE ANODES • CATHODIC PROTECTION ANODES VOLTAGE REGULATOR DISCS • WATER HEATER and PASTEURIZATION ELECTRODES • BEARINGS • WELDING CARBONS MOLDS and DIES • POROUS CARBON • SEAL RINGS • FRICTION SEGMENTS • CLUTCH RINGS • ELECTRIC FURNACE HEATING ELEMENTS • PUMP VANES • and many other products.

SARGENT SLOMIN

Motor-Stirred 5 Ampere

SARGENT HEAVY DUTY

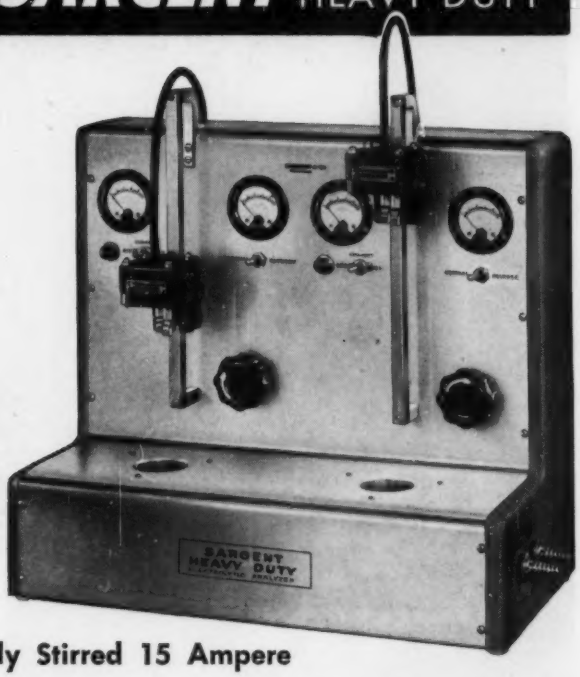

Magnetically Stirred 15 Ampere

Designed for continuous trouble-free performance, these electrolytic analyzers, manufactured by E. H. Sargent & Co., are durably constructed of the highest grade materials and component parts, including stainless steel front panel, cast aluminum end castings and stainless steel fittings.

Completely line operated, the Sargent analyzers employ self-contained rectifying and filter circuits. The deposition voltage between the electrodes is adjusted by means of auto-transformers, with meters indicating volts and amperes and controls on the panel. An easily replaceable fuse guards against circuit overload.

The Sargent-Slomin Analyzer stirs thorugh a rotating chuck operated from a capacitor type induction motor, motor having a fixed speed of 550 r.p.m. with 60 cycle A.C. current or 460 r.p.m. with 50 cycle A.C. current. Motors are sealed against corrosive fumes; are mounted on cast metal brackets, sliding on ½" square stainless steel rods, permitting vertical adjustment of electrode position over a distance of 4". Pre-lubricated ball-bearings support the rotating shaft.

The Sargent Heavy Duty Analyzer provides efficient stirring by the interaction between the cell current and the field established by a permanent magnet, tubular in shape and coaxial with the cell holder.

The Heavy Duty has recessed wells to hold the sample beakers, wells being 6¼" deep, designed to contain 250 ml electrolytic beakers. The wall of each well serves as an inner wall of the water jacket, for use in either heating or cooling. Two serrated nipples for rubber tubing connections for cooling or heating water are mounted on the right end casting. In plain copper analysis, 1 gram of copper may be deposited in 15 minutes with an accuracy of approximately 0.05% without the necessity of special techniques.

All electrolytic analyzers accommodate electrodes having shaft diameters no greater than 0.059 inch. Stainless steel spring tension chucks permit quick, easy insertion of the electrodes and maintain proper electrical contact. On the Heavy Duty Analyzer, the cathode chuck is eccentrically mounted, providing adjustability to accommodate electrodes up to 50 mm diameter. Special Sargent high efficiency electrodes are available for both analyzers.

Analyzers are complete with cord and plug for attachment to standard outlets. For operation from 115 volt, 50 or 60 cycle A.C. circuits.

	SARGENT-SLOMIN	HEAVY DUTY
Maximum D.C. current at each position	5 ampere	15 ampere
Maximum D.C. voltage at each position	10 volts	10 volts
Maximum power consumption	150* or 300 watts	400 watts
Height	18 inches	20¼ inches
Width	11¼* or 21 inches	21 inches
Depth	11¼ inches	11¼ inches
Net Weight	35* or 61 pounds	80 pounds
Shipping Weight	70* or 110 pounds	130 pounds

*One position unit

S-29459 ELECTROLYTIC ANALYZER — Motor Stirred, One Position, 5 Ampere, SARGENT-SLOMIN.....**$300.00**

S-29460 DITTO. But with adjustable sub-surface heater **$325.00**

S-29464 ELECTROLYTIC ANALYZER — Two Position, SARGENT-SLOMIN **$490.00**

S-29465 DITTO. But with two adjustable heaters, pilot lights and control knobs.....**$530.00**

S-29480 ELECTROLYTIC ANALYZER — Heavy Duty, Magnetically Stirred, Two Position, 15 Ampere, Sargent (illustrated top, right).....**$610.00**

SARGENT

SCIENTIFIC LABORATORY INSTRUMENTS • APPARATUS • SUPPLIES • CHEMICALS

E. H. SARGENT & COMPANY, 4647 W. FOSTER AVE., CHICAGO 30, ILLINOIS
MICHIGAN DIVISION, 8560 WEST CHICAGO AVENUE, DETROIT 4, MICHIGAN
SOUTHWESTERN DIVISION, 5915 PEELER STREET, DALLAS 35, TEXAS
SOUTHEASTERN DIVISION, 3125 SEVENTH AVE., N., BIRMINGHAM 4, ALA.

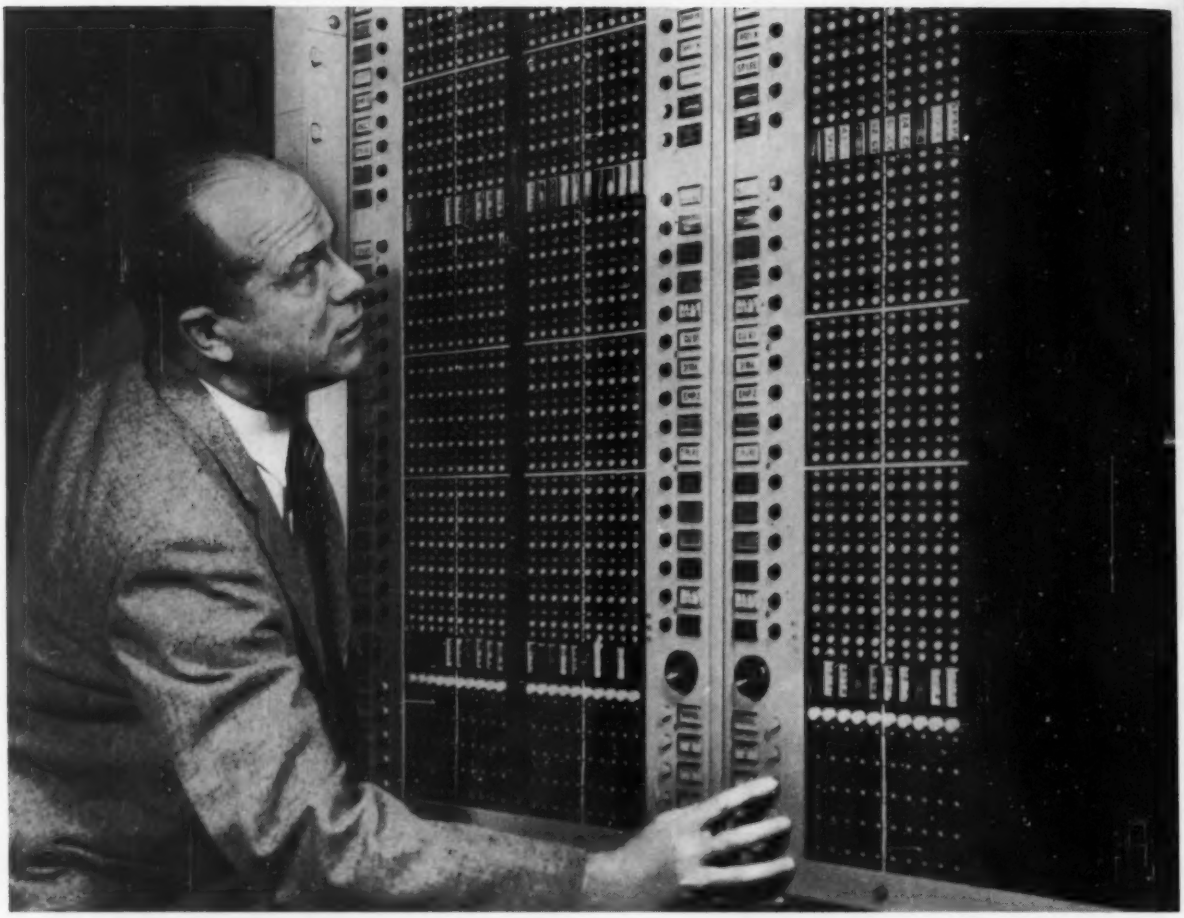

Bell Laboratories engineer Cyril A. Collins, B.S. in E.E., University of Washington, demonstrates new TV switching control panel for black and white or color. Complex switching connections are set up in advance; in a split-second a master button speeds dozens of programs to their destinations all over the nation. Special constant-impedance technique permits interconnection of any number of broadband circuits without picture impairment.

Telephone science speeds TV enjoyment

Telephone science plays a crucial part in your TV entertainment. An interesting example—one of many—is the latest TV switching center developed at Bell Telephone Laboratories.

Switching centers control the transmission of programs which come to your local TV station over Bell System facilities. To be available exactly on cue, programs must be switched at high speed and with very great accuracy.

To create the new switching center Bell Laboratories engineers borrowed from the switching control art which handles your dial telephone calls. They developed a special control panel which puts complex switching patterns within the easy grasp of one man. By pushing buttons, he sets up—and double-checks—forthcoming network changes far ahead of time. On cue he presses a master button which sends the programs racing to their respective destinations around the nation.

To connect the broadband circuits, the Laboratories engineers developed a new video switch which operates on a constant-impedance principle. The new switch permits the interconnection of any number of circuits, without the slightest impairment of transmission quality.

Thus the technology which serves your telephone also works for your TV enjoyment.

BELL TELEPHONE LABORATORIES

WORLD CENTER OF COMMUNICATIONS RESEARCH AND DEVELOPMENT

Editorial

Publication Problems

READERS of this JOURNAL will notice that the Current Affairs section has been reduced in size, while a larger number of technical papers is being published monthly. The Current Affairs section was given that name in 1950, and it was declared editorially that it would be maintained, and expanded if possible. The Editorial Committee has long believed that a good many subscribers find considerable interest in the news, announcement, and feature pages, and a real effort has been made to avoid curtailment of this section. However, so many worthy technical manuscripts are now received that an acute problem of publication has arisen. These original research reports obviously give the JOURNAL its lasting quality and deserve the highest publication priority they can get.

Actually, many items concerning industry and products, which might appear in this JOURNAL, can be found elsewhere at an earlier date. ECS news and announcements must, of course, be published. It is asked—Secretaries please note—that Division and Section reports be made brief. Pertinent news of electrochemical industry, a limited number of technical and regional feature articles, a few book reviews, will be continued.

Only recently the JOURNAL prided itself on its quick publication of technical papers, once they had been reviewed and accepted. Not so today: the number of manuscripts awaiting publication is so large that the delay is becoming intolerable. The bottleneck is, naturally, financial in nature. Money would pay for printing more pages, and for editorial assistance to prepare the material. Actually, the number of subscribers, the diversity of their interests, the success of the national meetings, would seem to warrant a much larger technical JOURNAL. Only a wide variety of material can assure the continued interest of every subscriber.

Various economies have been put into effect during the last two years. A rather small increase in the allowance for printing resulted in more efficient use of editorial time. A slightly thinner paper was adopted. A small reduction in type size enabled more words to be printed on fewer pages in 1956 than in 1955. You will notice that the JOURNAL now has a new printer, which will result in some savings and, it is hoped, will assure earlier distribution each month. Editorials may be discontinued or appear less frequently to save space, but the real need is for about 250 additional pages per year.

The Society's Board of Directors was able to appropriate, for JOURNAL operation in the current fiscal year—April 1, 1957 to March 31, 1958—several thousand dollars more than was available for the preceding year. All these things may keep the backlog of accepted manuscripts from growing in size for the coming year. After that, still more funds will be needed.

Recent increases in memberships and subscriptions have been helpful, but are not enough. Perhaps the time has come to consider an increase in subscription rates. In the JOURNAL, we are getting more material per dollar than we were 10 years ago. This is not true of food, clothing, housing, or luxuries. Each additional dollar invested in the JOURNAL now will bring a larger, more informative issue in the mail every month, and will help attract more subscribers to help share the cost.

—CVK

Choose from 4 grades of high purity magnesium

Now in volume—pig and ingot for production of titanium, uranium, zirconium, beryllium

Now—even purer grades of Dow magnesium are available in quantity lots to supplement Dow high purity (99.8%) magnesium. Magnesium pig and ingot of 99.9% purity and above are currently being produced in four different grades:

Grade mg 2, low manganese—(maximum .01% Mn)
Grade mg 3, low aluminum—(maximum .004% Al)
Grade mg 4, extra-low aluminum—(maximum .002% Al)
Grade mg 5, low iron—(maximum .003% Fe)

These specialized grades of high purity magnesium were developed for use in the manufacture of priority defense metals. They can be used in the reduction of titanium, uranium, zirconium and beryllium halides. Further information and data on maximum allowable impurities for the four grades are available on request. Contact the nearest Dow sales office or write THE DOW CHEMICAL COMPANY, Midland, Michigan, Department MA1437QQ.

YOU CAN DEPEND ON DOW

Effect of Pre-Oxidation in Oxygen on the Steam Corrosion Behavior of Zircaloy-2

D. E. Thomas and S. Kass

Atomic Power Division, Westinghouse Electric Corporation, Pittsburgh, Pennsylvania

ABSTRACT

The effect of pre-oxidation in dry oxygen gas on the corrosion behavior of Zircaloy-2 and unalloyed zirconium in steam was investigated. In the case of Zircaloy-2, pre-oxidation has no effect on corrosion behavior, the kinetics being the same whether all or part of the total exposure is in oxygen. A transition in kinetics from quasi-cubic to linear occurs in the corrosion of Zircaloy-2 in either medium, indicating that the transition is not associated with corrosion product hydrogen. On the other hand, unalloyed Zr shows neither transition nor breakaway (spalling) when exposed to oxygen, and exhibits breakaway on exposure to steam whether pre-oxidized or not, suggesting that breakaway is associated with corrosion product hydrogen. The phenomena of breakaway and transition are shown to be distinctly different.

The corrosion properties of Zircaloy-2 sponge Zr base with 1.5% Sn, 0.12% Fe, 0.10% Cr, and 0.05% Ni have been studied as a function of temperature and time (1, 2). The corrosion behavior in 750°F (400°C) steam at 1500 psi, Fig. 1, exhibits a change in slope ("transition") at a weight gain of 40 mg/dm² after 40 days (3). It has been shown that Zr and Zircaloy-2 pick up H during exposure to high temperature water or steam, and it has been suggested that the transition normally results when the pick-up of H during corrosion causes hydride to form at the metal/oxide interface or at some other site in the reaction zone.

If hydride formation is a factor in causing transition, specimens which have been exposed to dry oxygen for various periods of time and subsequently transferred to steam should show transition at total weight gains and total times greater than those for specimens not previously oxidized in dry oxygen. Furthermore, specimens which have been exposed only to dry oxygen should not show transition. The purpose of the work described here was to determine the effect of pre-oxidation in oxygen on the transition during subsequent exposure to steam at the same temperature, and thereby test the hypothesis.

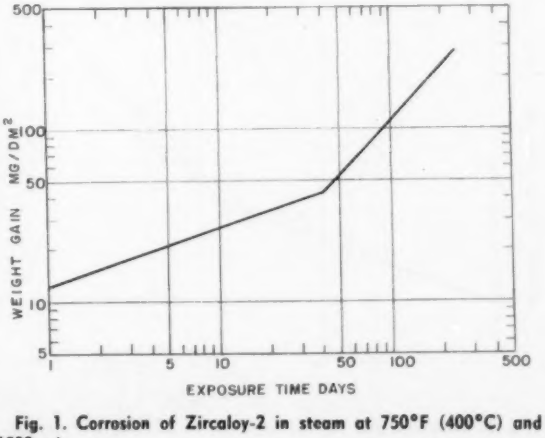

Fig. 1. Corrosion of Zircaloy-2 in steam at 750°F (400°C) and 1500 psi.

In the case of unalloyed, arc-melted sponge or crystal bar Zr, corrosion in high temperature water and oxygen is characterized by the formation of thin, adherent corrosion product which results in a protective or passive type of rate law relating weight gain and exposure time. After a time a new and more rapid corrosion rate sets in, coincident with the appearance of a nonadherent white corrosion product on the surface of the metal. This behavior has been called "breakaway". Specimens of crystal bar Zr were included in this study to provide a point of comparison with Zircaloy-2.

Experimental Procedure

Approximately forty specimens each of arc-melted crystal bar Zr and Zircaloy-2, measuring 1.0 in. x 0.5 in. x 0.1 in., were vacuum annealed for 1 hr at 775°C and furnace cooled. Specimens were bright etched in 38% HNO_3-5% HF-57% H_2O and were placed in the oxidation furnace. After a vacuum of 10^{-4} mm Hg was obtained, the entire system was flushed two or three times with tank oxygen dried by passing through "Drierite". After each addition of oxygen, the system was evacuated to 10^{-4} mm Hg. Finally, oxygen was added to the furnace until a pressure of 30-40 cm Hg was reached and heat was applied.

The temperature of 400° ±3°C was maintained by a thermocouple placed adjacent to the test specimens. This temperature was chosen since considerable data are available for comparison on the corrosion of Zircaloy-2 in 750°F (400°C) steam.

Three specimens each of crystal bar Zr and Zircaloy-2 were removed from the furnace after 1, 3, 7, 14, 28, 56, 84, and 112 days and subsequently transferred to steam at 750°F (400°C) and 1500 psi.

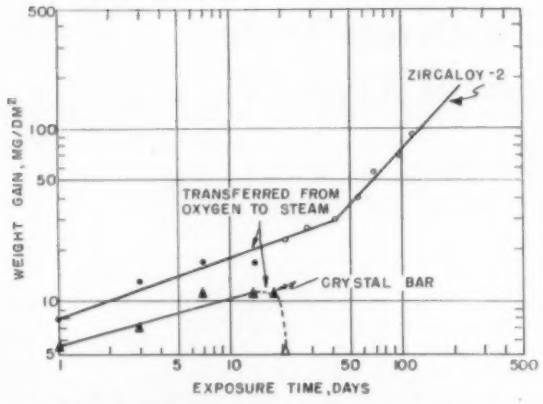

Fig. 2. Weight gain-time curves for exposure of crystal bar Zr and Zircaloy-2 at 750°F (400°C) for 14 days in oxygen followed by exposure to steam. Crystal bar Zr begins to lose weight on transfer. Solid circle, solid triangle = oxygen; open circle, open triangle = steam.

The evacuation and flushing technique outlined above was followed each time samples were returned to the furnace.

Weight gains were determined periodically during initial and final exposures. The corrosion product was not removed when samples were transferred.

Results

Results are represented graphically in Fig. 2, 3, 4, and 5.

Zircaloy-2.—The kinetics of the reaction of Zircaloy-2 with oxygen, shown in Fig. 4, are identical to those for reaction with steam shown in Fig. 1. Results shown in Fig. 2 and 3 are typical of those experiments in which the exposure was first in oxygen then in steam. It is seen that corrosion proceeds after transfer as though the entire exposure had been in steam. The interchangeability of exposure in the two media is exhibited in Fig. 5 in which data points for exposure to steam alone, oxygen alone, and to first oxygen then steam are combined. A single curve results within experimental error.

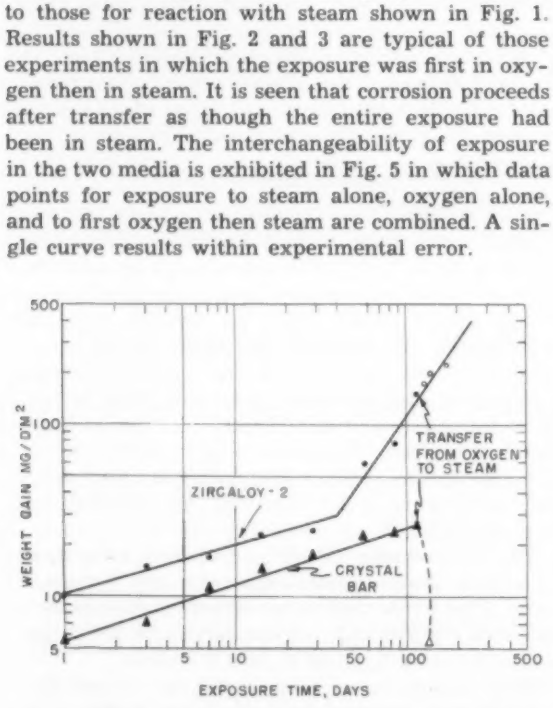

Fig. 3. Weight gain-time curves for exposure of crystal bar Zr and Zircaloy-2 at 750°F (400°C) for 112 days in oxygen followed by exposure to steam. Crystal bar Zr begins to lose weight on transfer. Solid circle, solid triangle = oxygen; open circle, open triangle = steam.

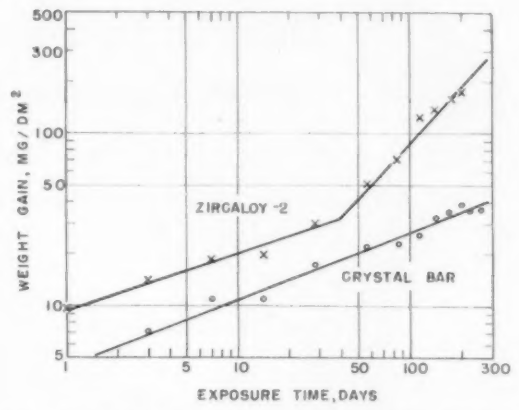

Fig. 4. Weight gain-time curve for corrosion of crystal bar Zr and Zircaloy-2 in oxygen at 750°F (400°C).

Crystal bar zirconium.—The kinetics of reaction of crystal bar Zr with oxygen are shown in Fig. 4. It is seen that the curve is quite different from that for Zircaloy-2. Significantly, transition is not apparent. This is not characteristic of the behavior of crystal bar Zr or sponge Zr in high temperature water or steam. No curves are shown for the attack of crystal bar Zr by 750°F (400°C) steam because "breakaway" and loss of oxide occur within the shortest exposure period investigated (1 day). Typical of the experiments in which crystal bar Zr was first exposed to oxygen then to steam are the results shown in Fig. 2 and 3. Upon transfer from oxygen to steam the specimens begin immediately to lose weight by spalling.

It should be noted here that the crystal bar Zr employed was of high purity. Isolated instances in which crystal bar Zr has shown higher resistance to attack by 750°F steam have been associated with the presence of somewhat greater than normal Fe, Ni, or Cr content.

Discussion

The observation that part of the H evolved by the reaction of Zr or Zircaloy-2 with water or steam is found in the unreacted metal has been thought to be

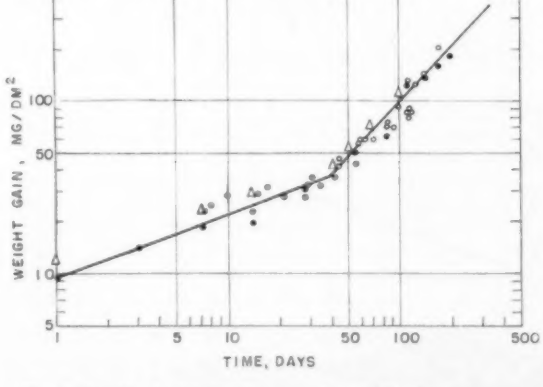

Fig. 5. Combined plot for the corrosion of Zircaloy-2 in oxygen, steam, and in oxygen followed by steam at 750°F (400°C). Solid circle = oxygen; open triangle = steam; open circle = oxygen and steam.

of considerable significance (1, 2, 4, 5). It has been suggested that the H content of the underlying metal may build up sufficiently to cause the precipitation of a zirconium hydride at the metal/oxide interface which could destroy coherency between metal and oxide, and result in more rapid corrosion locally, or possibly complete loosening of the oxide (1, 2). It was suggested that this would explain the phenomena of "breakaway" in the case of Zr and "transition" in the case of Zircaloy-2. In view of the fact that transition is observed for Zircaloy-2 whether the exposure is in oxygen or steam or both removes H from consideration.

On the other hand, the fact that crystal bar Zr does not exhibit transition or breakaway on exposure to oxygen suggests that H is in some way related to breakaway. Specimens of crystal bar Zr which had been exposed to steam for one day and which had begun to lose oxide were examined in cross section under the light microscope. No evidence for hydride was found. Thus, the circumstantial evidence points to H being associated with the breakaway phenomena, but it is evident that further work is necessary to secure direct evidence.

The results of these experiments suggest that a distinction is to be made between two terms which have been used to denote the point at which a change in kinetics occurs, namely breakaway and transition. Transition appears to be an abrupt change from protective-type kinetics (quasi-cubic) to linear corrosion kinetics, the newer corrosion rate being somewhat greater than that prevailing immediately prior to the change. The corrosion product remains adherent. It is not associated with the pickup of corrosion-product H, but is presumably associated with some as yet undetermined physical change in the oxide film. On the other hand, breakaway, while it refers to a change of kinetics in that a new corrosion rate sets in, is characterized by the loss of oxide at a relatively rapid rate, and is presumably associated in some way with the pickup of H. Since crystal bar Zr does not show transition or breakaway when exposed to oxygen, but does exhibit breakaway when exposed to steam, and since Zircaloy-2 exhibits transition but not breakaway in both oxygen and steam, it is apparent that the addition of Sn in combination with Fe, Ni, and Cr in Zircaloy-2 prevents the occurrence of breakaway. The elimination of breakaway by the addition of these elements may be associated with a change in the behavior of the material toward H in some way which is not apparent at present. Furthermore, it is not yet understood why Zircaloy-2 shows transition while crystal bar Zr does not.

Conclusion

1. Zircaloy-2 exhibits the same behavior in oxygen and steam at 750°F (400°C). Transition is not associated with the pickup of H.
2. Crystal bar Zr exhibits breakaway when exposed to steam. It exhibits neither breakaway nor transition when exposed to oxygen.
3. A distinction between "transition" and "breakaway" is made. Transition is not associated with H pickup during corrosion. Breakaway is presumably associated with H pickup.
4. The addition of some alloying elements to crystal bar Zr prevents the occurrence of breakaway, but promotes the occurrence of transition.

Acknowledgment

This work was performed under AEC Contract AT-11-1-GEN-14.

Manuscript received September 4, 1956.

Any discussion of this paper will appear in a Discussion Section to be published in the December 1957 JOURNAL.

REFERENCES

1. B. Lustman and F. Kerze, Editors, "Metallurgy of Zirconium," Vol. 4, Div. VII, Chap. II, McGraw Hill Book Co., New York (1955).
2. D. E. Thomas, "Aqueous Corrosion of Zirconium and its Alloys at Elevated Temperature", U.S. Paper No. 537, Geneva Conference (1955).
3. D. E. Thomas and S. Kass, *This Journal*, **103**, 478 (1956).
4. K. M. Goldman and D. E. Thomas, "Hydrogen Pickup during Corrosion Testing of Zirconium," unpublished work.
5. S. Kass, Work in progress.

A Hydrogen Effusion Method for the Determination of Corrosion Rates in Aqueous Systems at Elevated Temperature and Pressure

M. C. Bloom and M. Krulfeld

Metallurgy Division, Naval Research Laboratory, Washington, D. C.

ABSTRACT

This paper analyzes the limitations of weight change techniques at elevated temperature and pressure, and presents a description of a new technique based on the measurement of the hydrogen generated by the corrosion reaction. This H, which diffuses through the walls of a test specimen containing the aqueous solution, is collected and measured in a vacuum system of known volume which surrounds the test specimen; the corrosion rate is calculated from the hydrogen effusion rate. Results obtained with the technique show good reproducibility and compare well with results obtained by an independent method.

Corrosion rates of metals in aqueous solutions at elevated temperature and pressure have been obtained almost exclusively by weight gain or weight loss measurement of specimens subjected to corrosion in autoclaves of various types (1-4). Such measurements are inherently difficult. Loss of corrosion products by spalling or dissolution introduces serious errors into weight gain data. Weight loss data are reliable only if complete removal of corrosion products without attack on the uncorroded metal beneath can be obtained. Galvanic effects between autoclave and specimens may affect the results obtained if the two differ in composition or treatment history prior to the test. One of the most serious limitations is that from a single specimen only a single value of total corrosion can be obtained from which only an "average" corrosion rate over the period of exposure can be calculated. In the usual case, however, where corrosion resistance depends on the type of protection provided by corrosion product films, such average rates are misleading. The information needed in such cases is the differential corrosion rate. Using weight gain and weight loss methods, differential rates can be obtained only by corroding a large number of samples under the given conditions for varying times, the rates being obtained by differences between the gains or losses of the specimens at the different time intervals. Since reproducibility from sample to sample determines the accuracy of any rates calculated by difference, and since reproducibility using these techniques is usually not good, a large number of samples must be run simultaneously to obtain dependable average values for such calculations. These limitations of weight gain and weight loss methods are particularly serious when the corrosion rates are low.

To overcome the difficulties enumerated, a method was developed in which there is no error due to loss of oxide or of metal in the measuring process, the sample constitutes its own autoclave, samples need not be destroyed in the process of measurement, and observation can be continuous on a single sample so that a differential corrosion rate can be determined using only one specimen.

Theoretical Considerations

Examination of the reaction

$$\text{Metal} + H_2O \rightarrow \text{Metal Oxide} + H_2 \qquad \text{(I)}$$

indicates four possible methods of measuring corrosion rate, i.e., measurement of *(a)* metal consumed, *(b)* water consumed, *(c)* metal oxide formed, and *(d)* hydrogen formed. Methods *(a)* and *(c)* entail the difficulties outlined above, and method *(b)* involves analogous difficulties, so attention was turned to method *(d)*. Since H_2 diffuses rather readily through metals at elevated temperatures, the possibility of correlating effused H_2 with the corrosion reaction was investigated.

In a container of the metal under test, nearly filled with water or an aqueous solution, and heated to an elevated temperature, H_2 is generated by the corrosion reaction. It is generated initially as atomic H at the interface between liquid and container. It may pass through the container wall in this form to emerge on the other side and there combine to form molecular H_2, or it may recombine to form molecular H_2 within the container. In the latter case, the H_2 gas initially distributes itself between the liquid and the available vapor space but, as it builds up pressure, some of this H_2 also diffuses through the container wall. Thus, there are two sources of H_2 passing through the container wall. H_2 from the latter source permeates the wall at a rate governed by the equation

$$dQ/dt = S_T A \left(\sqrt{P_1} - \sqrt{P_2}\right)/d \qquad \text{(II)}$$

where dQ/dt is the amount effused per unit time, S_T is a constant determined by the nature of the metal and the temperature, A is the area of the metal, d is the thickness, P_1 is H_2 pressure on the high-pressure

side, and P_2 the H_2 pressure on the low-pressure side. If P_2 is maintained at a negligible value the equation reduces to

$$dQ/dt = S_T A \sqrt{P}/d \qquad \text{(III)}$$

where P is H_2 pressure within the container. As the corrosion reaction proceeds the pressure inside the container increases until *(a)* the rate of effusion from both sources becomes equal to the corrosion rate, or *(b)* the pressure inside the container continues to increase until the equilibrium pressure of the reaction is reached or the container is shattered. In the case of ferrous metals, the latter would be expected.

The data on S_T for mild steel (5, 6) indicate it is approximately 10^{-3} at 300°C when dQ/dt is in cc H_2 (STP)/hr, A is in cm^2, d is in mm, and P in atmospheres. Assuming a mild steel container with a wall 0.5 mm in thickness and an internal H_2 pressure of 1 atm, rates of H_2 effusion equivalent to a corrosion rate of 2700 mg/dm^2-mo are obtained based on the reaction $3Fe + 4H_2O \rightarrow Fe_3O_4 + 4H_2$. This is a much greater rate than would be anticipated for the corrosion of mild steel under these conditions (1) and indicates that a low H_2 pressure should be sufficient to obtain the required steady-state effusion rate.

In order to reach the steady state rapidly a maximum area to volume ratio, a minimum thickness of wall, and a minimum of vapor space are desirable. For a maximum A/V in a cylinder, where

$$A/V = \frac{2\pi r^2 + 2\pi rh}{\pi r^2 h} = \frac{2}{h} + \frac{2}{r} \qquad \text{(IV)}$$

the smallest dimensions feasible should be used. To avoid vapor space the capsule should be filled so that it develops a hydraulic pressure slightly in excess of the vapor pressure of the fluid at the temperature of test. This can be achieved by flattening a cylindrical container prior to complete filling and sealing. Upon heating, the flattened cylinder will react to the hydraulic pressure by expanding partially toward its original dimensions, developing an internal pressure which will depend on the amount of flattening and the thickness and character of the metal.

Based on the above considerations a technique was developed for the measurement of corrosion at elevated temperature and pressure employing a small, thin-walled, flattened capsule of the metal under test, heated within a vacuum system which was provided with means for measuring the amount of effused H_2.

Experimental Apparatus and Procedures

Metal tubing carefully fabricated to develop a smooth uniform interior surface free of foreign matter (preferably made in one lot from a single ingot) is used to encapsulate a small quantity of corroding fluid. A fluid-filled capsule, attached to a counterweight of magnetic material so that it can be moved up and down by an external magnet, is then inserted in the experimental apparatus shown in Fig. 1. After the capsule is dropped into the oven, H_2 is generated by corrosion and effuses through the capsule walls to build up a pressure in the surrounding

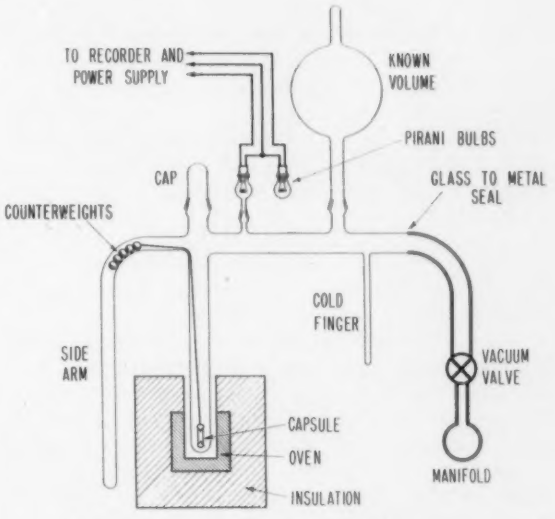

Fig. 1. Single system for hydrogen effusion measurement

glass envelope. This pressure is continuously recorded by the Pirani gauge circuit.

In actual operation a number of such systems are connected in parallel to a common furnace, pumping system, and associated apparatus. The furnace is a cast block of Al 8 ft long and 5 in. square drilled with 15 holes 1¼ in. in diameter and 3½ in. deep. The furnace is insulated with 2 in. of glass wool housed in an asbestos sheet duct 9 in. square and 3/16 in. thick. It is heated by means of cartridge heaters maintained at temperature by a thermocouple-actuated control circuit which maintains the temperature within ±2°C.

Fabrication of Capsules

The following description is based on operations with low-carbon steel, with which the work thus far has been mostly concerned. Procedures for other materials differ only in minor details.

One-foot lengths of seamless low-carbon steel tubing 0.25 in. in external diameter and 0.020 in. thick are washed in a hot detergent solution, degreased in hot trichloroethylene, and dried. They are then given a H_2 anneal, usually followed by a vacuum anneal, prior to fabrication in order to obtain clean oxide-free reproducible metal. The H_2 anneal is for 1 hr at 875°C, followed by cooling in the H_2 atmosphere to about 90°C in a water-cooled chamber. If a vacuum anneal is given, the tubing is placed in a vacuum furnace maintained at a pressure of less than 10^{-5} mm Hg, heated at 875°C for a minimum of 1 hr, and furnace cooled to room temperature.

In the fabrication procedure the annealed tubing is subjected first to a flattening operation with a hydraulically operated die. A second die with equally spaced flat teeth then outlines the capsule form. In this form the tubing, held vertically, is completely filled, by aspiration, with the fluid to be used as the corroding medium. Another die then closes the bottom flat section under a pressure of several tons per square inch. The die is moved upward to seal the ends of each filled capsule section successively. The

capsules are then separated by cutting across the centers of the flat sealed sections and are made pressure tight by spot welding across the flat ends. The over-all length of the finished capsule is 4 cm, of which the completely flattened, welded ends constitute 1 cm and the fluid-filled capsule section constitutes 3 cm. The over-all width of the capsule perpendicular to the flat sides is 0.28 cm.

Operation of Apparatus

Each capsule is connected by means of thin, flexible Pt-clad Mo wire to Ni-plated steel counterweights, and the capsule and counterweights are inserted in the vacuum system (Fig. 1). The capsules are maintained in the room temperature section of the apparatus by manipulation of external magnets. The system is sealed and then outgassed by opening the vacuum valve to the manifold. After overnight outgassing, a run is started by closing the vacuum valve to the manifold and raising the counterweights until the capsule drops into the furnace zone which is maintained at the desired temperature. The capsule heats rapidly as evidenced by a sudden, very rapid increase in the pressure within the system. The pressure rise, due to the corrosion-generated H_2 effusing through the capsule wall and collecting in the system, is measured by means of the Pirani bulb, connected in a calibrated bridge circuit whose output is recorded. To insure accuracy, the pressure measuring system is calibrated with pure dry H_2 gas and a McLeod gauge before each run.

When the pressure within the system reaches a value of about 50 μ, a pressure sufficiently low to make Eq. (III) valid, the system is pumped down to a pressure of less than 0.1 μ by opening the valve to the manifold and pumping system. After pumpdown the valve is again closed until the system pressure builds up again; the process is repeated as frequently as necessary.

The rate of pressure buildup for mild steel varies over a wide range. At the beginning of a run, a buildup of 50 μ in 3 min is not uncommon. After several months, when the formation of a protective film has reduced the corrosion rate, a buildup of the order of 2 μ a day is observed. Fluid leakage can readily be identified by chilling the cold finger shown in Fig. 1. If the presence of gases other than H_2 is suspected in the system, a rough check can be made by connecting an absolute gauge, such as a McLeod gauge, to the manifold. Unlike an absolute gauge, the Alphatron vacuum gauge shown connected to the manifold is sensitive to the nature of the gas being measured. If the Alphatron gauge, using the calibration curve for H_2, gives a pressure reading different from that indicated by the McLeod gauge after the unit has been opened to the manifold, the presence of gases other than H_2 is indicated. If it can be assumed that the foreign gas is air or water, the above readings also permit a rough calculation of the amount of foreign gas present. If more accurate analyses are desired, gas from any of the systems can be transferred to a gas analysis system.

A slight pressure rise not attributable to effusing H_2 has been encountered in gas-tight systems, varying from less than 0.01 μ/hr to a rise as high as 0.15 μ/hr, with average values of about 0.05 μ/hr being found most frequently. A pressure buildup of 0.05 μ/hr corresponds to a corrosion rate of approximately 4 mg/dm^2-mo under the conditions of operation. The exact nature of the residual pressure is not yet known, but it can probably be attributed to gas adsorbed on the walls and parts of the system which slowly desorbs at the low pressures normally used in making these measurements.

While the apparent corrosion rates due to causes other than corrosion within the capsules are low and do not affect significantly values obtained during early portions of a run when the corrosion rates are high, they become significant when the corrosion rate has diminished. They must, therefore, be evaluated and subtracted from the measured rates in order to obtain corrected corrosion rates. These "blank rates" for the individual system are obtained readily by raising the corroding capsule out of the hot zone of the system during the course of a run. The capsule then cools rapidly to room temperature, the corrosion rate dropping substantially to zero. The capsule is maintained in this position until sufficient pressure rise has been obtained for an accurate determination of the blank rate. Normally the rate is so low that at least five days of pressure buildup is required. The capsule is then returned to the hot zone of the system, with no disturbance other than the temporary change in temperature. Ordinarily the corrosion rate measured after the determination of the blank rate is approximately the same as that measured before the thermal shock imposed by the blank-rate measurement (Fig. 2). In a few cases some change in the corrosion rate has been encountered.

Determination of System Constants

The volume of a system is measured by expanding gas from a reservoir of known volume into the system. Pressures in the system and reservoir are measured before and after expansion and the system volume is calculated from these pressures using the gas laws. The arithmetic mean of several such

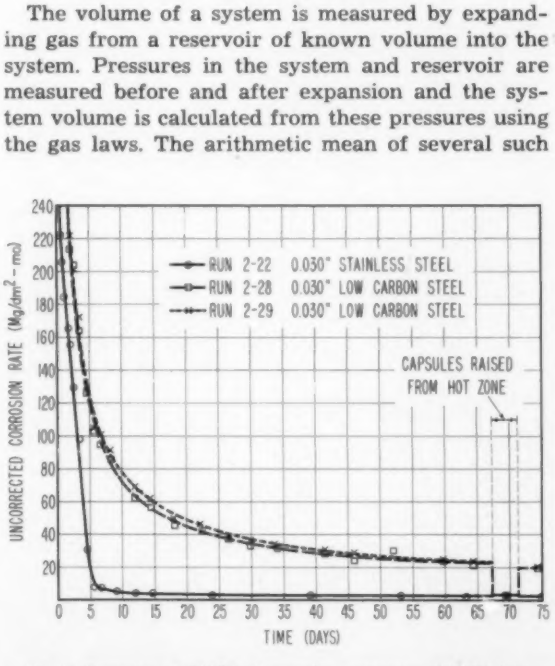

Fig. 2. Corrosion at 316°C of capsules containing NH_4OH (pH = 10.6 at room temperature).

measurements is taken to be the system volume. By this method the system volume is determined with an estimated accuracy of ±1.5%. These systems normally have a volume of about 2700 cc. If a more rapid rate of pressure buildup is desired, the system volume may be reduced by removing the bulb of known volume (approximately 2 liters) (Fig. 1), and replacing it with a cap.

The mean temperature of the gas in the system is taken to be the temperature of the room in which the apparatus is situated (maintained constant within ±1°C), modified by correcting for the higher temperature of that small part of the system which is in the heated zone. Data for this correction are obtained by thermocouple measurements of the temperature distribution within this heated zone. In this manner the mean temperature of the gas is determined with an estimated accuracy of ±1%.

Assuming that the surface area of a length of tubing undergoes negligible change in the flattening processes used in capsule fabrication, the inside surface area of a capsule is calculated from the length of tubing between the seals and the known dimensions of the tubing. The roughness factor was estimated as 1.2 from microscopic examination. Measurements on a large number of capsules indicate that variables in the fabrication process produce capsules which vary in length from 2.9 to 3.3 cm, the average length being 3.1 cm. There is a corresponding variation of inside surface area, the average surface area being 5.2 cm^2.

Determination of Pressure Rise

Pressures in the system are measured by means of a Pirani vacuum gauge that is a modification of that described by Schwartz and Lavender (7). The output of the Pirani circuit is recorded continuously to give a record of the pressure buildup within the system. At the beginning of each run the Pirani gauge is calibrated by determining the relationship between the Pirani output and the H_2 pressure in the system. The linear portion of this relation (pressures up to 60 μ) is then used for pressure determination. Although indications are that the errors involved are minor, certain gauge characteristics give rise to possible errors not yet evaluated. The Pirani gauge tends to exhibit some drift with time, which introduces uncertainty into the accuracy with which the pressure measurements can be made. It is clear that large errors could be introduced if the slope of the calibration curve changed markedly as a result of the drift. However, exploratory studies have indicated that this drift does not affect the slope of the linear portion of the curve appreciably. Another error which could be introduced is that resulting from drift in the interval between successive pressure measurements. Such errors are minimized by making successive pressure-rise measurements over the shortest time intervals practical and by the apparent fact that the drift is usually gradual. Due to the factors mentioned, it is not possible to make definite estimates of the probable errors in pressure-rise measurements. However, studies are contemplated to determine the errors more accurately and to improve stability in the pressure-measuring system.

Table I. Corrosion rate of low-carbon steel at 316°C after 40 days

Run	Sample: Vacuum Annealed	Sample: Fluid	Corrosion rate (mg/dm^2-mo): Uncorrected	Blank	Corrected
3–1	Yes	H_2O	35	6	29
3–2	Yes	H_2O	44	11	33
3–6	No	H_2O	30	14	16
3–7	No	H_2O	22	4	18
2–24	No	NaOH*	19	1	18
2–26	No	NaOH*	18	3	15
2–27	No	NaOH*	22	3	19
2–28	No	NH_4OH*	29	3	26
2–29	No	NH_4OH*	31	3	28

* Solution pH = 10.6 at room temperature.

Calculation of Corrosion Rates

The rate of corrosion of a sealed capsule is calculated from the rate of pressure rise corrected for system outgassing as explained above. From this rate of pressure rise, with the volume and temperature known, the gas laws are used to calculate the rate of H_2 increase within the system. This is equal to the rate of H_2 effusion from the corroding capsule. This rate of H_2 effusion is converted to corrosion rate per unit area by use of the internal surface area of the capsule combined with stoichiometric calculations from the equation $3Fe + 4H_2O \rightarrow Fe_3O_4 + 4H_2$.

Typical Results

The reproducibility obtained using the apparatus and procedures described is shown in Table I, which also illustrates the improvement obtained by blank rate correction.

The reproducibility obtainable during the course of a run on like samples is also indicated in Fig. 2, which shows the data on some typical runs including uncorrected corrosion rate and blank-rate data.

Discussion

One source of possible error in these measurements must be considered. High apparent rates may be indicated at the beginning of a run due to material adsorbed on the outside surface of the capsule which desorbs when the capsule is heated. Correction might be made for such errors by using blank capsules put through precisely the same treatment as the capsules under consideration but which contain dry air, inert gas, or a vacuum instead of the corroding fluid. Subtraction of the average values given by such blanks from the measured rates of corroding capsules would be expected to give more accurate corrosion data at the beginning of a run. Preliminary work in this direction indicates that such blanks may vary in magnitude. The indications are that the error from this source is normally negligible after the first few days of a run, but a few blank samples have shown significant outgassing for periods as long as several weeks. This matter is receiving further attention.

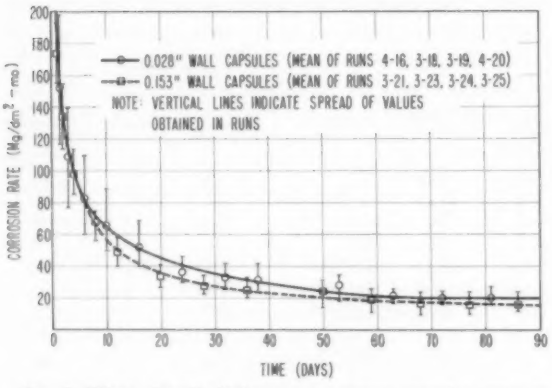
0.028" WALL CAPSULES (MEAN OF RUNS 4-16, 3-18, 3-19, 4-20)
0.153" WALL CAPSULES (MEAN OF RUNS 3-21, 3-23, 3-24, 3-25)
NOTE: VERTICAL LINES INDICATE SPREAD OF VALUES OBTAINED IN RUNS
CORROSION RATE (Mg/dm² - mo)
TIME (DAYS)

Fig. 3. Effect of wall thickness on apparent corrosion rates at 316°C.

Careful standardization of annealing operations prior to capsule fabrication is necessary. Table I indicates that vacuum annealing has an effect on the corrosion rate of low-carbon steel. Thus, standardization of conditions during the annealing operation is a prerequisite for the determination of the effect of other variables upon corrosion rates.

It is clear from Table I and Fig. 2 that fairly reproducible H_2 effusion rate data are obtained by employing the apparatus and techniques described. The question of the relationship between these hydrogen effusion rates and corrosion rates depends on how soon a steady state is reached. A categorical answer is not yet available, but there is evidence that, for mild steel treated as described above, it is achieved fairly rapidly.

The first piece of evidence deals with the effect of wall thickness on rates of H_2 effusion from corroding capsules. Fig. 3 exhibits data obtained from a series of experiments in which capsules of different wall thickness (0.153 in. vs. 0.028 in.) but otherwise identical in dimensions and machined from the same low-carbon steel rod were subjected to corrosion by distilled, deionized water at 316°C. Because the heavier-walled capsules could not be sealed readily by the usual welding technique, closure of all capsules in this series was effected by means of a threaded cap seating a 59-degree cone into a 60-degree conical opening. The capsules, after H_2 and vacuum annealing, were filled with the water to a level just sufficient to allow for heating to 316°C without exerting hydraulic pressure on the capsule walls. Results were not as reproducible from sample to sample as those obtained using the standard technique of sample preparation, but they suffice to demonstrate that the difference in H_2 effusion rates and corresponding calculated corrosion rates is small. If the diffusion rate through the metal wall were controlling the rate of effusion of H_2, such a fivefold increase in wall thickness would produce a much greater change in H_2 effusion rate than was observed. The data clearly indicate that diffusion through the metal wall of the capsule is not the controlling factor in H_2 effusion under the stated conditions. At least, this is true after the first few day of a run, and perhaps earlier.

A second piece of evidence confirms the rapid attainment of the steady-state rate. More important,

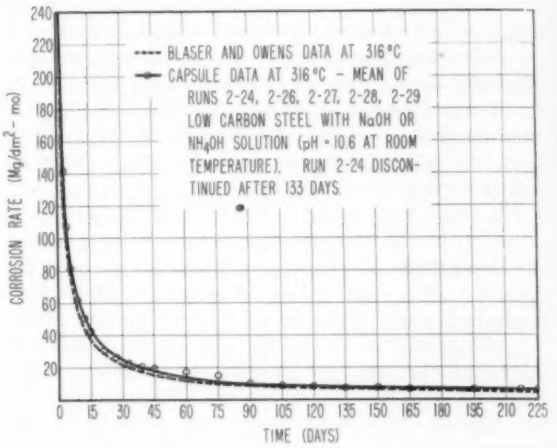
BLASER AND OWENS DATA AT 316°C
CAPSULE DATA AT 316°C - MEAN OF RUNS 2-24, 2-26, 2-27, 2-28, 2-29 LOW CARBON STEEL WITH NaOH OR NH4OH SOLUTION (pH = 10.6 AT ROOM TEMPERATURE). RUN 2-24 DISCONTINUED AFTER 133 DAYS.
CORROSION RATE (Mg/dm² - mo)
TIME (DAYS)

Fig. 4. Comparison of corrosion rates obtained by the H_2 effusion method with those obtained by the descaling method using multiple samples.

it demonstrates that the corrosion rates determined by the H_2 effusion method agree well with rates found on similar material by conventional methods. Fig. 4 exhibits a comparison of results obtained by the H_2 effusion method and those obtained by Blaser and Owens (8) in static systems (autoclaves) and semistatic systems (where the flow of fluid across the specimens was 1 ft/min or less) by means of descaled weight-loss measurements on a large number of samples. During their work, despite considerable variation from sample to sample, consistent average corrosion rates were obtained on low-carbon steel exposed to 315°C high purity water brought up to a *p*H (cold) of 11 with NH_4OH or LiOH. Within the limit of accuracy of the method, corrosion rates appear to be independent of the material used to produce the alkalinity. In Fig. 4 the average results obtained by Blaser and Owens are compared with the average results of five long-time runs in similar low-carbon steel capsules (not vacuum annealed) filled with air-saturated distilled water brought to a *p*H (cold) of 10.6, in two runs with NH_4OH and in the remaining three runs with NaOH. Agreement with the results of Blaser and Owens is excellent.

Douglas and Zyzes (9) measured corrosion rates of autoclaved specimens in high temperature water by mass spectrometric analyses of H_2 evolved. Their corrosion rates on Armco and high purity iron in water at 316°C are of the same order of magnitude as the measured corrosion rates of low carbon steel in 316°C water presented above.

These results indicate that, within the limitations herein stated, the H_2 effusion technique is capable of giving reliable corrosion data in aqueous systems at elevated temperature and pressure. The technique avoids the inherent experimental difficulties encountered in weight-gain or weight-loss methods and allows differential corrosion rates to be determined on a single specimen.

Acknowledgments

Particular thanks are due to W. A. Fraser, G. N. Newport, I. M. Patterson, P. N. Vlannes, and F. O.

Westfall, who operated the apparatus and made the measurements reported here and to G. M. Dinnick and D. I. Walter whose suggestions were especially helpful during the design stages.

Manuscript received April 16, 1956. This paper was prepared for delivery before the Pittsburgh Meeting, Oct. 9-13, 1955.

Any discussion of this paper will appear in a Discussion Section to be published in the December 1957 JOURNAL.

REFERENCES

1. C. R. Breden, S. Greenberg, R. M. Robinson, A. H. Roebuck, V. F. Saitta, and C. C. Scott, Argonne National Laboratory Rpt. ANL-4519, July 15, 1951.
2. S. C. Datsko, Argonne National Laboratory Rpt. ANL-5354, Oct. 4, 1954.
3. H. L. Solberg, G. A. Hawkins, A. A. Potter, and J. T. Agnew, *Trans. Am. Soc. Mech. Engrs.*, **59**, 725 (1937); **64**, 303 (1942); **65**, 47, 301 (1943); **66**, 291 (1944).
4. I. A. Rohrig, R. M. Van Duzer, Jr., and C. H. Fellows, *Trans Am. Soc. Mech. Engrs.*, **66**, 277 (1944).
5. W. Baukloh and W. Wenzel, *Arch. Eisenhüttenw.*, **11**, 273 (1937).
6. P. S. Flint, Knolls Atomic Power Lab. Rpt. KAPL-659, Dec. 14, 1951.
7. C. M. Schwartz and R. Lavender, *Rev. Sci. Inst.*, **19**, 814 (1948).
8. R. U. Blaser and J. J. Owens, Symposium on High-Purity Water Corrosion, ASTM Special Technical Publication No. 179, 1956.
9. D. L. Douglas and F. C. Zyzes, Knolls Atomic Power Lab. Rpt. KAPL-1376, Nov. 1, 1955.

Galvanic Corrosion

I. Current Flow and Polarization Characteristics of the Aluminum-Steel and Zinc-Steel Couples in Sodium Chloride Solution

M. J. Pryor and D. S. Keir

Kaiser Aluminum & Chemical Corporation, Spokane, Washington

ABSTRACT

Current flow, weight loss, and polarization measurements have been carried out on the aluminum-mild steel and zinc-mild steel couples in normal NaCl solution at 25°C. Under a wide variety of experimental conditions both aluminum and zinc are anodic to mild steel and completely protect it against corrosion. In both galvanic couples the current flow and weight losses of the anodes are proportional to the area of the steel cathode and are much less dependent on the anode area. Galvanic corrosion rates of both couples appear to be controlled by oxygen depolarization and are thus markedly increased by stirring. At high stirring rates, the aluminum-steel couple delivers a much higher galvanic current than the zinc-steel couple.

Zinc (1) and aluminum (2-4) are anodic to steel in many aqueous solutions and often corrode sacrificially to impart partial or complete protection to steel. This tendency of Zn and Al to protect steel cathodically has been reflected in the good corrosion resistance of galvanized and aluminized steel (5), particularly in marine environments (6, 7). Although cases are reported when Zn (8-10) and Al (3, 11, 12) reverse their polarity with respect to steel, it is generally true, at least for the zinc-steel couple, that the chance of a polarity reversal is much decreased in the presence of chloride.

Despite a large volume of research on galvanic corrosion, there has been little effort directed toward measuring the actual galvanic current flow in the aluminum-steel couple particularly at zero external resistance. Hoxeng and Prutton (10) carried out potential and current flow measurements on the zinc-steel couple during an extensive study of the effects of different anions in solution. However, many of their measurements refer to cases where the steel was anodic to Zn and are thus not directly comparable to results in NaCl when Zn functions as the anode. Akimov and his co-workers (12), using Cu cathodes coupled to a wide variety of dissimilar metal anodes in NaCl solution, demonstrated that the current flow was proportional to the area of the Cu cathode and was essentially independent of the area of dissimilar metal anode. This was a direct confirmation of the earlier work of Whitman and Russell (13) on the copper-steel couple. Later work by Evans (2) indicated that the additional corrosion produced by contact with a dissimilar metal cathode was approximately proportional to the area of the cathode only when the solution resistance was fairly low.

Because of the lack of quantitative information on the aluminum-mild steel couple in chloride solutions, the investigation described below was carried out. In this phase of the over-all investigation, currents flowing between Al and steel electrodes and between Zn and steel electrodes in normal NaCl were measured, together with weight losses of the electrodes. Polarization curves were determined for the two galvanic couples, and the effect of relative areas of anode and cathode on current flow, weight

loss, and electrode polarization examined. The effect of agitation of the solution on current flow and corrosion rate was also determined for both galvanic couples.

Experimental

Materials

The Al, Zn, and mild steel used in this investigation were in the form of cold rolled sheet 0.088 cm thick. Their compositions are: aluminum—Si 0.001%, Fe 0.001%, Cu 0.002%, balance Al; zinc—Si 0.08%, Fe 0.001%, Cu 0.009%, Pb 0.002%, balance Zn; mild steel—C 0.07%, Si 0.02%, Mn 0.45%, P 0.010%, S 0.005%, Cu 0.06%, Ni 0.08%, Mo 0.005%, Co 0.03%, balance Fe.

All solutions were made from C. P. chemicals and distilled water and were thoroughly shaken to insure saturation with dissolved air.

Steel samples were degreased in benzene, pickled in inhibited HCl, rinsed in distilled water, dried, rinsed again in benzene, and stored in dry air for 24 hr before use. Initial experiments were carried out in which Al specimens were etched in either HF or NaOH, rinsed, dried, and stored in dry air for 24 hr before use. The anodic weight loss, polarization data, and number of coulombs passing in the aluminum-steel couple in 96 hr were found to be insensitive to the surface preparation of the anodic metal. Consequently, Al and Zn specimens used in subsequent experiments received no surface pretreatment other than thorough degreasing in benzene.

Experimental Method

Current flow and weight loss determinations.—Two parallel dissimilar metal electrodes were held in position in a Lucite cell by means of micarta frames lined with neoprene gaskets. The backs of the specimens were masked with waterproofed Scotch pressure-sensitive tape to protect against seepage of the solutions. The masking and gasketing confined the area of each specimen in contact with the solution to 100 cm^2 unless smaller electrode areas were specifically desired.

The space between the electrodes was filled to a constant level with approximately 1600 ml of normal NaCl solution saturated with dissolved air. Evaporation was prevented largely by loosely covering the cell with Saran tissue. The cell was contained in a water bath thermostatted at 25° ±0.05°C.

Dissimilar metal electrodes were short-circuited for the test period of 96 hr. Current readings were taken periodically by introducing a zero resistance microammeter into the circuit. Potential measurements[1] of each electrode against a saturated calomel electrode showed that the closed circuit potentials of the anode and cathode were virtually the same and independent, to within 1 mv, of the position of the calomel electrode in the solution. Evidently any significant potential changes in the couple are limited almost entirely to the electrode-solution interfaces and do not occur gradually across the entire solution path as pictured by Akimov (19). These potential changes at the electrode surfaces may be regarded as energy barriers which alone control the rate of galvanic corrosion when the resistances of the external circuit and of the solution are very low. Measurements of both *p*H and conductivity of the solution were carried out before and after the experiment. After 96 hr, each test was discontinued and corrosion products removed chemically so that the weight loss of the electrodes could be determined. Steel specimens were cleaned by immersion for 2 min in 1:1 HCl inhibited with 3% Rodine 41; Al specimens were cleaned by immersion for 10 min in a solution containing 2% chromic acid and 5% syrupy H_3PO_4 at 80°C. Zn specimens were cleaned in 10% NH_4Cl solution followed by immersion in a boiling chromic acid/silver nitrate solution (14). Blank weight losses were determined for the cleaning procedures on uncorroded panels and were used in calculating corrected weight loss values of the corroded specimens. The total number of coulombs flowing in each experiment was calculated from the current/time curve. By also knowing the weight loss of the uncoupled specimens in normal NaCl solution, both the decrease in weight loss of the cathodic member of the couple and the efficiency of dissolution of the anodic member of the couple could be calculated.

Polarization studies.—The variation in potential of the anodes and cathodes with current was determined by short-circuiting the galvanic couple through a low variable series resistance and permitting both the current and potential to reach steady values at different arbitrary values of external resistance. It has been pointed out previously (15) that this method of measuring polarization curves is more truly comparable with conditions existing during galvanic corrosion, since in both cases the potential and galvanic current may vary together in achieving steady-state conditions.

Results

Potential measurements.—Potential/time curves in normal NaCl solution at 25°C for uncoupled specimens (100 cm^2) of Zn, Al, and mild steel are shown in Fig. 1. Whereas the potentials of Zn and mild steel are fairly steady after a short time, the potential of the Al shows considerable variation. The steady potential of the Zn is near the Nernst potential (16) corrected for Zn ion activity.

Effect of relative area of dissimilar metal electrodes on current flow and weight loss.—Triplicate experiments were carried out for 96 hr on the Zn-steel and Al-steel couples in normal NaCl solution

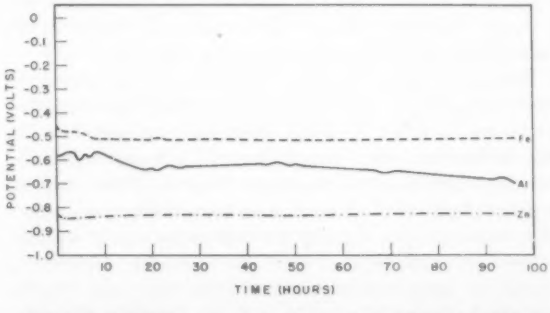

Fig. 1. Potential/time curves for Al, Zn, and mild steel in *N* NaCl solution at 25°C. Equal areas (100 cm^2) of uncoupled metals.

[1] All potentials in this paper are expressed on the Standard Hydrogen Scale.

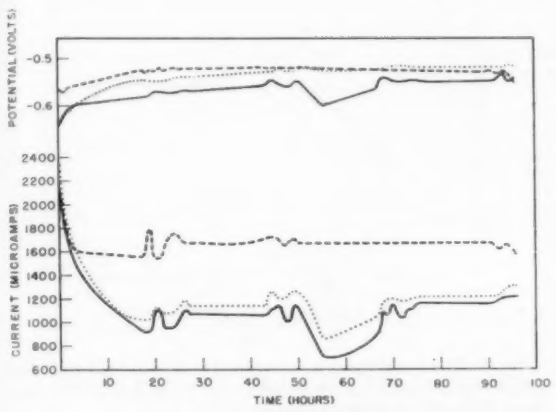

Fig. 2. Triplicate curves relating current flow and potential to time for the Al-mild steel couple in *N* NaCl solution at 25°C. Equal areas (100 cm²) of dissimilar metals.

at 25°C. Equal areas of dissimilar metals (100 cm²) were situated 15 cm apart in these experiments and were short-circuited through zero external resistance. The values of current flow at different times were not highly reproducible in replicate experiments, the degree of scatter between the current/time curves being shown for the Al-steel couple in Fig. 2 and for the Zn-steel couple in Fig. 3. During these experiments the pH of the solution increased from about 5.2 to 7.2 and the conductivity remained unchanged.

Similar experiments were carried out in which the distance of separation of the electrodes was held constant at 15 cm but in which the electrode areas were varied between 2 and 100 cm². Effect of cathode area on the weight losses of the Zn and Al anodes and on the total number of coulombs flowing in 96 hr is shown in Fig. 4. The effect of anodic area on anodic weight loss is shown in Fig. 5 and 6. These figures also contain the weight loss figures for the experiments with equal areas of Al, Zn, and steel. The experiments in which the area of the Al anode was varied (Fig. 5) gave less reproducible results than those in which the area of the steel cathode was varied.

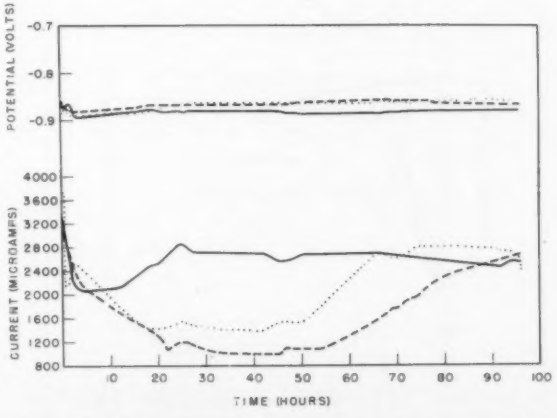

Fig. 3. Triplicate curves relating current flow and potential to time for the Zn-mild steel couple in *N* NaCl solution at 25°C. Equal areas (100 cm²) of dissimilar metals.

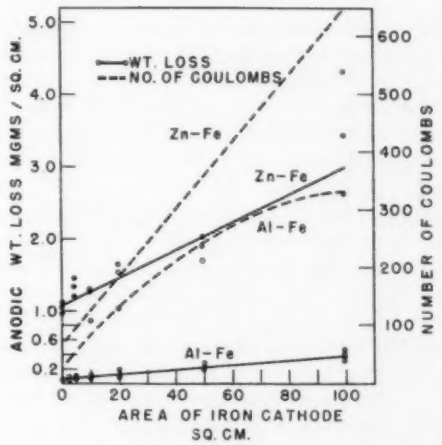

Fig. 4. Effect of area of mild steel cathode on the weight loss of Al and Zn anodes (of area 100 cm²) and on the number of coulombs flowing in the Al-mild steel and Zn-mild steel couples over a 96-hr period in 1*N* NaCl solution at 25°C.

In all experiments described in this paper the steel specimens were strongly cathodic to either Al or Zn and were, within the limits of experimental error, i.e., <0.01 mg/cm² completely protected against corrosion by coupling to either of these anodes. The weight losses of the Zn and Al specimens were, of course, markedly increased by coupling to the mild steel cathodes. In static solutions both the Al and Zn anodes were galvanically corroded in a uniform manner. From calculation of the number of coulombs flowing, it was apparent that the weight losses of the anodes were appreciably in excess of those calculated from the current flow data, particularly in the case of Zn. These additional losses in weight will be referred to as the "weight losses due to local action". Since the current was only measured on an intermittent basis, the estimation of the number of coulombs flowing is

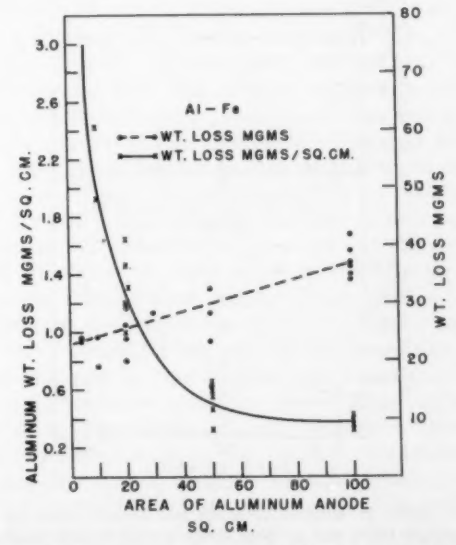

Fig. 5. Effect of area of Al anode on the total corrosion and on the intensity of corrosion of Al coupled to mild steel (100 cm² mild steel) over a 96-hr period in *N* NaCl at 25°C.

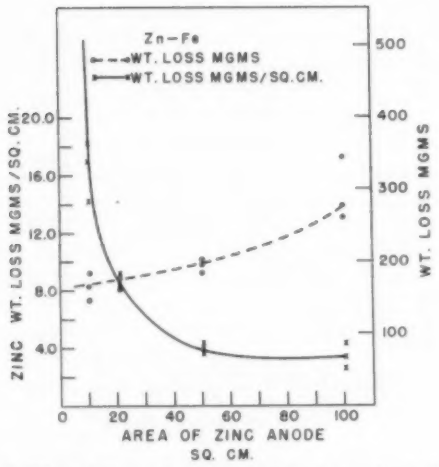

Fig. 6. Effect of Zn anode area on the total corrosion and on the intensity of corrosion of Zn coupled to mild steel (100 cm² mild steel) over a 96-hr period in *N* NaCl at 25°C.

less accurate than the measurements of weight loss. Consequently, the accuracy of the weight losses due to local action, which were calculated by difference, is not high, particularly for Al anodes where the total weight loss is relatively low. The variation in local action weight losses of Zn and Al with dissimilar metal electrode area is shown in Fig. 7.

Distance of separation of the electrodes.—Experiments were next carried out to determine the effect, if any, of distance of separation of the electrodes on the rate of galvanic corrosion of the Al-steel couple. In these experiments, weight losses alone were determined. The results (Fig. 8) show that the weight loss on Al anodes in experiments of 96 hr duration decreased somewhat as the electrodes approached each other closely. It must also be realized that, as the distance of separation decreased, the total volume of solution also became smaller. However, when the electrodes were 15 cm apart, the effect of small variations in distance of separation was insignificant.

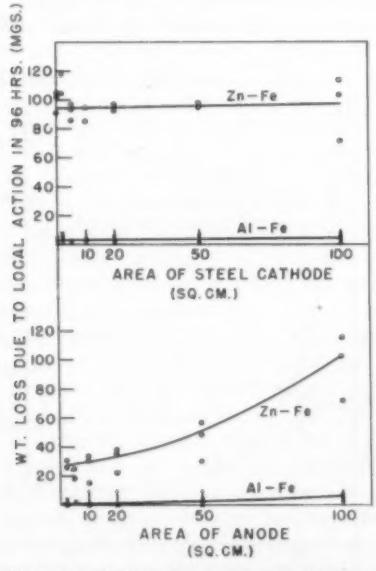

Fig. 7. Effect of variation of anode and cathode areas on the anodic weight losses due to local action in the Al-mild steel and Zn-mild steel couples in *N* NaCl solution at 25°C. When anodic area is variable the cathode area is constant at 100 cm²; when cathode area is variable the anodic area is constant at 100 cm².

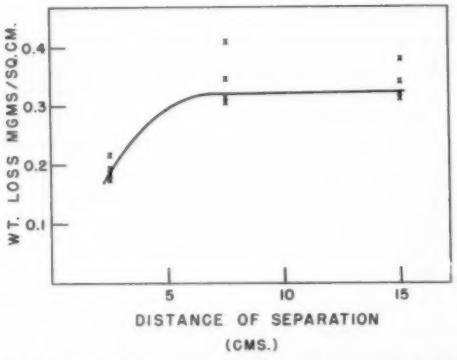

Fig. 8. Effect of distance of separation of Al and mild steel electrodes on the weight loss of Al anodes in *N* NaCl at 25°C. Equal areas (100 cm²) of dissimilar metals.

Polarization measurements.—Anodic and cathodic polarization curves were determined for both galvanic couples in the manner described above.

Variation of anodic and cathodic polarization curves as a function of cathode area was determined for both galvanic couples by employing a 15 cm electrode separation after a fixed time of 24 hr. Results are contained in Fig. 9 and 10 and may be used to assist in explaining the weight loss results shown in Fig. 4. Variation of the anode area had no significant effect on polarization curves determined in a similar manner.

Effects of stirring.—Experiments were carried out in which dissimilar metal electrodes having equal areas (20 cm²) were clamped 5 cm apart by means of a Lucite holder in a 400 ml beaker. A constant volume (320 ml) of normal NaCl at 25°C was used in these tests. The solution in the beaker was stirred by a variable speed stirrer located centrally in a

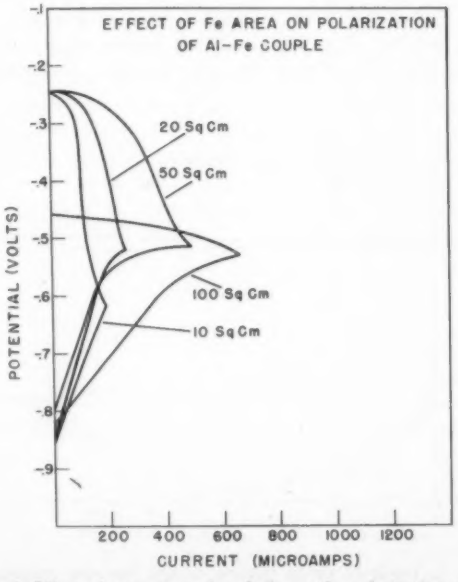

Fig. 9. Effect of area of steel cathode on the polarization curves for the Al-mild steel couple in *N* NaCl at 25°C using 100 cm² of Al.

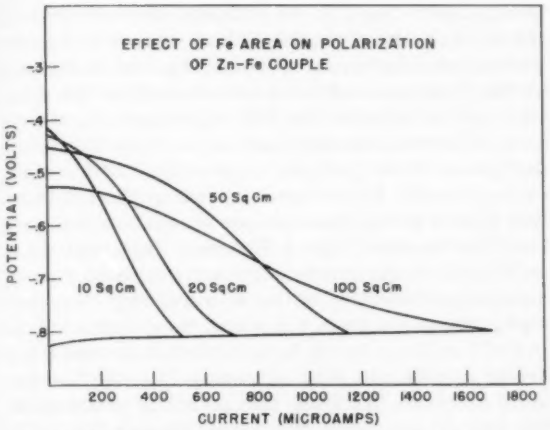

Fig. 10. Effect of area of steel cathode on the polarization curves for the Zn-mild steel couple in *N* NaCl at 25°C using 100 cm² of Zn.

fixed position between the electrodes. Experiments on the effects of stirring were carried out for a period of 24 hr on account of the greatly increased rate of galvanic corrosion. Weight loss, current flow, and potential measurements were made as described previously. The effect of stirring on weight loss and current flow in the Al-steel couple is shown in Fig. 11. In unstirred solutions, the Zn-steel couple delivered a higher galvanic current than the Al-steel couple. At 150 ppm both couples delivered the same galvanic current. At 300-500 rpm, the Zn-steel couple gave low and highly erratic current. For instance, at a stirring rate of 500 rpm the total number of coulombs flowing in six experiments on the Zn-steel couple varied between 105 and 202. In view of the highly irreproducible nature of the results on the Zn-steel couple at the higher stirring rates, a representative curve cannot be included in Fig. 11.

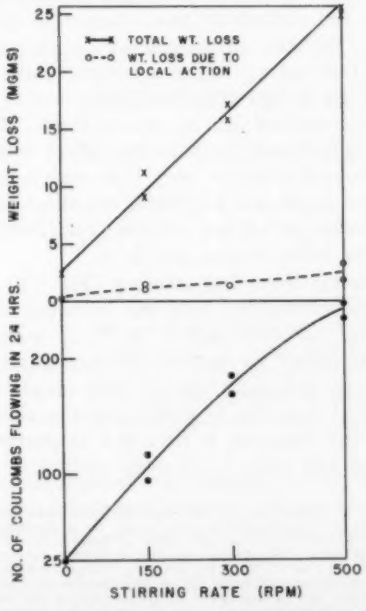

Fig. 11. Effect of stirring rate on the total Al weight loss, Al weight loss due to local action, and number of coulombs flowing (in 24 hr) in the Al-mild steel couple in *N* NaCl at 25°C. Equal areas (20 cm²) of Al and steel.

Discussion

It should be pointed out first that the results described in this paper are concerned primarily with the initial stages of galvanic corrosion. Such factors as the slow formation of protective films over long periods of time, which can markedly affect galvanic current flow, have not been investigated in this work.

The results of this investigation demonstrate that, in normal NaCl under a wide variety of experimental conditions, both Al and Zn are anodic to mild steel and completely protect it against corrosion, at least for periods up to 96 hr. Fig. 2, 3, and 4 demonstrate that the current flow under similar experimental conditions is somewhat greater in the Zn-steel couple than in the Al-steel couple except at rates of stirring in excess of 150 rpm. The current/time curves for both couples are quite erratic (Fig. 2 and 3) and show no evidence of settling down to really steady values. Whereas the potential of the Zn-steel couple is quite uniform at around −0.88 v (Fig. 3), irrespective of variations in current flow, the potential of the Al-steel couple shows much more variation (Fig. 2).

Fig. 10 shows that the galvanic corrosion of the Zn-steel couple is under cathodic control and that increasing currents may be drawn from a Zn anode with practically no change in potential. Indeed, as pointed out previously, the potential taken up by the Zn in NaCl solution containing dissolved air appears to be approximately the Nernst potential corrected for Zn ion activity. Consequently, variations in current flow must be tolerated without greatly altering the potential of the couple. From the form of the cathodic polarization curves for the Zn-steel couple (Fig. 10), it appears that the variations in current flow are due to the relative rates of consumption and replacement of dissolved oxygen at the cathode/solution interface.

Polarization curves for the Al-steel couple (Fig. 9) at first sight indicate that corrosion should be under mixed control. Furthermore, comparison with Fig. 1 shows that, as the Al is corroded galvanically, its open-circuit potential shifts substantially in the more anodic direction. Consequently, although the potential/time curves (Fig. 1) would indicate an open-circuit potential difference of around 150 mv for the Al-steel couple (and around 330 mv for the Zn-steel couple), Fig. 9 shows that, on coupling to 100 cm² of steel, there is actually an open-circuit potential difference of around 370 mv for the Al-mild steel couple. This is somewhat greater than that for the Zn-steel couple under similar conditions (Fig. 10). Since the potential of Al in NaCl is so far displaced from the Nernst potential (16), probably due to the formation of protective oxide films, factors increasing its corrosion rate and assisting in the breakdown of these protective films will displace its potential in the less noble direction. Evidently for metals such as Al, which behave in a highly irreversible manner, differences in corrosion or solution potential are a very unreliable guide to the true magnitude of open-circuit emf of galvanic corrosion. However, the magnitude of the galvanic

corrosion current will be controlled usually by the polarization characteristics of the electrode reactions.

Fig. 9 also shows that the anodic polarization curve for Al is not flat as is that for Zn. Therefore, changes in oxygen concentration due to relative rates of consumption and replacement of oxygen at the steel cathode will affect not only the current flow but also the potential of the Al-steel couple. That the more rapid decreases in current usually coincide with corresponding shifts in potential in the less noble direction (Fig. 2) supports the contention that the corrosion rate of the Al-steel couple is also controlled by oxygen depolarization. This is subsequently confirmed by the stirring experiments in Fig. 11.

In local-cell corrosion it is quite difficult to check the validity of polarization curves due to the experimental difficulty of separating anodic and cathodic areas. However, in studies of galvanic corrosion this difficulty does not exist to the same extent. Consequently, experiments with different relative areas of Al, Zn, and steel were carried out as described. Polarization curves for the Zn-steel couple (Fig. 10) indicate that the galvanic corrosion is under cathodic control. Therefore, the current flow and weight loss of the Zn should be proportional to the area of the steel cathode and should be less dependent on the area of the Zn anode. Experiments with partial areas of steel and Zn (Fig. 4 and 6) demonstrate that this is so, thereby affording a direct confirmation of the "Catchment Principle" (17). Furthermore it is evident that, since the weight loss of a Zn anode is only slightly affected by decreasing its area, the intensity of corrosion on the Zn must markedly increase with decreasing area (Fig. 6).

The polarization curves for the Al-steel couple with equal electrode areas are characterized by steeply sloping anodic polarization curves and relatively flat cathodic polarization curves (Fig. 9). Despite this, experiment shows that, as in the case of the Zn-steel couple, current flow and weight losses of the Al are almost directly proportional to the area of the steel cathode (Fig. 4) and are less dependent on the area of the Al anode, even though the results with variable areas of Al show much scatter (Fig. 5). Actually, these results and the polarization curves are not as mutually inconsistent as appears at first sight. Examination of the cathodic polarization curves for steel (Fig. 9) shows that the cathodic reaction (the reduction of dissolved oxygen) becomes diffusion controlled[3] at a current density of around 10-12 μamp/cm^2 under these experimental conditions. Whereas in the Zn-steel couple some gaseous H_2 can probably be evolved from the steel cathode, it is probable that when a steel cathode is coupled to Al in a NaCl solution containing dissolved oxygen, its potential cannot be depressed far enough to evolve significant quantities of H_2.[3] Consequently, the cathodic reaction in the Al-steel couple should be dependent primarily on oxygen depolarization. Thus, if the cathodic area is reduced, the current density at the cathode can only achieve a certain maximum value which depends on the rate at which oxygen diffuses from the bulk of the solution to the cathode. Further reductions in cathode area, therefore, should result in a proportional reduction in both galvanic current flow and weight loss of the Al. This effect is shown in the polarization curves in Fig. 9 and by the weight loss and current flow results in Fig. 4. However, the relative insensitivity of the current flow and corrosion rate to variations in the area of the Al is less easy to understand. It appears from Fig. 9 that the potential of Al in NaCl solution has to be ennobled to around 0.5 v before Al ions will migrate rapidly through the oxide film on the Al. Once this potential is achieved, the rate of migration of Al ions through the oxide film may be varied widely with little change in potential. This assists in explaining the very small effect of Al anode area on galvanic corrosion of the Al-steel couple.

The experiments in which the distance of separation of Al and steel electrodes was varied (Fig. 8) demonstrated that the rate of galvanic corrosion decreased as the electrodes approached each other more closely. Since the over-all volume of solution decreases as the distance of separation decreases, these experimental conditions favor the development of higher bulk pH values in the solution and, consequently, an increased absorption of CO_2 from the atmosphere. Separate experiments to be reported later have shown that, as with Zn (10), increasing concentrations of sodium bicarbonate progressively ennoble the potential of Al and thus decrease the open-circuit emf of the Al-steel couple. Alternatively, the change in geometry of the cell with decreasing distance of electrode separation certainly tends to reduce diffusion of dissolved oxygen from the surface of the solution to the lower portions of the steel cathode. This should reduce the area of steel acting as an effective cathode and, consequently, should proportionately reduce current flow and the weight loss on the Al anode. However, it should be pointed out that this effect is probably confined to solutions of very low resistance since, with higher resistance solutions, the effect of reducing the resistance of the solution path would tend to mask the effect shown in Fig. 8.

Experiments involving stirring (Fig. 11) further support the contention that the galvanic corrosion rate of the Al-steel couple in NaCl solutions is largely controlled by oxygen depolarization at the steel cathode. Although the Zn-steel couple delivers more current than the Al-steel couple in static NaCl solutions, the situation is reversed at stirring rates of 300 and 500 rpm. Very deep pitting of the Zn

[3] The cathodic reaction is said to be diffusion controlled with respect to oxygen when the rate-controlling step is the rate at which oxygen diffuses from the bulk of the solution to the solution-cathode interface.

[3] This view is supported by the fact that the potential of steel coupled to Al is not depressed far enough to cathodically reduce the air-formed oxide film on the iron cathode (18). Thus, with small areas of steel cathode the air-formed oxide film is probably reinforced due to contact with an alkaline, oxygen-containing solution. Consequently, as shown in Fig. 9, the open-circuit potential of the steel cathode can be markedly ennobled during galvanic corrosion due to a reduction in the ratio of film-free to oxide film-covered areas. However, during galvanic corrosion of the Zn-steel couple, the potential of the steel is shifted far enough in the active direction to reduce the air-formed oxide film on the steel cathodically. Therefore, as marked a shift in the open-circuit potential of the steel cathode in the noble direction is not observed (Fig. 10) since the cathode is free from oxide during the experiments.

anodes is observed at these stirring rates accompanied by low and erratic currents and high weight losses due to local action. On the other hand, the Al is uniformly attacked even at stirring rates of 500 rpm and weight loss due to local action increases only slightly over that in static solutions (Fig. 11). The potentials of both couples become ennobled with increasing stirring rate, but the shift in potential of the Al-steel couple is only about half of that of the Zn-steel couple (100 mv) under similar conditions. This suggests that the anodic polarization curve of Al is flatter than that of Zn within the current density range of 10-100 μamp/cm^2 as has been suggested previously.

Fig. 7 shows the weight losses (in 96 hr) due to local action on Zn and Al anodes of different areas coupled to various areas of mild steel. It may be seen that the local action weight loss on Zn is always very much greater than that on Al. This is probably due to the relative shapes of the anodic polarization curves of Al and Zn (Fig. 9 and 10). These indicate that the local cathodes on an Al anode should be suppressed more effectively by a relatively large shift in potential of around 300 mv in the noble direction during galvanic corrosion (Fig. 9) as compared with a shift of only around 20 mv (Fig. 10) in the case of Zn. Furthermore, this effect would be heightened by the fact, pointed out previously (20), that the cathodes on Al in NaCl solution containing oxygen are very small and comprise only about 5% of the total specimen area.

Acknowledgment

The authors wish to thank Dr. H. G. Oswin for his helpful comments and for his criticism of the paper.

Manuscript received May 3, 1956. This paper was prepared for delivery before the Pittsburgh Meeting, Oct. 9-13, 1955.

Any discussion of this paper will appear in a Discussion Section to be published in the December 1957 JOURNAL.

REFERENCES

1. R. M. Burns and A. E. Schuh "Protective Coatings for Metals," Reinhold Publishing Corp., New York (1939).
2. U. R. Evans, *J. Soc. Chem. Ind.*, **47**, 73T (1928).
3. G. D. Bengough and O. F. Hudson, *J. Inst. Metals*, **21**, 37 (1919).
4. J. D. Edwards and C. S. Taylor, *Trans. Electrochem. Soc.*, **56**, 27 (1929).
5. F. Fancutt and J. C. Hudson, *J. Oil & Colour Chemists Assoc.*, **35**, 396 (1952).
6. S. G. Clarke and W. N. Bradshaw, *J. Appl. Chem.*, London, **3**, 147 (1953).
7. M. L. Hughes and D. P. Moses, *Metallurgia*, p. 105, Sept. 1953.
8. G. Schikorr, *Trans. Electrochem. Soc.*, **76**, 247 (1939).
9. L. Kenworthy and M. D. Smith, *J. Inst. Metals*, **70**, 463 (1944).
10. R. B. Hoxeng and C. F. Prutton, *Corrosion*, **5**, 330 (1949).
11. M. R. Whitmore and J. Teres, *Ind. Eng. Chem.*, **31**, 608 (1939).
12. G. W. Akimov, S. A. Wruzewitsch, and G. B. Clark, *Korrosion u. Metallschutz*, **11**, 145 (1935).
13. W. G. Whitman and R. P. Russell, *Ind. Eng. Chem.*, **16**, 276 (1924).
14. H. H. Uhlig, Editor, "Corrosion Handbook," p. 1082, John Wiley & Sons, Inc., New York (1948).
15. M. J. Pryor, *This Journal*, **102**, 694 (1955).
16. W. M. Latimer, "Oxidation Potentials," p. 155, Prentice Hall, New York (1938).
17. U. R. Evans, "Metallic Corrosion, Passivity and Protection," p. 513, Edward Arnold and Co., London (1938).
18. M. J. Pryor and U. R. Evans, *J. Chem. Soc.*, **1950**, 1259.
19. G. V. Akimov, *Corrosion*, **11**, 515, (1955).
20. M. J. Pryor and D. S. Keir, *This Journal*, **102**, 605, (1955).

Inclusion of Fuchsin in Bright Nickel Deposits

Kedzie Chemical Laboratory, Michigan State University, East Lansing, Michigan

J. L. Dye and O. J. Klingenmaier

ABSTRACT

Fuchsin, a brightener used in nickel plating, was recovered from nickel deposits by dissolving the deposits in HCl. The amount of fuchsin recovered per gram of Ni was roughly linear in fuchsin concentration and decreased with increasing current density. Some pertinent properties of fuchsin were studied. The amount of fuchsin included and its brightening effect are correlated with a model which assumes preferential adsorption at grain corners and edges.

This investigation was carried out to determine whether an organic brightener of the second class (1) is included in Ni deposits without complete decomposition. When this was found to be the case, a study was made of the effect of brighter concentration and current density on the amount included in the deposit.

During plating, a gradual decrease occurs in the concentration of the brightening agent or agents. While decomposition products undoubtedly account for some of this loss, it seems reasonable to assume that some of the brightening agent or its decomposition products are included in the deposit.

The presence of carbonaceous matter in electrodeposited metals of the iron group has been reported by a number of investigators, and recently, Brenner and co-workers (2), found the carbon and sulfur contents of electrodeposited bright Ni to

range from 0.02 to 0.08%. A search of the literature failed to disclose any successful investigations of the identity of these inclusions.

A common brightener of the second class used in Ni plating is the organic dye, fuchsin, also known as rosaniline hydrochloride. Its molecular formula is: $C_{20}H_{20}N_3Cl$.

Fuchsin was chosen for study primarily because its intense color permitted the spectrophotometric determination of as little as 50 μg/l. A sensitive method of analysis was necessary in this investigation since the brightening agent is used in amounts as low as 1 mg/l. Accordingly, it was felt that only a small amount would be included in the Ni deposit. One of the drawbacks involved in the choice of fuchsin for study is that some decomposition could be expected because of its complex nature.

Experimental

The nickel stock solution used in the experimental work was a typical Watts-type bath of the following composition: $NiSO_4 \cdot 7H_2O$, 240 g/l; $NiCl_2 \cdot 6H_2O$, 45 g/l; boric acid, 30 g/l. The solution was purified by the method of Ewing (3). Bright baths were made by adding to the above solution (4): sodium naphthalene disulfonate, 4.5 g/l; sodium lauryl sulfonate, 0.1 g/l; fuchsin, 0.5-3.0 mg/l.

The fuchsin[1] was purified by two recrystallizations from water. The other chemicals used were analytical reagent grade and were used without further purification except that mentioned above.

Brass sheet stock 0.020 in. thick was electrocleaned and plated with dull Ni in the usual fashion. The surface was then buffed and passivated electrolytically. To accomplish this, the panel was alternately electrocleaned (anodically) and dipped in HCl 4 or 5 times. Plating was carried out in a one liter electrolysis jar at 55° ± 1°C. Agitation of the solution was provided by a low-pitch, glass stirring rod, rotating at 200 rpm. Anode bags were not used for these depositions because of the great tendency for fuchsin to adsorb on cloth. A current density of 0.02 amp/cm^2 was used, and all deposits were mirror bright. Fuchsin reduced with Ni and HCl was used in the first experiments. Because of the difficulty of preparing standard solutions of reduced fuchsin, as described later, plating was done with nonreduced fuchsin. The appearance of the deposits was identical to that obtained with reduced fuchsin.

A number of bright Ni deposits were also prepared from separate 250 ml amounts of bright Ni solution in a Hull cell (5). The deposits were then cut and combined to give five current density ranges for study.

In the course of this research, it was necessary to determine fuchsin quantitatively, both in the plating baths, and in the solutions obtained by dissolving the deposits. The procedure adopted was as follows: a 25 ml sample of the solution was heated with 1 g of nickel formate to 90°-95°C. The solution was cooled and transferred to a 125 ml separatory funnel. Successive small portions of methyl ethyl ketone were shaken with the solution to extract the dye. Whenever the fuchsin concentration was less than 2.5 mg/l, a total of 25 ml of extractant was used; otherwise, 50 ml was necessary. The absorbancy of the methyl ethyl ketone extraction at a wave length of 548 mμ (corresponding to the maximum absorbance) was determined with a Beckman Model DU Spectrophotometer using 1 cm cells. When working with solutions obtained by dissolving the deposits or with reduced fuchsin solutions, the absorbancy increased somewhat over a period of a few hours to a constant value.

Several methods of dissolving deposits containing fuchsin were attempted, including anodic dissolution, and the use of Classen's reagent (6). The only method which led to recovery of fuchsin was dissolution of the deposits in HCl solution. Ni foil, weighing about 1.2 g, was cut into small pieces and dissolved in 15 ml of 36% HCl. The process required 2-3 weeks at room temperatures, but only 4 hr at 70°-80°C. Both methods were used with about the same degree of success. The pH value of the solution was raised to the range of 2 to 3 with sodium carbonate, followed by the treatment with nickel formate as described previously.

Polarographic studies were made with a Sargent Model XXI Polarograph and infrared studies with a Perkin-Elmer Model 21 Recording Spectrophotometer.

Results

While fuchsin has many advantages in a study of this type, its principal disadvantage is the tendency to undergo complex reactions. Some of the reactions involving fuchsin are illustrated in Fig. 1*a* and 1*b*.

The reactions of fuchsin important in plating are its electrolytic reduction and oxidation. One liter of a solution containing 2.0 mg fuchsin and 10 g H_3BO_3, pH 3.2, was electrolyzed between graphite electrodes at a current of 0.1 amp for about 4 hr. Periodic sampling showed that the fuchsin content decreased roughly linearly with time at a rate of 0.4 millimoles/Faraday of electricity. A repeat experiment with a porous cup to separate the anode and cathode compartments showed that the loss of color was oc-

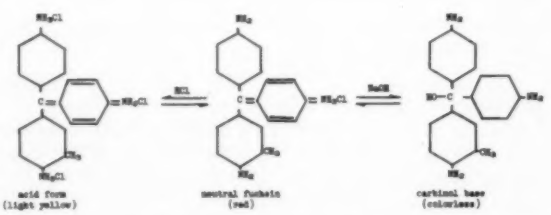

Fig. 1*a*. Acid-base behavior of fuchsin

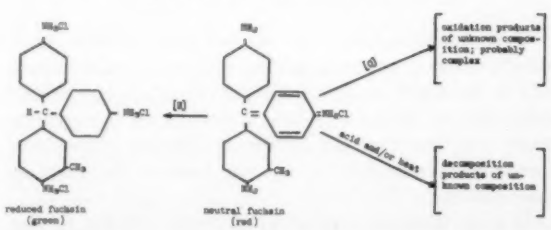

Fig. 1*b*. Oxidation-reduction and decomposition behavior of fuchsin

[1] A certified biological stain distributed by Eastman Kodak Co.

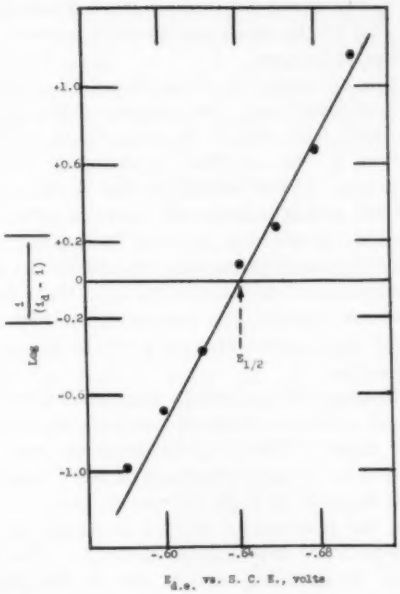

Fig. 2. Determination of the number of electrons involved in the primary reduction step for fuchsin from polarographic data.

curring in the anode compartment. This could not be made quantitative because of the strong adsorption of the dye into the porous cup. Attempts were made to analyze the oxidation products without success. The oxidation products appeared to be a complex mixture rather than a single pure substance.

Because reduced fuchsin is recommended as a brightening agent for Ni, the first deposits were made from a bath containing the reduced dye. This was made by heating fuchsin with Ni and HCl. This invariably resulted in the loss of 20-40% of the fuchsin. Since plates of excellent quality could be obtained with nonreduced fuchsin, use of the reduced material was abandoned.

Some polarographic studies of fuchsin were made to gain further insight into its electrolytic properties. It was found that excellent reduction waves could be obtained at the dropping mercury electrode. Fig. 2 shows a graph of $\log \frac{i}{i_d - i}$ vs. the dropping electrode potential relative to the saturated calomel electrode. The least-squares slope gives a value of 1.06 for n, the number of electrons involved in the reduction. While quantitative polarographic studies of the reduction were made at only two concentrations, it appears that the initial step in the reduction is the formation of a free radical. A corresponding oxidation wave could not be found with reduced fuchsin solutions. A rather poorly defined oxidation wave was obtained with fuchsin solutions at +0.28 v vs. the saturated calomel electrode when a rotating Pt electrode was used.

Fuchsin was recovered from the deposits by dissolving the deposits in HCl. A study was made of the effect of acid strength, temperature, and time of heating, on the decomposition of fuchsin. Thirty-one runs were made under various conditions. Results are given in Table I. They may be summarized by stating that high temperatures, high acid strengths, and long times of standing or heating resulted in the loss of fuchsin.

The absorption spectrum of solutions of fuchsin in water and in methyl ethyl ketone were determined at a number of concentrations. The molar extinction coefficients were found to be 65,000 in water at 545 mμ, and 91,000 in methyl ethyl ketone at 548 mμ. These wave lengths correspond to the absorption maxima in the two solvents.

Beer's Law was obeyed in both solvents within the experimental error. These calibration curves were used to evaluate the concentrations of the unknown samples.

A total of 19 depositions from solutions containing fuchsin were made, and both the fuchsin recovered from the plate and the fuchsin remaining in the bath were determined spectrophotometrically. Results are represented graphically in Fig. 3.

The effect of current density on the amount of fuchsin included in the Ni deposits was determined with a Hull cell (5). The 250 ml portions of bright Ni solution used in these experiments each contained 470 μg of fuchsin so that the concentration was 1880 μg/liter. Ni deposits were excellent in appearance. Table II gives results obtained in analyses of fuchsin from deposits covering five ranges of current density. There is a notable decrease in the

Table I. Recovery of fuchsin from HCl solutions subjected to different conditions of time and temperature

Fuchsin content (μg)	Amount of conc. acid (ml)	Temp, (°C)	Time (hr)	% Recovered
80	3*	95	0.1	94
40	5*	95	0.1	87
40	3*	70–90	0.1	94
40	3*	70–90	0.1	94
40	3*	70–90	0.5	77
40	3*	70–90	1.0	63
40	3*	25	0.2	100
40	5	25	0.2	100
40	15	90–95	4	58
40	15	90–95	4	58
41	15	60–70	4	64
41	15	60–70	4	65
42	15	50–55	1	64
42	15	50–55	2	66
42	15	50–55	3	58
42	15	50–55	4	60
84	15	50–55	6	72
40	5	25	24	86
40	10	25	24	84
40	15	25	24	84
40	10	25	72	60
40	15	25	168	57
40†	15	80–85	1	72
40†	15	80–85	4	46
40†	15	70–80	4	64
40†	15	60–70	4	60
40†	15	50–55	4	63
40†	15	50–55	4	60
40†	15	25	48	58
40†	15	25	168	58
40†	15	25	168	66

* Plus 25 ml of water.
† 1.2 g of pure Ni foil added to the acid solution.

Table II. Distribution of fuchsin in Hull cell deposits

Current density (amp/ft²)	Amount of Ni dissolved (g)	Fuchsin recovered (μg)	
		Per deposit	Per g of Ni
0–15	0.125	14	112
15–40	0.405	26	62
40–80	0.576	30	52
80–120	0.334	8	24
>120	0.409	12	29
	1.849*	90†	

* Total Ni deposited was 1.995 g.
† This value was 28% of the total decrease of fuchsin in the plating solutions.

amount of fuchsin recovered per gram of Ni as the current density is increased.

Conclusions

Even though conditions other than concentration were made as identical as possible during the various depositions, a considerable scatter of points resulted. This may be due to at least two important factors.

1. Unequal solution agitation at the electrode surface would certainly have a pronounced effect on the amount of fuchsin included in the deposit. It would be expected that too vigorous stirring would increase the amount of fuchsin destroyed by oxidation as well as the amount included in the plate. The data seem to indicate that this effect is operating.

2. Fuchsin is slowly destroyed in HCl solution, and by heat, as is shown in Table I. Lack of reproducibility of the results could well be due to this loss of fuchsin.

In spite of the difficulties encountered in obtaining quantitative data, several conclusions can be drawn from this study.

1. Fuchsin, when used as a brightener of the second class in Ni plating, is included in the deposits without being completely destroyed. About 30% of the total decrease of fuchsin in the plating bath could be recovered from the deposit. Probably much of the rest of the decrease resulted from the anodic oxidation of fuchsin.

2. The amount of fuchsin recovered from the deposits increased with the concentration of fuchsin in the bath from about 18 μg/g Ni at a bath concentration of 500 μg/liter, to about 90 μg/g Ni at 2500 μg/liter. These values are low because of losses of fuchsin, and it is believed that the values should be revised upward by 30-40% to obtain a better value of the fuchsin content in the Ni. Even if all of the decrease of fuchsin in the bath were due to its codeposition with Ni, the concentration of fuchsin in Ni could not exceed 500 μg/g Ni in this range of concentration.

3. The amount of fuchsin recovered from the deposits per gram of Ni decreases with an increase in current density. This is to be expected on a macro scale because of local depletion of the organic molecules at regions of high current density.

Since the percentage of fuchsin found in the deposits was very low (about 0.01%), it is possible that the brightening action occurs because of a preferential adsorption of fuchsin at points of high current density, such as grain corners and edges. Deposition of Ni would then be interrupted at these points and accentuated at low current density areas. Such action would tend to smooth out the deposit and produce randomly oriented small grains leading to a bright plate. To check the plausibility of this argument, the ratio of fuchsin molecules to Ni grains was calculated.

The amount of fuchsin recovered from 1 g Ni, plated from a bath containing 1800 μg of fuchsin/liter, was used as the basis for the calculation. Reference to Fig. 3 indicates that 65 μg fuchsin was recovered per gram of Ni. Assuming 35% loss of fuchsin in the process of solution of the deposit, a value of 100 μg, or 3×10^{-7} gram-moles of fuchsin/g Ni was chosen. This figure corresponds to 1.8×10^{17} molecules/g Ni. Using a density of 8.9 g/cc for Ni and the information that the grain size of bright Ni deposits is less than 10^{-4} mm (7), the number of fuchsin molecules per grain of Ni would vary from 1600 at a grain size of 10^{-4} mm to 1.6 at a grain size of 10^{-5} mm. Table III shows that, depending on the grain size produced, it would be possible for the included fuchsin molecules to cover the edges of each grain, or merely the corners.

Attachment of organic molecules at the grain corners and edges during deposition could restrict grain growth. A higher fuchsin concentration in the

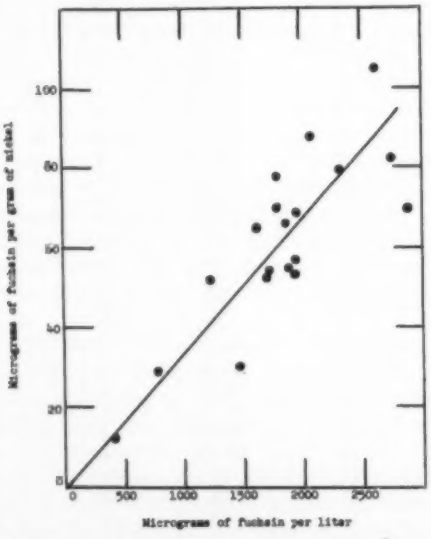

Fig. 3. Effect of fuchsin concentration in the bath on the amount recovered from Ni deposits.

Table III. Distribution of 100 μg of fuchsin in 1 g Ni

Grain size (mm)	Fuchsin molecules per grain	Length of grain edge per fuchsin molecule (A)
1×10^{-4}	1600	1.9
5×10^{-5}	200	7.5
4×10^{-5}	100	12.0
3×10^{-5}	43	21.0
2×10^{-5}	13	47.0
1×10^{-5}	1.6	—
9×10^{-6}	1.2	—
8×10^{-6}	0.8	—

solution would then increase this effect by making a larger number of molecules available at the surface. The concentration of brightener could thus play an important role in determining the grain size, with more brightener producing smaller grains, but at the same time more brittle deposits.

Acknowledgments

The authors wish to acknowledge the helpful advice of Dr. A. Timnick, who aided in the polarographic studies reported in this paper. Credit is also due to Mr. P. O. Sawyer for his discussions of the mechanism of plating with one of the authors.

Manuscript received August 6, 1956. This paper was prepared for delivery before the Cleveland Meeting, Sept. 30 to Oct. 4, 1956, and work on it was performed by O. J. Klingenmaier in partial fulfillment of the requirements for the M. Sc. degree from Michigan State University.

Any discussion of this paper will appear in a Discussion Section to be published in the December 1957 JOURNAL.

REFERENCES

1. A. G. Gray, Editor, "Modern Electroplating," Chap. 13 on Nickel by W. L. Pinner, G. Soderberg, and W. A. Wesley, pp. 311-317, John Wiley & Sons, Inc., New York (1953).
2. A. Brenner, V. Zentner, and C. W. Jennings, *Plating*, **39**, 865 (1952).
3. D. T. Ewing, R. J. Rominski, and W. M. King, *ibid.*, **36**, 1137 (1949).
4. R. Lind, W. J. Harshaw, and K. E. Long (to Harshaw Chemical Co.) U. S. Pat. 2,198,267, April 23, 1940.
5. R. O. Hull, *Monthly Rev. Am. Electroplaters' Soc.*, **26**, 753 (1939).
6. P. K. Froelich, *Trans. Electrochem. Soc.*, **46**, 87 (1924).
7. W. L. Pinner, G. Soderberg, and E. M. Baker, *ibid.*, **80**, 539 (1941).

Throwing Index

A New Graphical Method for Expressing Results of Throwing-Power Measurements

Robert V. Jelinek and Hero F. David[1]

Department of Chemical and Metallurgical Engineering, Syracuse University, Syracuse, New York

ABSTRACT

A new direct method is proposed for expressing the results of throwing-power measurements made on plating solutions in a conventional rectangular throwing-power box with plane parallel electrodes. The metal distribution ratio (M) is plotted vs. the linear ratio (P) on arithmetic coordinates. The reciprocal of the slope of this plot is called "Throwing Index" and represents a direct measure of bath throwing-power. Experimental data on several solutions are presented and advantages of this method are discussed.

Of prime importance in establishing the practical value of a commercial electroplating solution is "throwing-power," the capacity for producing uniform coatings on both accessible and inaccessible cathode areas. This paper presents a new graphical method for analyzing directly the results of throwing-power measurements in terms of "Throwing Index".

Haring and Blum (1) introduced the rectangular cell with plane parallel electrodes as a device for measuring throwing-power. They proposed the definition,

$$\text{Throwing power} = (P - M)/P \qquad \text{(I)}$$

where P = linear (or primary) ratio and M = metal distribution ratio between the two equi-potential plane parallel cathodes placed at different distances from the anode.

Two modified equations are (2-4):

$$\text{Throwing Efficiency} = (P - M)/(P - 1) \qquad \text{(II)}$$

$$\text{Throwing power (BSI)} = (P - M)/(P + M - 2) \qquad \text{(III)}$$

[1] Present address: Solvay Process Div., Allied Chemical & Dye Corp., Syracuse, N. Y.

These reduce the effect of P on the numerical results.

Valid objections have been raised to the throwing-power box. Chief among these are that it is an empirical device with an electrode arrangement dissimilar to many actual configurations, that numerical values obtained from it are dependent on cell dimensions, and that results may even be misleading for small differences in throwing-power. However, the fact remains that it is a simple and useful test apparatus which permits direct and rapid comparison of different plating solutions or operating conditions with sufficient precision for most practical purposes.

Throwing Index

In a recent study of the electrodeposition of alloys (5), the throwing-power of several solutions was compared under varied operating conditions. Measurements were made in a cell of the Haring-Blum type, 1 in. wide x 6 in. long, with 2 in. solution depth.

Table I presents the results of a typical group of runs, showing measured values of M and P, together with throwing-power calculated by means of each of the three equations above. None expresses

Table I. Throwing-Power measurements*

Linear ratio (P)	Metal ratio (M)	Throwing Power [Eq. (I)]	Throwing efficiency [Eq. (II)]	Throwing Power-BSI [Eq. (III)]
Tin-zinc cyanide bath:				
(150°F, 30 amp/ft²)		%	%	%
2.17	1.49	31.4	58.1	41.0
5.40	2.25	58.4	71.5	47.4
9.50	3.05	67.9	76.0	61.1
(75°F, 30 amp/ft²)				
2.02	1.18	41.5	82.4	70.0
3.80	1.25	67.1	91.0	83.5
5.70	1.42	75.0	91.2	83.5
Lead-tin fluoborate bath:				
(80°F, 40 amp/ft²)				
2.30	2.22	3.5	6.2	3.2
4.50	3.84	14.7	18.9	10.4
9.50	7.63	19.7	22.0	12.3
(80°F, 30 amp/ft²)				
2.08	1.95	6.3	12.0	6.4
4.85	3.88	20.0	25.2	14.4
9.50	7.02	26.1	29.2	17.1
Cadmium cyanide bath:				
(80°F, 15 amp/ft²)				
2.11	1.26	40.4	76.5	62.0
4.30	1.70	60.5	78.8	65.0
9.00	2.23	75.1	84.5	73.5
Acid zinc sulfate bath:				
(80°F, 15 amp/ft²)				
1.25	1.25	0	0	0
1.85	1.87	−1.1	−2.4	−1.2
4.76	5.27	−10.7	−13.6	−6.3
6.00	6.94	−15.7	−18.8	−8.6

* Haring-Blum type throwing-power box, 1 in. x 6 in., 2 in. solution depth. Thin polished-steel cathodes.

throwing power satisfactorily in terms of a fairly constant value over a range of linear ratios for one bath at constant plating conditions. Such a value would be useful for expressing variations in throwing-power with changes in current density, temperature, etc.

Accordingly, the simple procedure of plotting metal ratio vs. linear ratio on arithmetic coordinates was tried for a group of runs. The result was a linear relationship for each bath over the full range of the data. Fig. 1 shows such a plot for the data in Table I. Table II identifies the plating baths tested.

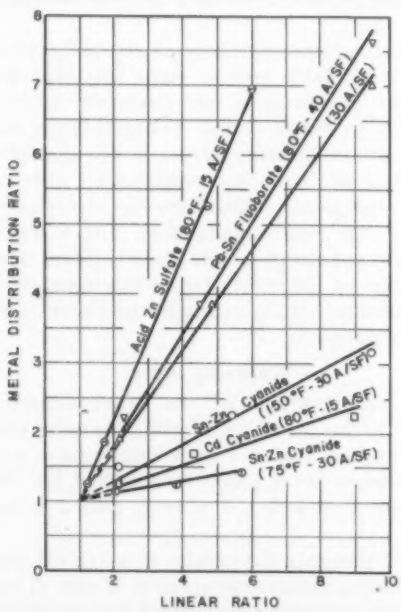
METAL DISTRIBUTION RATIO
LINEAR RATIO
Acid Zn Sulfate (80°F - 15 A/SF)
Pb-Sn Fluoborate (80°F - 40 A/SF)
(30 A/SF)
Sn-Zn Cyanide (150°F - 30 A/SF)
Cd Cyanide (80°F - 15 A/SF)
Sn-Zn Cyanide (75°F - 30 A/SF)

Fig. 1. Throwing Index plot

Table II. Solution composition

Tin-zinc cyanide:	
Sodium stannate	16.0 oz/gal
Zinc cyanide	1.2
Potassium cyanide	2.8
Potassium hydroxide	0.87
Lead-tin fluoborate:	
Lead	11.8 oz/gal
Total tin	0.98
Stannous tin	0.80
Free fluoboric acid	5.4
Free boric acid	3.4
Acid zinc sulfate:	
pH	3.3
Zinc	5.7 oz/gal
Cadmium cyanide:	
Cadmium	2.10 oz/gal
Total cyanide (as NaCN)	1.74
Alkalinity (as NaOH)	0.17

At first it was thought the result might be fortuitous for the particular throwing-box and solutions used in this work. To test the method, data were taken from the papers of Pan (3) and Gardam (6) and plotted in the same way. Pan used a Haring-Blum box measuring 10 x 10 x 60 cm; Gardam's data are from two cells, one 10 x 10 x 60 cm, and the other 2 x 2 x 12 cm. These data are shown in Fig. 2 and 3.

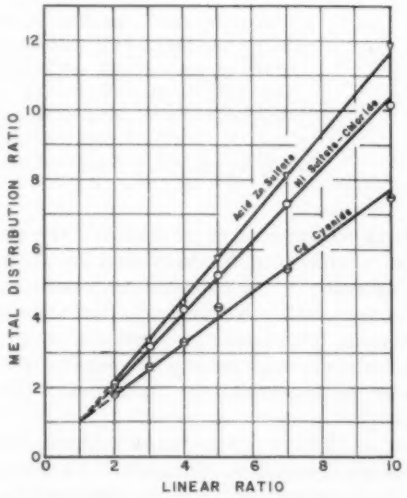

Fig. 2. Throwing Index plot, data of Pan (3)

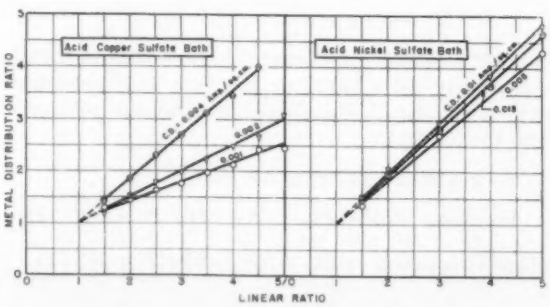

Fig. 3. Throwing Index plots, data of Gardam (6)

Table III. Values of Throwing Index

Bath	Temp (°F)	Current density (amp/ft²)	Throwing Index
Authors' Data:			
Sn-Zn cyanide	75	30	10.0
	150	30	3.68
Pb-Sn fluoborate	80	30	1.38
	80	40	1.24
Cd cyanide	80	15	5.75
Acid Zn sulfate	80	15	1.19
Data of Pan (3):			
Cd cyanide	68	15	1.34
Acid Zn sulfate	77	15	0.83
Ni sulfate-chloride	80	28	0.96
Data of Gardam (6)			
Acid Cu sulfate	75	0.92	2.58
	75	1.85	1.98
	75	3.70	1.18
Acid Ni sulfate	75	4.63	1.19
	75	9.25	1.04
	75	13.9	1.10

The point $M = 1$, $P = 1$ should be common to all of the curves, and so each of the lines on Fig. 1, 2, and 3 was extended to include this point. A solution with ideal throwing characteristics would produce a horizontal line at $M = 1$, and one with poor throwing-power would show a very steep line on this type of plot. Thus it was reasoned that the slope of the line could be used as an indication of throwing-power. In order to have larger values associated with better throwing-power, the reciprocal of the slope was used. The designation "Throwing Index" is suggested for this number, in order to distinguish it from Throwing Power and Throwing Efficiency used in the literature.

Values of Throwing Index obtained from Fig. 1, 2, and 3 are listed in Table III. Fig 4 presents the relation between Throwing Index and current density for two solutions, as shown by Gardam's data (6).

Discussion

There are several advantages associated with the new Throwing Index method:

1. Experimental data from the familiar Haring-Blum cell are used directly and conveniently. No formulas are required, and there is no question as to which equation was used when the results are reported.

2. A single number is obtained, characteristic of a range of linear ratios. This makes it convenient to follow experimentally the effects of temperature, current density, bath concentration, and other plating variables.

3. Throwing Index is obtained from several experimental points, minimizing errors in measurement at any one point. The three formulas in use at present all require individual throwing-power calculations at each point; relatively small errors in one or two points can then produce an anomalous throwing-power curve when the data are graphed.

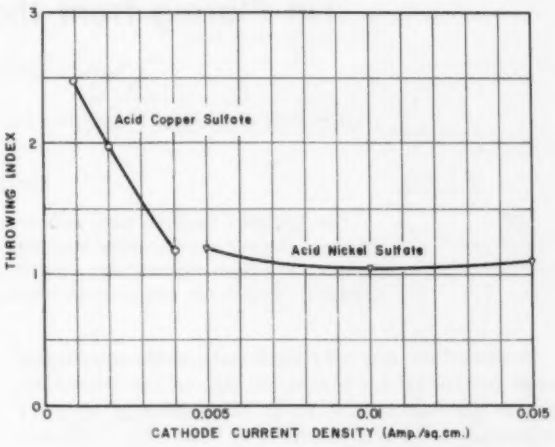

Fig. 4. Throwing Index vs. current density, data of Gardam (6)

The method does not present any new theoretical approach to the throwing-power problem. It is subject to the same limitations that have already been pointed out for the Haring-Blum cell (7-9). Throwing Index is offered principally as a useful empirical tool, convenient for practical electroplating studies, operating specifications, and production control tests.

Acknowledgment

The authors wish to express their appreciation to the Crouse-Hinds Co. for support of this work through a contract with the Syracuse University Research Institute. Thanks are also due to Walter Beck and C. S. Grove, Jr., for their advice and encouragement and to Ardeshir Aidun for analytical assistance.

Manuscript received August 6, 1956. This paper was prepared for delivery before the Cleveland Meeting, Sept. 30 to Oct. 4, 1956.

Any discussion of this paper will appear in a Discussion Section to be published in the December 1957 JOURNAL.

REFERENCES

1. H. E. Haring and W. Blum, *Trans. Electrochem. Soc.*, **44**, 313 (1923).
2. A. H. Heatley, *ibid.*, **44**, 283 (1923).
3. L. C. Pan, *ibid.*, **58**, 423, (1930).
4. S. Field, *J. Electrodep. Tech. Soc.*, **9**, 144 (1934).
5. H. F. David, "Electroplating of Tin-Zinc and Lead-Tin Alloys," M.Ch.E. Thesis, Syracuse University, May 1956.
6. G. E. Gardam, *Trans. Faraday Soc.*, **34**, 698 (1938).
7. T. P. Hoar and J. N. Agar, *Disc. Faraday Soc.*, No. 1, 162 (1947).
8. C. Kasper, *Trans Electrochem. Soc.*, **77**, 353, 365 (1940); **78**, 131 (1940).
9. M. Schlotter and J. Korpiun, *ibid.*, **62**, 129 (1932).

Tin Plating from the Pyrophosphate Bath

J. Vaid and T. L. Rama Char

Department of General Chemistry, Indian Institute of Science, Bangalore, India

ABSTRACT

The complex $Sn_2P_2O_7$ bath was found satisfactory for the electroplating of Sn since it gave good quality deposits over a wide range of experimental conditions. Addition agents like dextrin-gelatin increased the brightness of the deposits. This bath has several advantages over the stannate bath.

Acid sulfate and alkali stannate baths are widely used for industrial plating of Sn. In the literature, use of pyrophosphate baths is mentioned only by Roseleur (1-3) and Marino (4). Recently, Safranek and Faust (5) used the $Sn_2P_2O_7$-copper cyanide bath for deposition of Sn-Cu alloys.

The principal advantages of using pyrophosphate solutions for electroplating relate to high solubility, nonpoisonous nature, stability, and low metal ion concentration due to complex formation. Detailed investigations on the electrodeposition of various metals and alloys from this bath were undertaken to study the electrochemistry of metal pyrophosphate solutions, optimum operating conditions for satisfactory deposition, and to compare its performance with that of well-established baths. Electrodeposition of Sn, Zn, Cu-Sn alloy and Ni from the pyrophosphate bath has been reported briefly in preliminary notes from this laboratory (6-9). This paper presents in detail the work on the deposition of Sn.

Experimental

Plating solutions were prepared by dissolving $Sn_2P_2O_7$ in $Na_4P_2O_7$ solution, resulting in formation of a complex: $Sn_2P_2O_7 + Na_4P_2O_7 \rightarrow 2Na_2[Sn(P_2O_7)]$. Potentiometric and conductimetric titrations showed that the ratio of pyrophosphate to Sn in the complex is 1:1. The Sn ion concentration in the solution as found from potential measurements was of the order of 10^{-14} g-ion/l (10). The pyrophosphate content of the bath was always in excess of that required for complex formation. $Sn_2P_2O_7$ was prepared by adding $Na_4P_2O_7$ solution to a solution of $SnCl_2$ in HCl. The precipitate formed was washed thoroughly, dried, and kept for use. Stannous pyrophosphate was analyzed for Sn by the cupferron method, and for pyrophosphate by decomposition to orthophosphate and then volumetric estimation by the ammonium molybdate method. Composition (by weight) was: Sn, 54.0, pyrophosphate 39.5, and water 6.5%.

It was possible to maintain a fairly high Sn content in the plating bath because of the high solubility of $Na_4P_2O_7$ in water. Keeping in view the cost, drag out losses, and necessity for the presence of a high free pyrophosphate content (and consequently the tendency of the bath to crystallize at low temperatures), it was not advisable to go beyond a Sn content of 33 g/l. The $Na_4P_2O_7$ concentration in the range 80-480 g/l was found suitable for the metal concentrations used, the ratio (by weight) of $Na_4P_2O_7$ to $Sn_2P_2O_7$ being from 4:1 to 8:1. The free pyrophosphate improved anode corrosion, conductivity, and throwing power. Nine bath compositions were studied, the $Sn_2P_2O_7$ content being 20, 40, and 60 g/l, and the ratio of $Na_4P_2O_7$ to $Sn_2P_2O_7$ being 4:1, 6:1, and 8:1.

Chemicals employed for the plating bath were of C.P. quality, $SnCl_2$ being "Bakers Analyzed" and sodium pyrophosphate British Drug Houses brand. Fresh solutions were run for each experiment. Canning and Co. Sn anodes (3 x 1 x ⅛ in.) and Cu sheet cathodes (3 x 1 x 1/32 in.) were used, the inter-electrode distance being 1 in., immersed area of each electrode 2 $in.^2$, and plating time 20-30 min. Experimental details concerning cleaning electrodes, plating equipment, current efficiencies (on the basis of divalent Sn), temperature, agitation (speed 500 rpm approximately), pH, and resistivity were the same as described previously (11, 12). The pH was varied by the addition of H_3PO_4 or NaOH.

Cathode and anode potentials during deposition were determined as follows. The electrode whose potential was to be measured was coupled with a saturated calomel electrode and the emf of the combination determined by using a Tinsley potentiometer. The connection to the electrode was made by an agar-agar bridge whose tip, drawn into a capillary of approximately 1 mm diameter, pressed lightly against the electrode, minimizing thereby the error due to potential drop through the electrolyte. A thick layer of Sn was deposited on the cathode before taking measurements. Then, commencing from the static potential, emf readings were taken at various current densities. Sufficient time, approximately 2-3 min, was allowed for each measurement to enable the potential to reach a steady value. Plating conditions were carefully controlled to obtain results of the accuracy of ±0.001 v, as far as possible. Potential values refer throughout to the H scale.

The limiting C.D. was found from (*a*) C.D.-cathode potential curves, there being a sudden change in the form of the curve at the limiting C.D., and (*b*) current efficiency-C.D. data. Both methods gave practically the same values. The throwing power was calculated from the equations of Schlotter-Korpiun (13) as well as those of Gardam (14). In the latter case, the equation for a linear relationship between cathode potential and log C.D. was used, and as approximation, the inter-electrode distance was substituted for l_2 of the equation.

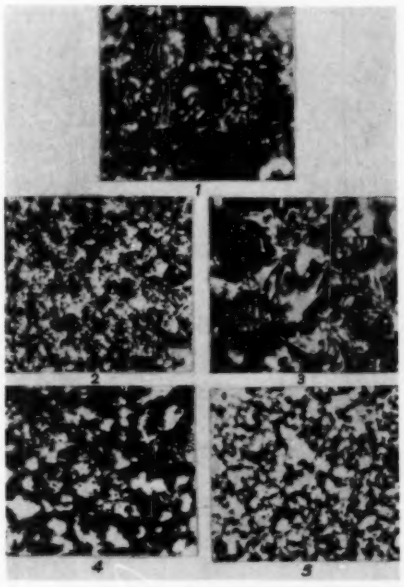

Fig. 1. Photomicrographs of deposits from $Sn_2P_2O_7$ 60, $Na_4P_2O_7$ 360 g/l, Cu cathode. Magnification 1 x 500 before reduction for publication. *Plate 1*. Fine-grained, bright deposit at 80°C and 1.6 amp/dm², from stannate bath (composition, Table II); *Plate 2*, fine-grained, semibright deposit at 50°C and 0.54 amp/dm², from pyrophosphate bath; *Plate 3*, coarse-grained, semibright deposit at 80°C and 0.54 amp/dm²; *Plate 4*, fine-grained, bright deposit at 80°C and 1.6 amp/dm²; *Plate 5*, fine-grained and brighter deposit with same conditions as Plate 4 and with 10 g/l dextrin and 1 g/l gelatin.

To study the structure, a thick coating of Sn was deposited under various conditions on polished cathode plates, and photomicrographs were taken with a Vicker's projection microscope at 500 magnification, using Kodak B20 process plates.

Results

A detailed study of the effect of important variables on deposition was made, and results are presented graphically in Fig. 1-11 and Tables I and II. Results obtained for all concentrations studied have not been covered graphically to avoid overlapping; for the same reason points corresponding to 100% efficiencies or static potentials have not been marked. The data correspond to good quality deposits. The decomposition potential for the plating solution was 2.5-2.6 v and the bath voltage 0.30-1.00 v. The standard stannate bath composition was modified to bring the Sn content on a par with that of the pyrophosphate bath.

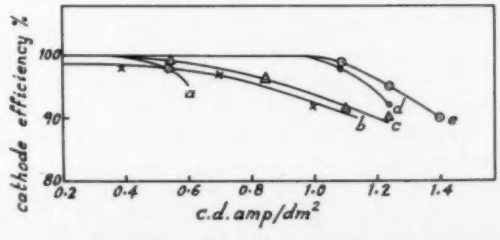

Fig. 2. (a) $Sn_2P_2O_7$ 20 g/l, ratio 6; (b) $Sn_2P_2O_7$ 40 g/l, ratio 6; (c) $Sn_2P_2O_7$ 60 g/l, ratio 4; (d) $Sn_2P_2O_7$ 60 g/l, ratio 6; (e) $Sn_2P_2O_7$ 60 g/l, ratio 8; temp, 60°C.

Table I. Effect of addition agents on current efficiency and quality of deposit

$Sn_2P_2O_7$ 60 g/l, $Na_4P_2O_7$ 360 g/l, temperature 60°C, pH 9.0, cathode Cu, anode Sn, still plating. Quality of deposit: A—marked improvement, B—slight improvement, C—no effect, D—deterioration.

No.	Addition agent	Amount added g/l	C.D. amp/dm²	Current efficiency % Cathode	Current efficiency % Anode	Brightness of deposit
1.	Nil	—	0.85	100	103	—
			1.01	100	103	—
			1.24	92	104	—
2.	Sodium nitrate	15.0	0.85	99	106	C
			1.01	98	104	C
			1.16	97	106	C
3.	Ammonium citrate	15.0	0.85	93	107	B
			1.01	93	105	B
			1.16	95	101	B
4.	Sodium oleate	5.0	0.85	97	103	D
			1.01	92	97	D
5.	Sodium tartrate	15.0	1.01	100	106	A
			1.16	96	105	B
			1.32	95	103	C
6.	Sodium acetate	15.0	1.16	98	105	C
			1.32	90	104	C
7.	Resorcinol	20.0	0.85	100	98	D
			1.16	92	103	D
8.	Dextrin	5.0	1.01	100	105	A
			1.16	99	104	A
			1.32	95	103	B
9.	Dextrin	10.0	1.32	100	105	A
			1.47	100	105	A
			1.63	96	104	A
10.	Gelatin	0.5	1.32	93	105	C
			1.47	90	100	C
11.	Gelatin	1.0	1.01	100	105	B
			1.32	94	106	B
			1.63	95	101	C
			1.94	95	100	D
12.	β-naphthol	1.0	1.16	96	104	A
			1.32	92	100	B
13.	Dextrin + Gelatin	10.0 + 1.0	1.32	94	105	A
			1.63	94	102	A
			1.94	90	100	A
			2.25	91	99	A
			2.71	88	99	C

Nature of deposit.—The bath gave matte, white, smooth, and adherent deposits of Sn on Cu (steel or brass) cathodes over a wide range of plating conditions: metal content, ratio of $Na_4P_2O_7$ to metal pyrophosphate, pH (8.0, 9.0, and 9.5). Increase in C.D. gave finer-grained deposits and increase in temperature or agitation gave coarser grained ones. The addition of dextrin or dextrin-gelatin combination, tartrate, and β-naphthol in optimum concentrations increased brightness. The dextrin-gelatin combination was the best and gave deposits com-

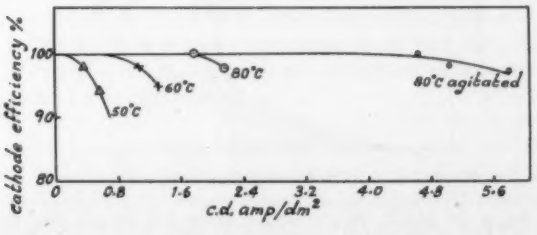

Fig. 3. Concentration (d) of Fig. 2.

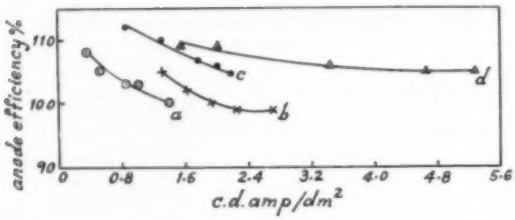

Fig. 4. (a) $Sn_2P_2O_7$ 60 g/l, ratio 6, temp, 60°C; (b) $Sn_2P_2O_7$ 60 g/l, ratio 6, temp, 60°C + (gelatin 1, dextrin 10 g/l); (c) $Sn_2P_2O_7$ 60 g/l, ratio 6, temp, 80°C; (d) $Sn_2P_2O_7$ 60 g/l, ratio 6, temp, 80°C (agitated).

parable with those obtained from the stannate bath (Fig. 1, plates 1-5). The effect of various addition agents on quality of the deposit and current efficiency is recorded in Table I.

Current efficiencies.—In the working C.D. range, cathode efficiency was nearly 100%, anode efficiency was a bit higher, 100-110%, although the anode did not dissolve chemically in the plating solution. Current efficiencies remained practically unaffected by changes in concentration, temperature, agitation, pH (not recorded), or use of addition agents (Fig. 2-4 and Table I).

Current density.—The C.D. range and limiting C.D. increased with increase in metal content, the ratio of $Na_4P_2O_7$ to metal pyrophosphate (to a small extent), rise in temperature, agitation, and the addition of few substances like dextrin, gelatin or their combination. pH variation had little effect. It

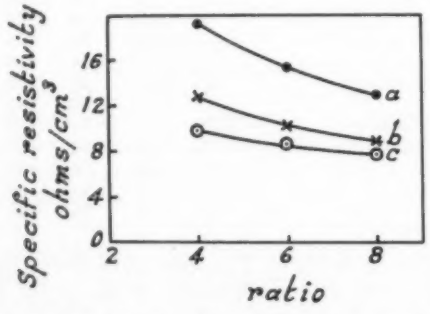

Fig. 5. (a) $Sn_2P_2O_7$ 20 g/l; (b) $Sn_2P_2O_7$ 40 g/l; (c) $Sn_2P_2O_7$ 60 g/l; temp, 60°C.

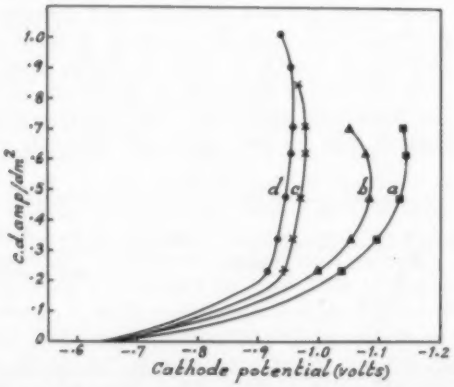

Fig. 6. (a) $Sn_2P_2O_7$ 20 g/l, ratio 4; (b) $Sn_2P_2O_7$ 20 g/l, ratio 8; (c) $Sn_2P_2O_7$ 60 g/l, ratio 4; (d) $Sn_2P_2O_7$ 60 g/l, ratio 8; temp, 60°C.

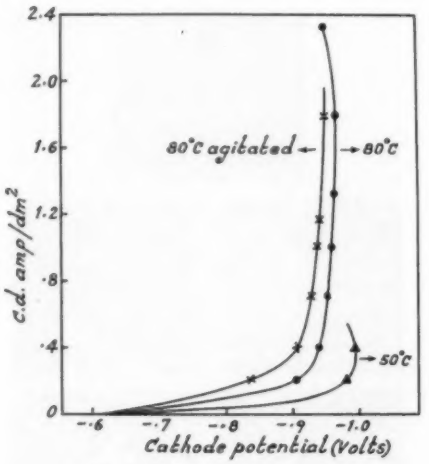

Fig. 7. $Sn_2P_2O_7$ 60 g/l, ratio 6

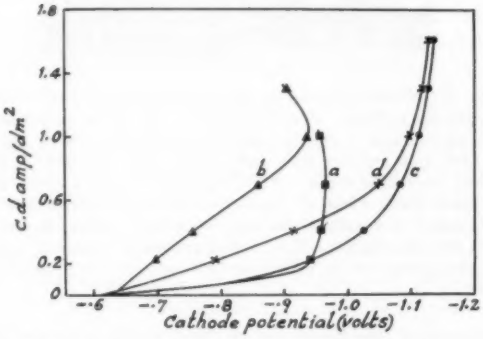

Fig. 8. Concentration as in Fig. 7, temp, 60°C: (a) addition nil; (b) addition ammonium citrate 15 g/l; (c) addition gelatin 1 g/l; (d) addition gelatin 1, dextrin 10 g/l (dextrin only also).

was possible to go up to 5 amp/dm². There was no interference with anode dissolution due to film formation, etc., even at high C.D. (Fig. 2-4 and Table I).

Specific resistivity.—Increase in metal content, ratio of $Na_4P_2O_7$ to metal pyrophosphate, or temperature (not shown) and decrease of pH (slightly) lowered the resistivity (Fig. 5). The addition of dextrin-gelatin combination had no effect.

Polarization.—Cathode polarization decreased with increase of metal content (keeping the ratio same), ratio, temperature, agitation, and pH (not recorded). Addition of dextrin, gelatin, or dextrin-gelatin combination had the general effect of increasing polarization; at low C.D., however, a lowering was observed. Ammonium citrate decreased polarization. In all cases it increased with rise in C.D. up to the limiting C.D. only. After this stage, a decrease was observed from the available data. Current efficiency then decreased, H evolution commenced, and the deposit was not good (Fig. 6-8). C.D.-potential curves for stannate bath are also recorded in Fig. 9.

The effect of variables on anode polarization was similar to that on cathode polarization. No limiting value for the anode C.D. was found in the C.D. range studied. Dextrin-gelatin decreased polarization (Fig. 10).

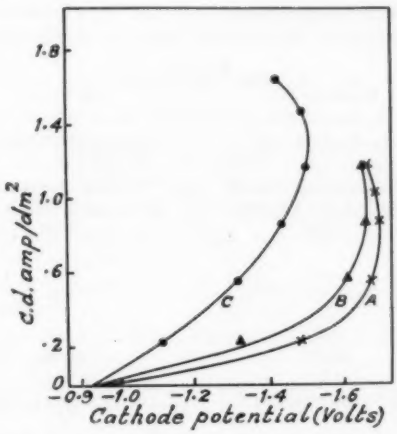

Fig. 9. Concentration Table II: (A) temp, 50°C; (B) temp, 60°C; (C) temp, 70°C.

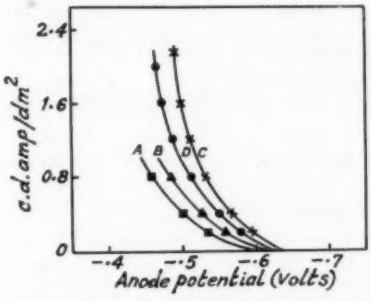

Fig. 10. $Sn_2P_2O_7$ 60 g/l: (A) ratio 4, temp, 60°C; (B) ratio 6, temp, 60°C; (C) ratio 6, temp, 80°C; (D) ratio 6, temp, 60°C + (gelatin 1, 10 dextrin g/l).

Throwing power.—The plating solution possessed good throwing power. Calculations on the basis of the Schlotter-Korpiun equation showed that the throwing power increased with rise in metal content and temperature, and with the use of dextrin, gelatin, or their combination, while it decreased with increasing C.D., and to a small extent with rise in pH and agitation. The Schlotter-Korpiun throwing power values were in the range 5.7-10.8 for the pyrophosphate, and 9.8-16.4 for the stannate baths. For the optimum pyrophosphate bath, the Gardam value was 59% as against 64% for the stannate (Fig. 11, curves A and D, Table II).

Control and maintenance of bath.—The bath was quite stable and did not decompose with high temperatures. Composition did not change appreciably after electrolysis, since current efficiencies were high and practically balanced, and there were no difficulties due to anode corrosion. In a typical case with a solution containing 60 g/l of $Sn_2P_2O_7$ and 360 g/l of $Na_4P_2O_7$, changes before and after electrolysis for 40 min at 0.7 amp/dm², 60°C, were: metal content, 32.4-32.6 g/l; total pyrophosphate (P_2O_7), 164.2-164.3 g/l; pH, 9.0-9.2; specific resistivity, 8.65-8.66 ohms/cm³. The solutions did not contain orthophosphate before and after electrolysis as estimated by the method of Kolthoff and Stenger (15). A freshly prepared solution could be used for 4-5 runs without any deterioration in its performance (quality of deposit, C.D. range, current efficiencies, etc.). A solution which was aged for about two months was equally satisfactory.

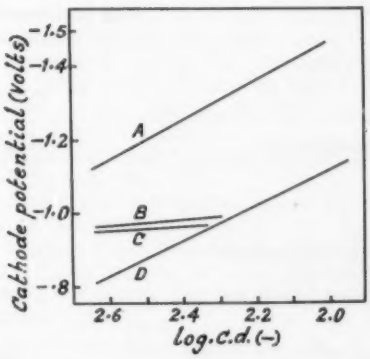

Fig. 11. (A) $Na_2Sn(OH)_6$ bath concentration Table II, temp, 70°C; (B) $Sn_2P_2O_7$ 40 g/l, ratio 6, temp, 60°C; (C) $Sn_2P_2O_7$ 60 g/l, ratio 6, temp, 60°C; (D) $Sn_2P_2O_7$ 60 g/l, ratio 6, temp 60°C + (gelatin 1, dextrin 10 g/l).

Testing of deposits.—Coatings of any desired thickness of 0.0005 in. or above (calculated from area and weight) could be obtained by varying the plating time. Adherence of deposits to the base metal as determined by bending and breaking tests was good. Ferricyanide (steel base) and hot water tests showed that they were free from porosity. Corrosion resistance was good in the laboratory atmosphere (4-6 mo). Sn content of the deposits was above 99.8%.

Optimum plating conditions.—A study of experimental results led to the following optimum bath composition and operating conditions for the best performance of the $Sn_2P_2O_7$ bath. Bath composition: $Sn_2P_2O_7$ 60 (tin content 32.4), $Na_4P_2O_7$ 360, dextrin 10, gelatin 1 g/l. Operating conditions: Cathode C.D.: 0.2-2.3 amp/dm² (still, 60°C), up to 5.0 amp/dm² (agitated, 80°C, without addition agents); pH 9.0, temperature: 60-80°C; time to deposit 0.001 in. thickness at 2.2 amp/dm², 80°C: 25 min.

Comparison of pyrophosphate and stannate baths.—Table II gives an idea of the relative performance of the pyrophosphate and stannate baths for Sn plating. Data recorded for stannate bath were obtained experimentally as well as from literature (1, 16, 17).

The $Sn_2P_2O_7$ bath is superior to the stannate bath in the following respects: *(a)* current efficiencies up to the limiting cathode C.D., *(b)* bath voltage, *(c)* stability, *(d)* wide range of anode C.D., and *(e)* absence of critical anode C.D. which facilitates bath control. It compares well with the stannate bath in throwing power, quality of deposit, and cost of plating solution. In view of these considerations, it can be stated that the pyrophosphate bath compares favorably with the commercial stannate bath and is suitable for Sn plating.

Discussion

The $Sn_2P_2O_7$ bath gives satisfactory deposits of Sn on steel, Cu, or brass over a wide range of operating conditions and has many advantages over the conventional stannate bath. Roseleur (2) used a

Table II. Comparison between pyrophosphate and stannate baths

No.		Pyrophosphate	Stannate	
			Experimental	Literature
1.	Composition g/l	$Sn_2P_2O_7$ 60 $Na_4P_2O_7$ 360	$Na_2Sn(OH)_6$ 74 NaOH 7.5 Sodium acetate 11 30% H_2O_2 3 drops	$Na_2Sn(OH)_6$ 90 NaOH 7.5 Sodium acetate 15.0 H_2O_2 (100 vol) 0.5 ml
2.	Tin g/l	32.4	32.4	40.0
	Free pyrophosphate (P_2O_7) g/l	116.4	—	—
3.	Addition agents g/l	Dextrin 10.0 Gelatin 1.0	— —	— —
4.	*pH*	9	12	—
5.	Temp, °C	60-80	60-70	60-80
6.	Bath voltage, v, 80°C	0.3-1.0 (0.6-2.3 amp/dm²)	4.5 (0.4-2.3 amp/dm²)	3.0-4.5 (1.1-2.7 amp/dm²)
7.	Specific resistivity 60°C, ohms/cm³	8.65	8.56	—
8.	Cathode C.D. (max) amp/dm²	5.0	1.6	1.1-2.7
9.	Anode C.D. (max) amp/dm²	5.0	1.6	1.1-4.3
10.	Cathode current efficiency, %	91-100	70-83	60-90
11.	Anode current efficiency, %	99-112	80-98	60-90
12.	Cathode polarization 60°C, v	0.28-0.60 (0.4-2.3 amp/dm²)	0.40-0.73 (0.23-1.60 amp/dm²)	—
13.	Throwing power, 60°C, Schlotter-Korpiun (0.54 amp/dm²)	10.8	16.3	—
	Gardam % (0.39 amp/dm²)	59	64 (70°C)	68-74
14.	Stability of bath	Good	Fair	Fair
15.	Quality of deposit	Good	Good	Good
16.	Time in min to deposit 0.001 in. at 1.6 amp/dm² 80°C	34	—	70
17.	Cost of bath, dollars per liter (approx)	0.76	—	1.00

solution of the composition: fused $SnCl_2$ 1.0-1.5, $Na_4P_2O_7$ 10.0-12.5 g/l. However, no mention was made of the plating conditions except that this bath was unable to give heavy deposits. Another Roseleur solution (3) was made up of $SnCl_2$ 9.4, $Na_4P_2O_7$ 75.0, dextrin 6.25 g/l; operating conditions: 60°C and C.D. of 5 amp/ft². Solutions used in the present investigation were simpler in composition, addition agents being used only to obtain some beneficial effects. The metal content was high, and it was possible to work the bath at current densities up to 5 amp/dm².

Organic brighteners like dextrin, gelatin, and β-naphthol in the pyrophosphate bath were also used in the acid Sn bath. Henricks (18) attributed the brightening action to their acid pickling inhibiting tendency. Tartrate had some brightening effect, as in the deposition of Cu from the pyrophosphate bath; it is perhaps due to complex formation. The grain size became finer and the cathode polarization increased with addition of dextrin-gelatin.

Cathode polarization was fairly high, although slightly less than that of stannate bath. The relationship between cathode potential and log C.D. is linear for the pyrophosphate as well as the stannate bath (Fig. 11) and both of them give fine-grained deposits (Fig. 1). Gardam (19) suggested that the logarithmic type, i.e., $\Delta E \alpha \log I$, indicates frequent formation of new grain nuclei, viz., production of fine-grained deposits. Experimental results are in accordance with the Gardam theory. However, it should be stated that exhaustive polarization measurements were not made for the stannate bath. The anode potential measurements showed that no limiting C.D. was found for anode dissolution. This is one of the important advantages of the pyrophosphate bath against the stannate, where there is a limit to the anode C.D. The throwing power of the bath, Schlotter-Korpiun as well as Gardam, was of the same order as that of stannate bath. The latter is among the best of the plating baths, so far as this property is concerned.

In the electrodeposition of Sn from the complex pyrophosphate bath, the metal ion concentration was low; smooth, fine-grained, and bright deposits were obtained at electrode efficiencies close to 100%. The cathode polarization was high, and the throwing power of the bath was very good. The performance of the bath was in accordance with the general expectations for a complex salt plating bath. The present work indicates that this bath shows promise and is suitable for further investigation on a commercial scale.

Acknowledgment

The authors are thankful to Professor K. R. Krishnaswami, Head of the Department of General Chemistry, for his keen interest in the work.

Manuscript received November 14, 1955. This paper is based in part on a thesis presented by J. V. to the graduate faculty of Punjab University in partial fulfillment of the requirements for the degree of Master of Science.

Any discussion of this paper will appear in a Discussion Section to be published in the December 1957 JOURNAL.

REFERENCES

1. F. F. Oplinger and F. Bauch, *Trans. Electrochem. Soc.*, **80**, 617 (1941).
2. E. F. Kern, *ibid.*, **23**, 193 (1913).
3. S. Field and A. D. Weill, "Electroplating", Ch. 21, p. 428, Sir Isaac Pitman and Sons, London (1951).
4. P. Marino, Brit. Pat. 10,133, July 12, 1915; *Chem. Abstr.*, **11**, 121 (1917).
5. W. H. Safranek and C. L. Faust, *Plating*, **41**, 1159 (1954).
6. J. Vaid and T. L. Rama Char, *Current Sci. India*, **21**, 310 (1952).
7. J. Vaid and T. L. Rama Char, *J. Sci. Ind. Research, India*, **11B**, 503 (1952).
8. J. Vaid and T. L. Rama Char, *Current Sci. India*, **22**, 170 (1953).
9. S. K. Panikkar and T. L. Rama Char, *J. Sci. Ind. Research India*, **14B**, 603 (1955).
10. J. Vaid and T. L. Rama Char, *Current Sci. India*, **22**, 170 (1953); *Chem Abstr.*, **48**, 4353 (1954).
11. T. L. Rama Char and N. B. Shivaraman, *This Journal*, **100**, 227 (1953).
12. T. L. Rama Char and R. Sadagopachari, *J. Indian Inst. Sci.*, **35A**, 298 (1953).
13. M. Schlotter and J. Korpiun, *Trans. Electrochem. Soc.*, **62**, 129 (1932).
14. G. E. Gardam, *Trans. Faraday Soc.*, **34**, 698 (1938).
15. I. M. Kolthoff and V. A. Stenger, "Volumetric Analysis," Vol. II, p. 140, Interscience Publishers, New York (1947).
16. P. R. Pine, *Trans. Electrochem. Soc.*, **80**, 631 (1941).
17. "Instructions for Electrodepositing Tin," p. 9, Tin Research Institute, England (1946).
18. J. A. Henricks, *Trans. Electrochem. Soc.*, **82**, 113 (1942).
19. G. E. Gardam, *Disc. Faraday Soc.*, **1**, 182 (1947).

A Simplified Procedure and Apparatus for Measuring Surface Area of Fine Powders By Gas Adsorption

F. M. Starkweather and D. T. Palumbo[1]

Chemistry Laboratory, Sylvania Electric Products Inc., Flushing, New York

ABSTRACT

A modification of the standard Brunauer-Emmett-Teller (BET) gas adsorption technique for the determination of surface areas of fine powders is presented. Data show that values usually within 10% of those by the standard method are obtained for Ba, Sr, Ca carbonates, ZnS, CdS, and Zn_2SiO_4. A simplified design of the conventional gas adsorption apparatus is described. It is simple to operate, less subject to accidental damage, and can be set up with simpler accessories than are required for the standard BET system.

In the investigation of the preparation of triple carbonates for use in oxide cathode studies, a reliable measure of the particle size is required. Past practice has been to measure the surface area by the BET gas adsorption method (described below) and to calculate the mean particle diameter (MPD) assuming spherical particles. Ordinary gravitational sedimentation methods are not suitable for these materials as the mean particle diameters are in the range 0.07-1 μ. The Fisher Sub-Sieve Sizer (FSSS), which has been used for control of commercial preparation of carbonates, was also unsuitable. Here, the size values obtained depended, in part, on the degree of agglomeration of the precipitate. For particles of rough external or with large internal surface, the air permeation method (FSSS) would not be expected to give values comparable to the gas adsorption method. However, large internal surface can result from the agglomeration of individual particles with smooth surface. In these cases, the air permeation method would not indicate whether the agglomerate size, crystallite size, or both have changed.

The major drawback of the BET procedure is the time required for a determination. Unless overnight outgassing is used, at least two days' elapsed time per sample are required for the measurement. Actual operational time required is approximately 6 hr. The result is that any experimental program which depends on BET measurements is slowed down correspondingly.

In preliminary experiments, such as those where various procedures for preparation of carbonates are surveyed, a surface area value within 25% of the true area is usually sufficient for meaningful results. A simplification of the BET method to reduce the time per determination to about 1 hr with a negative error usually no greater than 10% of the standard BET value is discussed below. The magnitude of the error is a function of sample composition and surface area. In general the error increases with samples of larger surface area. The design and construction of a simplified unit, particularly suited for rapid measurements, is described.

The major saving in the time of a determination results from the use of a single point surface area determination, elimination of the dead space determination, and a short outgassing schedule. Other workers have proposed and employed these modifications. Emmett (1), for example, points out that the slope of an adsorption curve using a zero inter-

[1] Present address: Sylvania Electric Products Inc., Towanda, Pa.

cept and one measured point is usually within 5% of the slope determined by three or four points. Bugge and Kerlogue (2) have shown that shorter outgassing time and avoidance of the dead space determination gave results only slightly lower (ca. 3%) than values obtained by the standard method. Amron and Starkweather (3) have shown that <2% error is introduced by using two or three points for determining the curve rather than five or more and had considered the feasibility of a single point adsorption run. The modifications described below represent the natural extension and integration of these ideas into a unit simple to construct and operate and a method which permits determinations of surface area in a minimum of time.

Experimental

Standard BET adsorption method.—The apparatus used for the determination of surface area is of standard design (4). A complete run entails the following steps: sealing a weighed sample in an adsorption bulb onto the system; outgassing at elevated temperature to remove adsorbed water and gases; calibration of the adsorption bulb for volume, using helium; measurement of nitrogen taken up by the sample as a function of pressure at constant temperature; calculation of the surface area from the adsorption isotherm (1).

The time for a run is determined by the outgassing procedure and the number of experimental points measured on the adsorption curve.

Simplified BET procedure.—The apparatus used for the simplified procedure may be the same as for the standard method, with the sample tube position fitted with a ground glass joint. This eliminates a glass sealing operation. Further simplifications are possible, including elimination of the diffusion pump, McLeod gauge, and mercury reservoirs. The simplified method incorporates the following features: *(a)* outgassing at room temperature 10-20 min to a pressure of 1 μ or less; *(b)* sample tube calibrated for volume with ground glass connection to the system; *(c)* a one-point run at about 15 cm pressure and assumption of zero intercept.

With samples of known density and a calibrated sample tube volume, the helium run can be omitted.

The accuracy of the proposed method was checked by determining the surface area of samples of interest (phosphors and triple carbonates) by both procedures.

A Simplified Gas Adsorption Apparatus

A simplified BET apparatus is shown in Fig. 1a, b, c. The major points of difference are the substitution of a variable volume manometer for the fixed volume manometer and a fixed "calibrated" volume for the "variable" calibrated volume of the standard apparatus. These modifications eliminate the mercury reservoir and eliminate adjustment of the mercury levels. The elimination of the need for mercury level adjustment represents a considerable simplification in the procedure. Other modifications include the use of: *(a)* restricted capillaries in the helium and nitrogen entrance lines to reduce the possibility of pressure surges damaging the apparatus; *(b)* ground glass joints for attaching sample tubes, helium and nitrogen reservoirs to the system; (c) a sample tube volume which can be isolated from the calibrated volume, gas inlets, and manometer.

Direct pumping on the sample tube volume is possible without disturbing the gas metering portion of the system. Entrained powder, resulting from too rapid an evacuation, is prevented from depositing in the calibrated volume (requiring a cleaning of the system and recalibration). A two-way stopcock in the sample tube line also permits initial outgassing of the sample through a restricted capillary, further reducing the possibility of powder entrainment into the system.

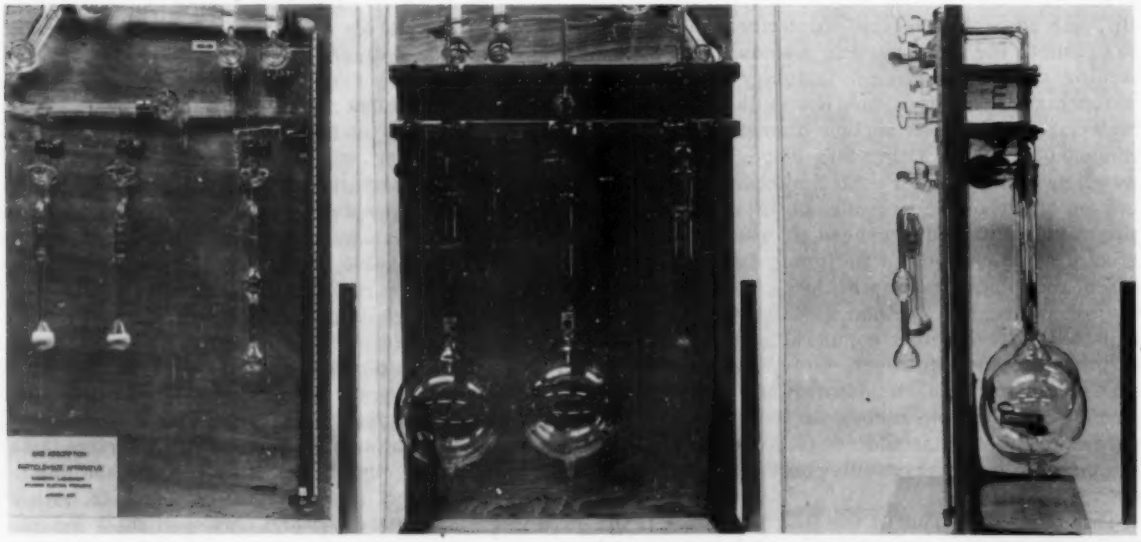

Fig. 1a. (*Left*) Front view. From left to right, sample tubes—$\overline{\$}$ 10/30 joints, gas buret, manometer. Fig. 1b. (*Center*) Rear view. From left to right, N_2 and He supply—$\overline{\$}$ 19/38 joints, cold trap—$\overline{\$}$ 29/42 joint. Fig. 1c (*Right*) Side view.

Table I. Comparison of standard and simplified BET systems (simplified gas adsorption method)

Sample	Standard system m^2/g	Standard system MPD	Simplified system m^2/g	Simplified system MPD
Cadmium sulfide	19.0	0.0656	17.8	0.070
	19.1	0.0653	18.3	0.068
Triple carbonate #2	2.20	0.713	2.20	0.713
	2.23	0.705	2.10	0.745
Zinc sulfide #1	20.3	0.072	18.8	0.078

Table II. Reproducibility of gas volume measurement for simplified gas adsorption system

Sample tubes	Volume, cc	Avg dev, %
#1	10.55	0.48
	10.45	
#2	6.14	0.13
	6.12	
	6.12	
#3	4.00	0.13
	3.99	

The manometer, made from precision bore tubing, and gas buret of the system are calibrated for volume (with mercury) before the system is assembled. The tubing volume, i.e., from the zero level of the manometer to stopcocks of calibrated volume, gas bottles, and sample tube, is then determined by introducing He into the evacuated system at known pressure and temperature, then measuring the change in pressure when the calibrated volume is thermostated with liquid N_2.

The validity of this method of calibration was checked by determining the volume of the buret with He at liquid N_2 temperature and comparing this value to the calibration made with mercury. In the calculation for determining the tubing volume it is assumed that there is no temperature transition zone from the section at liquid N_2 temperature to that at room temperature. The buret was attached to the conventional BET system for the volume measurement. Mercury and helium calibrations agreed to within 0.1%. A comparison of runs on typical powders made with the standard and simplified systems using the rapid procedure (short outgassing time and one point adsorption) are given in Table I. In general, there is close agreement in the values for surface area obtained on the two systems.

To indicate the inherent accuracy of the simplified system, Table II gives results of volume measurements with the simplified system. In all cases the average deviation of duplicate determinations was less than 0.5%. Where conventional runs were made on both systems (powder outgassed at 140°C for 4 hr, three adsorption points) the surface area values agreed within experimental error. For example, a CdS powder gave a value of 20.9 m^2/g on the conventional system and 21.3 m^2/g on the simplified system.

Comparison of the Methods

Reproducibility of each method.—For the standard procedure, Table III gives the areas of samples

Table III. Reproducibility of standard BET determinations* (samples re-run without removal from system)

$BaCO_3$ m^2/g	$BaCO_3$ MPD, μ	$CaTiO_3$ unmilled m^2/g	$CaTiO_3$ unmilled MPD, μ	$CaTiO_3$ milled 65 hr m^2/g	$CaTiO_3$ milled 65 hr MPD, μ
4.88	0.277	4.21	0.348	9.79	0.149
4.88	0.277	4.14	0.353	9.58	0.153
4.96	0.274	4.21	0.348	10.01	0.146
4.96	0.274	4.22	0.347	10.06	0.145
4.79	0.283				
5.27	0.257				
5.14	0.263				
5.40	0.251				
5.03±0.17		4.19±0.04		9.86±0.18	

* Mean particle diameters computed from surface area values by the relation MPD = 6/surface area x density.

Table IV. Reproducibility of standard BET determinations of surface area and mean particle diameter

(Different samples of same materials used for runs 1 and 2)

Sample	Area m^2/g	MPD, μ	Avg dev, %
Triple carbonate #1	5.76	0.273	0.17
	5.74	0.274	
Triple carbonate #2	2.45	0.642	0.00
	2.45	0.642	
Triple carbonate #3	9.31	0.169	1.67
	9.00	0.175	
$CaTiO_3$	4.33	0.338	0.12
	4.22	0.339	

that were remeasured without being removed from the system. The average deviation was found to vary from 0.95 to 3.3%. In cases where duplicate samples were run (Table IV) the average deviation was 0 to 1.8%. With duplicate samples using the simplified method the average deviation was 0.26 to 1.5% (Table V).

Agreement of surface area values between the two methods.—In most cases it was found that the simplified BET method gave values that varied less than 10% from the standard BET value (Table VI). Only in the case of a ZnS with a large surface area was the simplified method appreciably in error (about 27% low). Also, reported values are always on the low side of the standard BET value. It should be pointed out that although in this case the simplified method gives a value of 0.072 μ MPD compared to 0.052 μ MPD by the conventional method, the Fisher Sub-Sieve Sizer and optical microscope examination would give values of 6 μ.

Discussion of Results

In determining the reproducibility of surface area measurements a distinction must be made between the system accuracy and the sample stability. The former is a function of the physical design (i.e., accuracy of volume and pressure measurement) of the system, the latter a function of composition and previous history of the sample.

For a standard BET determination a minimum of four pressure readings are required for a single adsorption point, namely, two readings each for a he-

Table V. Reproducibility of simplified BET determinations of surface area and mean particle diameter

(Different samples of same material used for runs 1, 2, and 3)

Sample	Area m^2/g	MPD, μ	Avg dev, %
Zinc sulfide #1	20.5	0.0715	0.78
	20.3	0.0722	
	20.6	0.0711	
Zinc sulfide #2	0.277	5.28	1.25
	0.284	5.16	
Triple carbonate #1	5.18	0.303	0.38
	5.22	0.301	
Triple carbonate #2	2.20	0.713	0.68
	2.23	0.705	
Cadmium sulfide	19.0	0.0656	0.26
	19.1	0.0653	

Table VI. Comparison of standard and simplified BET surface area determinations

Material	Standard BET m^2/g	Standard Value MPD	Simplified BET m^2/g	Simplified Value MPD	Error, % standard value for surface area
ZnS (Fired)	0.30	4.9	0.28	5.2	— 6.1
ZnS (Unfired)	27.9	0.0524	20.4	0.0722	—26.9
Zn_2SiO_4	0.90	1.7	0.84	1.8	— 5.9
CdS	20.9	0.0596	19.1	0.0653	— 3.9
Triple carbonate	2.45	0.642	2.21	0.711	— 9.8
Triple carbonate	5.74	0.279	5.20	0.302	— 9.4

lium and a nitrogen run. With the standard BET system, pressure readings are accurate to ±0.02 cm, or 0.1% for a 20 cm height. In the worst case, the error expected would be 0.4%. In general, duplicate determinations show deviations of this order of magnitude (Tables IV and V). Larger deviations may be the result of incomplete outgassing of the samples or actual changes in the surface area.[2] From Table III (Col. 1 and 5) there is noted a trend to a larger surface area when the same sample is measured repeatedly on the system. Here it is possible that the apparent increase in surface area is a result of more complete outgassing.

In evaluating this method it was pointed out that the surface area values obtained were, in general, lower than those given by the standard procedure. That this is attributed to the shortened outgassing procedure is shown in Table VII. Outgassing efficiency (for fixed time and temperature) should increase with decreased surface area and degree of agglomeration of the powder. However, there appears to be little difference in outgassing efficiency over a wide range of pumping conditions (Table VIII). For example, outgassing for 15 min at liquid N_2 temperature (77.4°K) gave a surface area only 6% lower than for outgassing at 300°K.

In the calculation of the surface area of powders using a single point adsorption measurement the assumption was made that the curve had a zero intercept. The data of Table IX show that if the value of

[2] Changes in surface area as a result of the preparation history of triple carbonates is currently under investigation. This work will be described in a future report.

Table VII. Effect of time and temperature of outgassing on surface area. Outgassing schedule

Time, min	Temp, °C	Simplified BET m^2/g	Simplified Value MPD	Error, % of standard value
10	25	20.3	0.0722	—26.9
30	110	24.2	0.0605	—13.4
90	140	25.6	0.0511	— 9.4
360	140	27.9*	0.0524	0

* Standard method—outgas 2 hr at room temperature, 6 hr at 140°C.

the intercept is assumed greater than zero (usually the case in an actual run) the simplified BET value approaches the standard value more closely.

The accuracy of the simplified procedure is much better than the data imply. Although the simplified procedure gives values that are 3-27% lower than the standard run for a variety of materials, for a particular material in a given size range the surface area values by both procedures differ by a relatively constant factor. For example, for triple carbonates with surface areas of 2.45 and 5.76 m^2/g the modified value was from 9.0 to 10.2% lower than the standard value. Based on these data, it is possible to predict the surface area that would be obtained by a standard run within 2% of the actual value obtained by measurement. The accuracy of this procedure was demonstrated in a batch precipitation of triple carbonate. It was required that a 2-lb sample be prepared having a mean particle diameter of close to 0.64 μ.

There being no previous background in precipitations with the particular reagents used, trial preparations were measured by the one point adsorption method. Based on a difference of 11% between the standard and one point adsorption run on a typical sample, the trial runs were designed to give a sample 11% lower in area when measured by the simplified procedure. The 2-lb batch was then prepared based on data from the trials. When measured by

Table VIII. Effect of outgassing samples with varied pumping procedures. Outgassed 15 min

Method of outgassing	Temp, °C	Pressure μ	Surface area m^2/g
Welch duo seal pump	25	~4	18.3
Two stage oil diffusion pump	25	<2	18.3
Two stage oil diffusion pump	—195.8*	<2	18.3

* Liquid nitrogen temperature.

Table IX. Effect of assumed values of intercept on surface area of triple carbonate

Run No.	Intercept	Surface area	MPD, μ	Error, % of standard value for surface area
1	0.000	5.22	0.301	—9.3
	0.003	5.31	0.296	—8.0
	0.015	5.71	0.275	—1.2
2	0.000	5.18	0.303	—9.8
	0.003	5.25	0.299	—8.5
	0.007	5.36	0.293	—6.6

the conventional procedure, it had a mean particle diameter of 0.63 μ compared to the desired size of 0.64 μ.

Manuscript received July 13, 1955. This paper was prepared for delivery before the Cincinnati Meeting.

Any discussion of this paper will appear in a Discussion Section to be published in the December 1957 JOURNAL.

REFERENCES

1. P. H. Emmett, "Advances in Colloid Science," Vol. I, Chap. I, Interscience Publishers Inc., New York (1942).
2. P. E. Bugge and R. H. Kerlogue, *J. Soc. Chem. Ind., London*, **66**, 377 (1947).
3. I. Amron and F. M. Starkweather, Unpublished data.
4. P. H. Emmett, *ibid.*

Temperature Dependence of Electroluminescence

C. H. Haake

Lamp Division, Westinghouse Electric Corporation, Bloomfield, New Jersey

ABSTRACT

Electroluminescent brightness measurements were carried out on several zinc sulfide phosphors over wide ranges of temperature and frequency. From the temperature dependence of photoluminescence a thermal extinction factor was derived which, when introduced in the electroluminescent brightness values, led to an ideal electroluminescent brightness unaffected by thermal quenching. In general, this ideal brightness was found to increase or tend to saturation with increasing temperature, but did not decrease. The temperature sensitivity of the ideal electroluminescence is explained on the basis of a two-step mechanism: the excitation process and the return process. Luminescence is assumed to occur only during the latter process. On the phosphors studied the temperature dependence of the ideal electroluminescent brightness seems to be due mainly to the thermal behavior of traps during the return process, since the electron return is impeded by traps.

This work constitutes an attempt to obtain the temperature dependence of electroluminescence of some zinc sulfide phosphors detached from thermal quenching of luminescence and to arrive at conclusions as to which mechanism is mainly responsible for the temperature sensitivity of electroluminescence in these phosphors. Electroluminescence of powdered samples was measured between −180° to +150°C at various frequencies and voltages of operation. Measurements of photoluminescence were carried out on the same phosphor samples over the same temperature range. By combining photoluminescence and electroluminescence at any given temperature in a proper manner, an ideal electroluminescence was derived which is that expected if no thermal quenching were effective. Thus it was possible to consider the temperature dependence of electroluminescence due to thermal quenching and that due to an intrinsic temperature sensitivity of the ideal electroluminescent brightness separately.

The mechanism which leads to electroluminescence is believed to occur in two steps which are separated in time and space. The excitation process provides a number of electrons liberated from centers in a high field zone by field ionization and inelastic collisions. These electrons are rapidly swept out into low field zones where they become trapped. Only when the electrons return to empty luminescence centers upon field reversal (return process) does luminescence occur.

Experimental Arrangement

The phosphor powders investigated were inserted into a condenser-type cell. The phosphor was embedded in air which excluded any brightness variations due to thermal changes of the dielectric properties of the embedding medium. Premature electrical breakdown was avoided by a thin transparent film (Mylar). The thickness of this film was about 5 μ compared to ~85 μ thickness of the phosphor layer. Hence, thermal changes of the dielectric properties in the film affected the field across the phosphor particles only to a minor degree. The cell parts were made of aluminum and Teflon.

The unit in which the cell could be subjected to temperatures from −180° to +150°C is shown in Fig. 1. The cell was inserted into a copper chamber

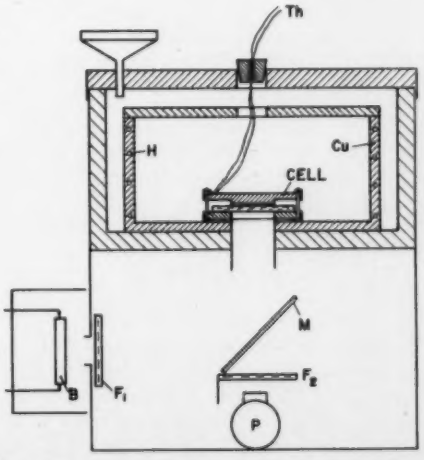

Fig. 1. Apparatus for measuring the temperature dependence of electroluminescence.

(Cu). It could be cooled by liquid N_2 or warmed by heating elements (H) in the walls. The heating current was controlled by a Variac. The phosphor in the cell was excited to luminescence either electrically or by u.v. light from a high pressure mercury lamp (B) over a semi-transparent mirror (M). An audiofrequency generator connected to a power amplifier served as a voltage source to operate the cell. The voltage applied to the u.v. lamp (B) was stabilized electronically. The u.v. intensity could be varied by varying the distance of (B) to the inlet. The light emitted from the phosphor was measured by a photomultiplier (P) (1P21) operated on a regulated power supply.

The time averaged photocurrent was measured by a Keithley vacuum tube electrometer. The temperature of the phosphor was obtained by means of a copper-constantan thermocouple (Th) screwed onto the metal back electrode of the cell. The thermo-voltage was measured by a L&N precision potentiometer. The filter F_1 transmitted only u.v. radiation in the neighborhood of 3500Å (Corning 5860). The filter F_2 cut off u.v. light and thus prevented it from falling onto the cathode of the photomultiplier. F_2 transmitted mainly between 4600-7000Å (yellowish Schott-filter). Since no vacuum was applied, care had to be taken to avoid condensation of water vapor on the glass parts of the temperature system at low temperatures. This was accomplished by inserting vessels in the cell chamber and around the photomultiplier which contained an efficient drying agent.

Elimination of Thermal Quenching

It is assumed that thermal quenching as observed with photoluminescence also occurs with electroluminescence such that the brightness tends to decrease with increasing temperature (1). One may then define the electroluminescent brightness (I_{el}) actually measured as equal to an ideal electroluminescent brightness (I_{el_0}) modified by the probability of thermal quenching of luminescence ($p_f = I_{el}/I_{el_0}$). This probability is assumed to be the same as that for photoluminescent brightness (I_f) at any temperature T. Hence

$$p_f(T) = \frac{I_{el}(T)}{I_{el_0}(T)} = \frac{I_f(T)}{I_{f_0}} \qquad (I)$$

where I_{f_0} stands for the photoluminescent brightness which is unaffected by thermal quenching and thus usually occurs only at low temperatures. Here I_{el_0} is a function of temperature because of the temperature sensitivity of pure electroluminescence but not of quenching.

Thus with Eq. (I)

$$I_{el}(T) = I_{el_0}(T) \cdot \frac{I_f(T)}{I_{f_0}} \qquad (II)$$

If the luminescence probability $I_f(T)/I_{f_0}$ were dependent only on temperature, one plot of I_f over the whole temperature range of interest would be sufficient, since $I_{el}(T)$ need be divided simply by $p_f(T)$ in order to obtain $I_{el_0}(T)$. However, p_f is also dependent on the intensity of the exciting radiation (2). This may lead to an increase of photoluminescent brightness faster than linear with increasing excitation intensity (3). More specifically, at a given temperature the effect of thermal quenching may be less pronounced at higher brightnesses I_f. This phenomenon must also be expected with electroluminescence. In order to account for this effect, not only must the ratios of Eq. (I) be considered equal but also either numerator and denominator. Hence, Eq. (II) can be written

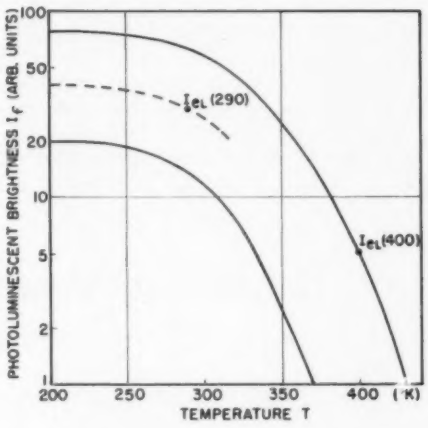

Fig. 2. Schematic procedure for finding I_{el_0} from $I_f(T)$ plots

$$I_{el}(T) = I_{el_0}(T) \frac{I_{el}(T)}{I_{f_0}}$$

or simply

$$I_{f_0} = I_{el_0}(T) \qquad (III)$$

This means that there must be a known I_f-value equal to each I_{el}-value measured at any temperature T. Consequently a series of plots of $I_f(T)$ must be taken with different exciting u.v. intensities in order to cover the whole range of the I_{el}-values at any temperature.

The principle of the procedure to determine $I_{el_0}(T)$ is illustrated in Fig. 2. For example, let an electroluminescent brightness of $I_{el} = 5$ units be measured at 400°K. Among the number of various plots of photoluminescent brightness $I_f(T)$ there must be one plot which also shows a brightness of 5 units at 400°K. The maximum brightness of this particular plot of photoluminescence then is the appropriate value of I_{f_0} (here about 80 units) according to Eq. (III). If at $T = 290$°K an electroluminescent brightness $I_{el} = 30$ units is measured and none of the $I_f(T)$-plots previously obtained goes through this I_{el}-value, the $I_f(T)$-plots must be sufficiently close to each other so that interpolation is possible. In this particular case I_{f_0} is found to be about 40 units. From these examples it becomes obvious that I_{f_0} in Eq. (III) is a function of I_{el} and one should therefore write

$$I_{f_0}(I_{el}) = I_{el_0}(T) \qquad (IIIa)$$

With this procedure a spectral emission shift with temperature which would cause a falsified response of the photomultiplier is excluded from the I_{el_0} values, since both I_{el} and I_f show about the same emission color at any given temperature (4). This, however, is true only if the frequency of the alternating field applied to the phosphor has no effect on

the emission color. Fortunately there are some single-band phosphors for which the shift of the emission color is negligible from 15 to 10,000 cps. Only those phosphors were studied here.

This procedure is based on the assumption that both electroluminescence and photoluminescence are uniformly emitted throughout the phosphor crystals. However, it has been observed (5, 6) that electroluminescence occurs preferentially in a number of single spots. Hence, the electroluminescent spot brightness is higher than the photoluminescent brightness when the electrometer connected to the photocell reads the same photocurrent. The I_{e1_0}-values obtained can, therefore, be taken only as first approximations.

Experimental Results

The temperature dependence of electroluminescence was measured on a number of powdered single-band zinc sulfide phosphors containing Cu, Cu-Pb, oxygen and Cl impurities (heating rate about 3°/min). Two of these phosphors were chosen at random and subjected to a more intensive study: WL77 (ZnS.ZnO activated with Cu and Pb, coactivated with Cl, fired in air) and WL702 (ZnS activated with Cu, coactivated with Cl, fired under special conditions).[1] At room temperature both phosphors emitted in the green nearly independent of frequency up to 10 kc. Fig 3*a* and *b* show the averaged electroluminescent brightnesses I_{e1} as functions of temperature on WL77 and WL702 at an average field strength of about 5 x 10^4 v/cm (corresponding to 400 v rms across the cell) with 15, 100, 1000, and 10,000 cps (gas discharge and breakdown did not occur below 6-7.10^4 v/cm). After the phosphors were kept at about +50°C for 1 hr, during which time the above field alternating with about 500 cps was applied, the curves proved reproducible in shape, regardless of the direction of the temperature change.

Fig 3*a* and *b* clearly illustrate the shift of the brightness curves to higher temperatures with increasing frequency. This phenomenon has been observed before by several workers (7-10). Brightness curves are less sensitive to changes of the electric field strength. In general, the brightness peaks shift but slightly to lower temperatures with increasing field strength and usually some minor changes occur on the low temperature side of the peaks.

Employing the method described above the electroluminescent brightness, I_{e1}, was converted to the ideal electroluminescent brightness, I_{e1_0}, which would exist without interference from thermal quenching of luminescence. For this purpose a set of photoluminescent brightness plots as functions of temperature was measured such that the whole scope of the brightnesses I_{e1} at any temperature was covered or at least easily accessible to extrapolation. The conversion of the I_{e1}-values to corresponding I_{f_0}-values as demonstrated in Fig. 2 was carried out in a more convenient way by plotting log (I_{f_0}) as a function of log (I_f) with the temperature T as parameter (Fig. 4). As can be seen in Fig. 4 the phosphor has acquired a linear emission at about −80°C. Below this temperature photoluminescence is constant and only upon further decrease of temperature begins to decrease slightly, which is due to changes of the u.v. absorption characteristics (2). However, this has no bearing on the present considerations of electroluminescence. Thus, I_{f_0} is assumed constant for all $T < -80°$.

The general result is consistent with both phosphors. I_{e1_0} increases steadily with increasing temperature or exhibits a tendency to saturation, but it does not decrease. Fig. 5 shows such a step-curve. Similar curves have been reported by Alfrey and Taylor (7) in temperature ranges where thermal quenching is not yet predominant. The shape of the

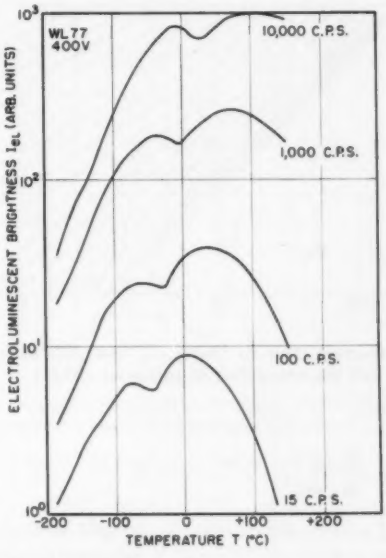

Fig. 3*a*. Electroluminescent brightness as function of temperature at 400 v rms and various frequencies. WL77.

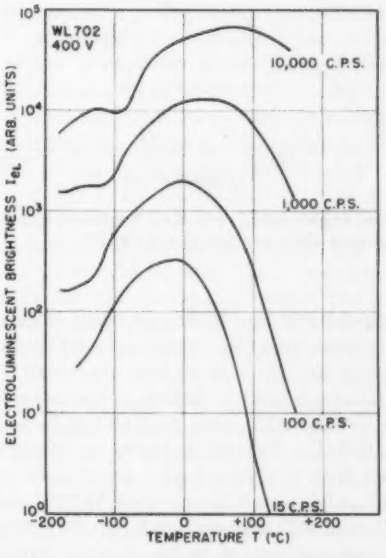

Fig. 3*b*. Electroluminescent brightness as a function of temperature at 400 v rms and various frequencies. WL702.

[1] Both phosphors were prepared by W. Lehmann in this laboratory.

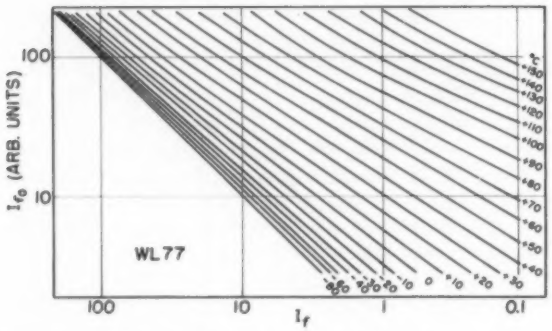

Fig. 4. Practical chart for finding I_{el_0} from plots of I_{f_0} as function of I_f with the temperature as parameter (WL77).

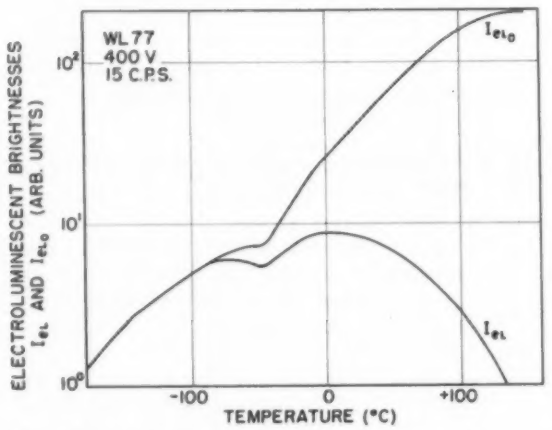

Fig. 5. Real brightness, I_{el}, and ideal brightness I_{el_0}, as function of temperature at 400 v rms and 15 cps (WL77).

$I_{el_0}(T)$-plots leads one to expect some kind of thermal activation energies which should become revealed when log (I_{el_0}) is plotted over 1000/T (°K). [A first attempt in this direction has already been made by Mattler (11) who plotted log I_{el} as a function of 1000/T.] Indeed, a series of straight lines was found with average slopes which correspond to about 0.02; 0.05; and 0.16 e.v. with WL77, and 0.006; 0.08; 0.13; and 0.24 e.v. with WL702 (Fig. 6). Sometimes the slopes ceased to be straight lines at the high temperature side of the straight lines and log I_{el_0} became only weakly dependent on 1000/T. An indication of this behavior is found in Fig. 6 near 1000/T = 4. The activation energies are dependent on frequency such that increasing frequency tends to increase the activation energies. Also, decreasing voltage shows a pronounced increase of the activation energies, and the straight lines of log (I_{el_0}) vs. 1000/T sometimes appear broken so that effectively the number of activation energies found between −180° and + 150°C seems to increase. Table I shows results obtained on both phosphors for various frequencies and voltages across the cell.

In order to compare the activation energies with the trap depths, glow curves were taken for both phosphors (*see* Fig. 7). Trap depths were calculated according to a method described by Curie and Curie (12) [heating rate ~ 2.5°/min (WL77), and

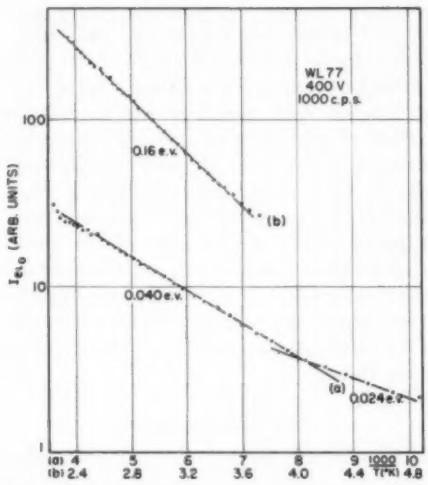

Fig. 6. Plot of log (I_{el_0}) as function of 1000/T for 400 v rms and 1000 cps (WL77).

~ 3°/min (WL702), s = 5 x 10^8 sec^{-1}]. Results are given in Table II. (The values in brackets are derived from unresolved glow peaks.)

Table III shows a correlation of the temperatures T_{max} and T_{min} at which electroluminescent brightness extrema occur, the activation energies, and the temperature ranges in which these activation energies are observed as straight lines from the plots of log I_{el_0} as a function of 1000/T for various frequencies and a voltage of 400 v rms across the cell. It will be noted that the temperature ranges in which the activation energies occur exhibit the same tendency to shift to higher temperatures with increasing fre-

Table I. Activation energies at various frequencies and voltages

WL77 Frequency (cps)	Voltage (v)	Activation energies (e. v.)			
15	400	0.024	0.035		0.15
100	400	0.022	0.038		0.17
	250	0.032	0.049		0.23
1000	400	0.024	0.040		0.16
	250	0.028	0.056		0.23
10000	400	0.025	0.055		0.16
	250	0.043	0.06; 0.105		0.25
	150	0.06	0.10; 0.12; 0.15; 0.18		0.32

WL702 Frequency (cps)	Voltage (v)	Activation energies (e. v.)			
15	400	—	0.077	0.099	0.14
100	400	0.006	0.076	0.096	0.18
	200	0.018	0.11	0.13	0.21
1000	400	0.006	0.084	0.13	0.26
	200	0.014	0.132	0.17; 0.23	0.33
10000	400	0.0095	0.094	0.27 (?)	0.36 (?)

Table II. Trap depths of WL77 and WL702

Phosphor	Trap Depths (e. v.)			
WL77	(~0.2)	0.25	(~0.3)	0.38
WL702	—	(~0.26)	0.30	(?)

Table III. Survey of experimental results with respect to temperature and frequency

Frequency (cps)	EL. brightness T_{max} (°C)	T_{min}	Activation energy (e.v.)	Temp. range of act. energy (°C)
WL77:				
15			0.02	−168 to −131
	−75		0.04	−120 to − 76
		−45		
	+ 6		0.15	− 37 to +124
100			0.02	−172 to −151
	−65		0.04	−137 to −65
		−30		
	+37		0.17	− 18 to +120
1000			0.02	−168 to −150
	−38		0.04	−142 to −13
		− 5		
	+70		0.16	+6 to +150
10000			0.03	−176 to −142
	− 9		0.06	−120 to −8
		+25		
	+100		0.16	+30 to +144
WL702:				
15			?	?
			0.08	−127 to −56
	−10		0.10	−43 to +9
			0.14	+22 to +80
100			0.006	−174 to −144
			0.08	−120 to −40
	0		0.10	−28 to +30
			0.18	+36 to +108
1000			0.006	−174 to −122
			0.08	−104 to −44
	+31		0.13	−30 to +20
			0.26	+36 to +148
10000	−123		0.01	−180 to −120
		−97		
			0.09	−84 to +12
	+72		0.27(?)	+20 to +84
			0.36(?)	+86 to +150

quencies as the extrema of the electroluminescent brightness.

Discussion and Interpretation

Ideal Brightness

If one relates the exponential factor of I_{el_0} which leads to the observation of activation energies to a thermal release process of electrons from certain centers, the activation energies appear as energy "depths" E^*. The probability p of electron escape from such centers is facilitated in the presence of an electric field (13):

$$p \propto \exp - E^*/kT = \exp - [E - f(F)]/kT \quad \text{(IV)}$$

[E, depth of center in the absence of a field; F, field strength; $f(F)$, function of field strength such that $f(F)$ increases with increasing F]. The influence of frequency on E^* is most likely due to capacitive effects. Combinations of high field regions and low field regions as exist inside the phosphor crystals form some sort of microcapacitors across which the potential drop decreases with increasing frequency. Hence increasing frequency reduces the effective field and E^* increases as observed. If now the values of Table II are compared with those of Table III, one finds that with low voltages and high frequencies the high values of E^* approach those of the trap depths

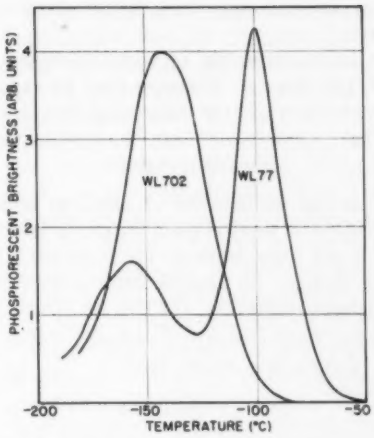

Fig. 7. Glow curves on WL77 and WL702

as determined from glow curves. Therefore, it seems justifiable to identify E in relation (IV) with a trap depth. Then the low values of E^* observed at low temperatures would correspond to traps which are too shallow to be detectable by glow curves.

The temperature behavior of electroluminescence can now be considered in a simplified model based on the action of electron traps. There is ample evidence that the essential processes of electroluminescence are confined to certain high field regions and adjacent low field regions. The high field regions may occur either in potential barriers (14) or near sharp points or edges of conducting segregations in the host crystal (e.g., Cu_2S) (15). In these regions electrons field-ionized from donors or injected electrons are accelerated and thus become able to collision-ionize luminescence centers. The electrons, quickly increasing in number, are swept out into the low field regions where the energy gain by field action is lower than the energy loss by impact. Thus the electrons become trapped to an extent determined by temperature and frequency. During this part of the process (excitation process) hardly any emission occurs, since the transit time of electrons through the high field region is extremely small (*see* Appendix). Particularly in the case of conducting segregations in the host crystals, the high field region reverses its sign with the next half-cycle of the applied voltage and conduction electrons are attracted from the low field region to the high field region where they recombine with empty luminescence centers. It is this part of the process (return process) which gives the major contribution to light emission. Experimental proof for the time-separation of excitation and return process was obtained when the buildup of electroluminescence on previously quenched phosphors was studied (16). No light emission could be observed during the first half-cycle of the voltage applied, in agreement with Waymouth and Bitter (6).

Both processes are functions of field, frequency, and temperature. The production and behavior of conduction electrons in the high field zone during the excitation process, however, probably is determined mainly by the comparatively high field and

its frequency and only to a lesser degree by temperature.

Let m be the number of traps occupied by electrons at the time t. Disregarding retrapping, the time dependence of trap emptying can then be described by

$$dm/dt = -pm$$

where p is the probability of electron escape from traps in the low field region, as given by Eq. (IV). $f(F)$ in p not only depends on time but also in an unknown fashion on spatial coordinates. However, as a first approximation, $f(F)$ is set proportional to an averaged field strength $\overline{F}$ which renders p independent of time and space. Thus

$$m = m_0 \exp(-pt)$$

where m_0 is the number of traps at the beginning of the return process and depends mainly on the excitation process, i.e., on field and frequency.

If it is assumed that each electron ejected from a trap is quickly carried away to luminescence centers in the high field zone during the time the return process is in effect, dm/dt is a measure of the momentary light emitted so that the mean emission during one half-cycle is

$$I_{el_0} \propto -2fp \int_0^{1/2f} m\, dt = 2f\, m_0(f)\,[1-\exp(-p/2f)] \quad \text{(V)}$$

$I_{el_0}(T)$ increases steadily with temperature as long as $p << 2f$, i.e.,

$$I_{el_0} \alpha\, m_0(f)p = m_0(f)s \exp -[E - \text{const}\,\overline{F}]/kT \quad \text{(Va)}$$

A straight line appears on plotting log (I_{el_0}) as a function of $1/T$. As the temperature is further increased, $p > 2f$ and I_{el_0} tends to saturation as actually observed. The temperature range in which this tendency prevails occurs at higher temperatures for higher frequencies. This agrees very well with experiment where, however, more than one activation energy appears. This is because trapping levels of different depths have different p-functions. Whenever $p_1 >> 2f$ prevails with one group of traps, the next deeper traps with $p_2 << 2f$ may begin to show in I_{el_0}.

A quantitative expression of the shift of the brightness curves to higher temperatures along the temperature scale can be derived by defining a normalized ideal brightness which is the ratio of I_{el_0} to I_{el_0} at $p >> 2f$

$$W_{T,f} = \frac{2f\, m_0(f)\,[1-\exp(-p/2f)]}{2f\, m_0(f)} = 1 - \exp(-p/2f)$$

Fig. 8 shows a schematic diagram of two plots of the normalized ideal brightness for two different frequencies. The relative brightness found at a temperature T_1 with a frequency f_1 can only be reproduced at a higher frequency f_2, if the temperature T_1 is increased to T_2 which is derived from the equality condition

$$W_{T_1,\, f_1} = W_{T_2,\, f_2}$$

or

$$1 - \exp(-p_1/2f_1) = 1 - \exp(-p_2/2f_2)$$

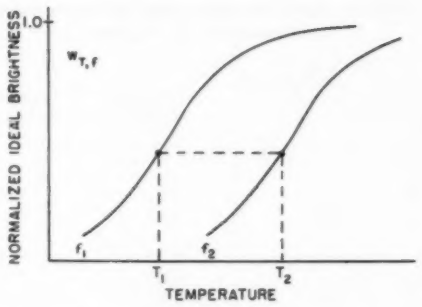

Fig. 8. Shift of the normalized electroluminescent brightness to higher temperatures with increasing frequency.

or

$$p_1/2f_1 = p_2/2f_2$$

Hence $p/2f$ is constant for corresponding points of the normalized brightness curves, so that

$$f = \text{const} \exp -E^*/kT_c \quad \text{(VI)}$$

where T_c denotes the temperatures at corresponding points. This expression was first postulated by Alfrey and Taylor and should always appear when trap emptying is time restricted by the frequency of operation. However, it is hard to find such corresponding points in the unnormalized $I_{el_0}(T)$-curves.

Real Brightness I_{el}

It is now easy to see what determines the shape of an $I_{el}(T)$-curve. In the temperature range where thermal quenching has not yet become effective, I_{el} is equal to I_{el_0}. The brightness measured will increase with increasing temperature or tend to saturation as the lifetime p_1^{-1} of electrons in a certain group of traps decreases to $p_1^{-1} << 1/2f$. Then the next deeper group of trapping levels begins to eject electrons discernibly so that I_{el} again increases. At this point let thermal quenching become effective. At first, quenching will be weak and I_{el} still increases although with a slightly lower rate. On approaching the condition $p_2^{-1} << 1/2f$, thermal quenching, however weak it may be, causes I_{el} to decrease and a brightness maximum is observed. If this last group of traps were the deepest one in the phosphor, I_{el} would decrease continuously with increasing temperature as determined by quenching. However, if a deeper trapping group exists, I_{el} can rise again, because thermal trap emptying may temporarily overcompensate thermal quenching. Therefore, a minimum of I_{el} occurs. With further temperature increase, thermal quenching gains more and more importance so that a maximum of I_{el} is observed, and then I_{el} decreases again. These conditions are illustrated in Fig. 5.

However, the life time p^{-1} not only decreases with increasing temperature but also with increasing field strength. Following this reasoning, a maximum of I_{el} should be found at a lower temperature on increasing the voltage. This could be confirmed by experiment, although with the relatively small range of voltage used the temperature shift of the brightness maxima never exceeded 10°. A good example of these conditions, however, has been given

by Mattler (4) who varied the voltage applied to his ZnS.Cu phosphors up to a factor of 6.

It was stated earlier that it is hard to find corresponding points in the unnormalized I_{el_0}-curves which relate the frequency of operation to T_c according to Eq. (VI). Exact normalization from experimental plots is difficult, especially on phosphors with several trapping groups. Therefore, one may attempt to find these corresponding points from the I_{el}-curves actually measured. The only outstanding, easily localized points are the extrema of the I_{el}-curves. However, it is not quite correct to regard these as corresponding points. As has been shown above, brightness maxima (or minima) arise from a competition process of trap emptying and thermal quenching. If, e.g., a maximum occurs at a temperature T_1 for a frequency f_1, the maximum will be shifted to $T_2 > T_1$ for a frequency $f_2 > f_1$. However, at the temperature T_2 thermal quenching is much more effective than at the lower temperature T_1. Hence, this increased effect of quenching gives a maximum occurring at the temperature T_2, which is lower than that expected from Eq. (VI). Upon plotting the maxima positions logarithmically according to Eq. (VI) one would find more or less distorted straight lines and the E-values derived from their slopes are higher than those which one would obtain from plots of exactly corresponding points.

The two maxima in WL77, and the single maximum in WL702 were treated as approximately corresponding points and plotted according to Eq. (VI). As expected, the values of E obtained are higher than the thermal activation energies of I_{el_0} and even higher than the trap depths derived from the glow curves, as can be seen in Table IV.

Summary and Conclusions

Measurements of electroluminescence and photoluminescence carried out on several zinc sulfide phosphors over a wide temperature range permitted determination of an ideal electroluminescent brightness which is unaffected by temperature quenching of luminescence. The thermal behavior of this ideal brightness seems to imply that trap emptying is the major effect of temperature on electroluminescence apart from thermal quenching. Various authors have realized the significance of electron traps [*see*, e.g., references (9, 17-21)]. However, there is still some controversy as to whether the traps in the high field region or those in the low field region are predominantly responsible for the thermal behavior of electroluminescence. The present study indicates the importance of traps in the low field region. This conclusion is based on the assumption that electroluminescence occurs in a coupled two-step process. During excitation electrons are freed in the high field zone and caught in traps in the low field zone. The number of electrons returning for luminescent recombinations is mainly determined by the rate of thermal and field release of electrons from traps. A simple model can explain the general trend of electroluminescent brightness with varying temperature and frequency.

These conclusions lead to the practical consequence that, beside other qualities, a good electroluminescent phosphor should have only a few shallow traps and no deep traps. The temperature at which thermal quenching sets in should be high. Unfortunately, the latter can be accomplished only by compromising with another essentiality. Experiment shows that good electroluminescent phosphors need a high copper concentration, but that thermal quenching sets in at a temperature which decreases with increasing copper concentration (22).

As a final comment it should be emphasized that the above explanation of trap action on electroluminescence is not all-embracing. It predicts extrema in electroluminescence-temperature curves only in temperature regions where thermal quenching is already effective. However, Johnson, Piper, and Williams (9) have shown that a ZnS.Al.Cu phosphor exhibited extrema in a temperature range far below the onset of thermal quenching. Some measurements were carried out on the same phosphor in these laboratories. This effect must be accounted for as a temporary super-position of a different temperature action on the one outlined above. Fig. 9 shows a plot of log (I_{el_0}) as a function of $1000/T$ obtained from this phosphor. It can be seen that with this phosphor straight lines (activation energies) also occur, except in the comparatively small temperature range between 150°-220°K.

Acknowledgment

The author is indebted to Dr. H. F. Ivey, Dr. B. Rosenberg, and Mr. W. Lehmann for helpful discussions, and to Dr. P. D. Johnson (General Electric Co.) for kindly supplying one of his phosphor samples.

Table IV. Activation energies derived from Eq. (VI) with T_c as temperatures of brightness maxima

	WL77	WL702
E_1 (e.v.)	~0.57	~0.55
E_2 (e.v.)	~0.7	

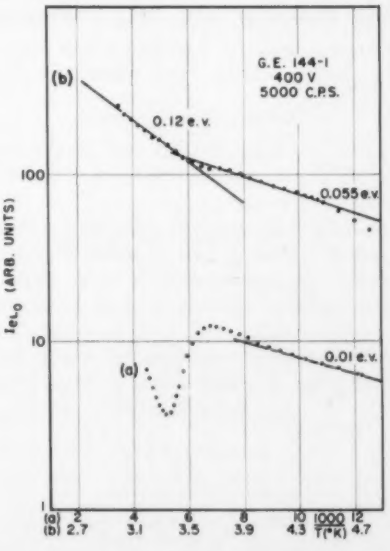

Fig. 9. Plot of log (I_{el_0}) as function of 1000/T at 400 v rms and 5000 cps (G.E. 114-1).

APPENDIX

Recombination Probability in High-Field Regions

If it is agreed that, because of inelastic scattering with lattice atoms, on the average, conduction electrons cannot exceed a kinetic energy higher than that of the band-to-band gap (23), the following energy balance is valid in ZnS

$$e\bar{F}\,\lambda_o \sim 3.5 \text{ e.v.}$$

(e, electron charge; $\bar{F}$ average electric field; λ_o, mean electron path between two exciting collisions). With $\bar{F} \sim 10^6$ v/cm

$$\lambda_o \sim 3.5 \cdot 10^{-4} \text{ cm}$$

With m^* as effective electron mass, x as distance an electron has traveled in the field-direction, and dx/dt as drift-velocity

$$\frac{m^*}{2}\left(\frac{dx}{dt}\right)^2 = e\bar{F}x$$

Integration results in

$$\tau_o = \sqrt{\frac{2m^*\lambda_o}{e\bar{F}}} = 7.10^{-14} \text{ sec}$$

as the time required for an electron to drift the distance $\lambda_o \cdot (m^* \sim m)$. If the width of a high field region is assumed to be of the order of 10^{-3} to 10^{-5} cm which is about 300 to 3 times λ_o, the transit time of an electron through this region is of the order of $\tau = 10^{-11}$ to 10^{-12} sec.

If n conduction electrons are created per cm^3 of the high field region per second, the total number of possible recombinations is n. The capture volume of one empty center available for recombinations per second is βcm^3/sec so that the total number of capture volumes per second is βn. Then the favorable number of recombinations is determined by βn, by the number of available electrons, n, and by the time τ actually available for these transitions. Hence the probability of radiative return per electron is

$$\frac{(\beta n)\, n\tau}{n} = \beta n\tau$$

With n being of the order of 10^{16} cm^{-3} or less, and $\beta = 10^{-14}$ cm^3 sec (24) this probability becomes 10^{-7} to 10^{-9} or less which indeed is negligible. [This value is in accord with findings of Zalm (24).] Consequently there should be virtually no electroluminescence during the excitation process.

Manuscript received July 12, 1956.

Any discussion of this paper will appear in a Discussion Section to be published in the December 1957 JOURNAL.

REFERENCES

1. D. Curie, *J. Phys. Radium*, **14**, 672 (1953).
2. G. F. J. Garlick, "Luminescent Materials," Oxford University Press, Oxford (1949).
3. F. Urbach, A. Urbach, and M. Schwarz, *J. Opt. Soc. Amer.*, **37**, 122 (1947).
4. J. Mattler, *J. Phys. Radium*, **17**, 42 (1956).
5. E. E. Loebner and H. Freund, *Phys. Rev.*, **98**, 1545 (1955); G. Diemer, *Philips Research Rpts.*, **10**, 194 (1955).
6. J. F. Waymouth and F. Bitter, *Phys. Rev.*, **95**, 941 (1954).
7. G. F. Alfrey and B. Taylor, *Brit. J. Appl. Phys.*, Suppl. #4, p. S44 (1955).
8. C. H. Haake, *Phys. Rev.*, **98**, 1544 (1955).
9. P. D. Johnson, W. W. Piper, and F. E. Williams, *This Journal*, **103**, 221 (1956).
10. R. E. Halsted and L. R. Koller, *Phys. Rev.*, **93**, 349 (1954).
11. J. Mattler, Private Communication.
12. G. Curie and D. Curie, *J. Phys. Radium*, **16**, 199 (1955).
13. N. F. Mott and R. W. Gurney, "Electronic Processes in Ionic Crystals," p. 42, Oxford University Press, Oxford (1948).
14. W. W. Piper and F. E. Williams, *Brit. J. Appl. Phys.*, Suppl. #4, p. S39 (1955).
15. W. Lehmann, *Bull. Am. Phys. Soc.*, II/1, 113 (1956).
16. C. H. Haake, *ibid.*, II/1, 113 (1956).
17. D. Curie, *J. Phys. Radium*, **13**, 317 (1952).
18. A. Fischer, *Physik. Verhandl.*, **5**, 64 (1954).
19. C. H. Haake, Symposium on Electroluminescence and Photoconduction in Inorganic Phosphors, Brooklyn (1955).
20. W. A. Thornton, *Phys. Rev.*, **102**, 38 (1956).
21. G. F. Neumark, *ibid.*, **103**, 41 (1956).
22. G. F. Alfrey, *Phys. Radium*, **17**, 719 (1956).
23. G. Diemer, H. A. Klasens, and J. G. Van Santen, *Philips Research Rpts.*, **10**, 401 (1955).
24. P. Zalm, *J. Phys. Radium*, **17**, 777 (1956).

Transport Numbers and Structures in Fused $AgNO_3$-$NaNO_3$ Mixtures

Frederick R. Duke, R. W. Laity,[1] and Boone Owens

Institute for Atomic Research and Department of Chemistry, Iowa State College, Ames, Iowa

ABSTRACT

The transport numbers of the ions in $NaNO_3$-$AgNO_3$ mixtures are very closely proportional to the mole fractions. The transport number of the nitrate ion remains essentially constant. It is thus concluded that there are no complex species in $NaNO_3$ or $AgNO_3$ and that all cations present are structurally in identical positions. This argues strongly against any concept except complete dissociation in this nitrate system.

A complete transport number-composition curve for a binary fused salt mixture has not been obtained previously. Such data are of much interest because transport numbers should be sensitive probes to changes in structure of salt mixtures with composition. For such a binary mixture two types of data are needed to yield a complete determination of transport numbers: Hittorf cell data concerning changes in relative composition of salt near the electrodes, and volume-change data, to determine total change in equivalents of salt in each electrode compartment. In principle, both types of data could be obtained in a single experiment of proper design, but in practice it was found simpler to perform separate experiments.

The fundamental equations relating to the Hittorf experiments were developed by Wetmore and Aziz (1) who performed some experiments on the $AgNO_3$-$NaNO_3$ mixture.

Experimental

Hittorf type of transport data was obtained by using a cell made from 4 mm ID Pyrex tubing bent into the shape of a very broad U tube. This tube was placed in a muffle furnace maintained at 305° ±5°C and was filled by pouring the molten salt into one end. Silver electrodes were inserted into the ends of the tube and about 30 coulombs of electricity passed. An alternating current of about 100 ma (five times the direct current) was superimposed to help prevent trees from growing out from the cathode. The tubes were carefully removed and cooled and cut into three parts, an anode section, a cathode section, and a short center section. These sections were analyzed by titrating the Ag^+ (Volhard) and determining the net weight of salt in each section. Only those tubes with center sections closely corresponding to the original mixture (approximately 10% of the runs) were used. Total equivalents of current were measured by using a silver coulometer.

An alternative procedure was to place an ultrafine, sintered glass membrane in the center of the U, the membrane thus corresponding to Hittorf center compartment. The two portions obtained after electrolysis and after breaking the cell at the membrane were analyzed. The use of this type of cell eliminates the overlap of the anode and cathode compartments due to convection which is found in a majority of the cells not containing the membrane.

The volume change in the electrode compartments was determined by using a modified cell similar to that described by Duke and Laity (2). The modification consisted of omitting the capillary with the bubble and measuring directly by changes in height the volume change in the electrode compartments. The moving bubble could not be used because it responds to density as well as to volume changes. The electrodes were Ag plated from aqueous cyanide onto tungsten. The level was measured in a capillary (two 1-mm capillaries were sealed to the top of each electrode compartment to facilitate filling) which constituted the upper part of each cell compartment. It was found that differences in head across the ultrafine membrane produced a slight leakage (about 0.06 cm^3/hr/cm head). This leakage was calibrated and taken into account for each run. A d-c current of about 50 ma was used, and from 5 to 10 measurements were taken over periods of 2000 sec on a given mixture. In case of pure $NaNO_3$, Ag-$AgNO_3$ electrodes were used.

Results and Discussion

Consider first the Hittorf type of experiment. For the anode compartment, $n_1 - n_{o_1} = Z - t_1 Z$, and

$$n_2 - n_{o_2} = -t_2 Z$$

where n_1 and n_2 are the final numbers of equivalents of $AgNO_3$ and $NaNO_3$, respectively, in the anode compartment after Z equivalents of current have been passed, n_{o_1} and n_{o_2} are the original number of equivalents of these salts in the anode compartment, and t_1 and t_2 are the transport numbers of Ag^+ and Na^+, respectively. A silver anode is used. Combining these equations with the following,

$$t_1 + t_2 + t_3 = 1 \qquad \text{(I)}$$

$$\frac{n_{o_1}}{n_{o_1} + n_{o_2}} = N_{o_1}, \text{ and}$$

[1] Present address, Frick Chemical Lab., Princeton University, Princeton, N. J.

Table I. Variation of ϕ with composition

N_{o_2}	ϕ
0.91	0.94
0.70	0.69
0.50	0.50
0.29	0.30

$N_{o_1} + N_{o_2} = 1$, where t_3 is the transport number of the nitrate ion and N_{o_1} and N_{o_2} are the original equivalent fractions of $AgNO_3$ and $NaNO_3$, respectively, Eq. (II) is obtained

$$\phi \equiv \frac{N_{o_2} n_1 - N_{o_1} n_2}{Z} = 1 - t_1 - N_{o_1} t_3 \qquad \text{(II)}$$

where ϕ combines all of the experimental values as a function of the transport number and can be seen to be t_2 if the reference point is the nitrate ion ($t_3 = 0$). This equation was first derived by Wetmore and Aziz (1). Notice that the reference point is not fixed by this equation which contains one degree of freedom. Values of ϕ are shown in Table I. The authors cannot account for the reasons for the discrepancy between these results and those of Wetmore and Aziz (1) on the same system.

The volume change equations for the anode are:

$$V_a = (1 - t_1)\, Z\, \overline{V}_{AgNO_3} - t_2 Z\, \overline{V}_{NaNO_3} - Z\, V_{Ag} \qquad \text{(III)}$$

where the $\overline{V}$'s are the partial molal volumes in the mixture, and V_{Ag} is the equivalent volume of silver. Then Eqs. (I), (II), and (III) may be solved for the transport numbers t_1, t_2, and t_3, if n_1, n_2, Z, V_a, $\overline{V}_{AgNO_3}$ and $\overline{V}_{NaNO_3}$ and the original compositions are known. Eq. (III) combined with (I) and (II) fixes the reference point as being the porous disk; this point is a fixed point in the liquid providing the liquid is not allowed to leak past the disk due to pressures caused by gravitational head and momentum changes at the disk. Any leakage must be properly calibrated and taken into account. Another possibility is that the disk affects the transport numbers by preferential adsorption of an appreciable fraction of one of the ions; this seems unlikely in view of the small surface to volume ratio inside the disk, and in this work it is assumed that the disk has no preferential effect. The volume changes observed are listed in Table II.

Table II. Volume changes in the anode compartment of the cell using mixtures of $AgNO_3$ and $NaNO_3$

No_2	$V_a \times 10^{+3}$ (cc)	$Z \times 10^3$ (Equivalents)
1.00	2.0 ± 2.0	1.00 ± 0.03
0.73	-1.0 ± 3.0	0.52 ± 0.03
0.50	0.7 ± 0.3	0.52 ± 0.03
0.30	$+0.6 \pm 0.6$	0.52 ± 0.03
0.00	$+1.0 \pm 3.0$	0.52 ± 0.03

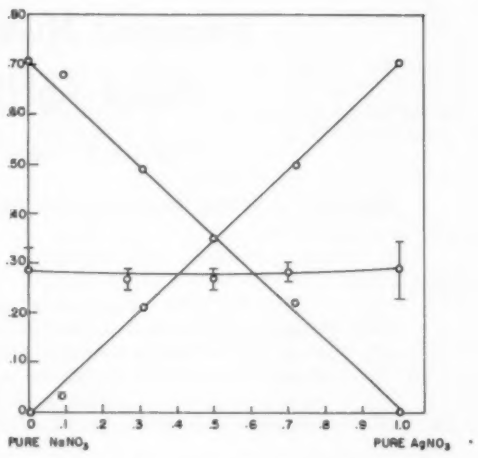

Fig. 1. Transport numbers vs. composition in $AgNO_3$-$NaNO_3$ mixtures.

The results of Byrne, Fleming, and Wetmore (3) on densities and total conductivities show that the molal volumes are essentially identical to the molar volumes ($V_1 = 43.86$ cc and $V_2 = 44.43$ cc), and, combined with the authors' results, show that the mobilities of the ions are constant (total conductivity being linear and almost constant with composition). The final results are shown in Fig 1. The lack of dependence of mobility on composition, mobility being t/X where X is the ion fraction, shows that there is no systematic change in the character of either salt when diluted with the other. If complex ions or incomplete dissociation were present, one would expect a change in mobility at low concentrations due to a change in degree of dissociation under these conditions. Thus it has been shown by nonthermodynamic considerations that these fused nitrates essentially are completely dissociated in mutual mixtures and the pure salts.

Manuscript received August 16, 1956. This paper was prepared for delivery before the San Francisco Meeting, April 29-May 3, 1956. This is Contribution No. 482; the work was performed in the Ames Lab. of the U. S. Atomic Energy Commission.

Any discussion of this paper will appear in a Discussion Section to be published in the December 1957 JOURNAL.

REFERENCES

1. P. M. Aziz and F. W. Wetmore, *Can. J. Chem.*, **30**, 779 (1952).
2. F. R. Duke and R. W. Laity, *J. Phys. Chem.*, **59**, 549 (1955).
3. J. Bryne, H. Fleming, and F. W. Wetmore, *Can. J. Chem.*, **30**, 922 (1952).

The Mechanism of Titanium Production by Electrolysis of Fused Halide Baths Containing Titanium Salts

J. G. Wurm, Lucien Gravel, and Roger J. A. Potvin

Laval University, Quebec, Quebec, Canada

ABSTRACT

Titanium was produced by electrolyzing a molten bath of a sodium and potassium chloride mixture containing potassium fluotitanate, K_2TiF_6, and sodium fluotitanate, Na_2TiF_6. The formation of trivalent titanium double fluorides of sodium and potassium always preceded the production of metallic titanium during the electrolysis. These new trivalent titanium compounds were positively identified as K_2NaTiF_6, K_3TiF_6, and Na_3TiF_6. Free metallic sodium was deposited at the same time as titanium when using a cooled cathode. This fact together with the measured polarization voltage and the presence of trivalent titanium compounds indicate that production of metallic titanium proceeds by secondary reactions in two steps: first, tetravalent titanium is reduced to the trivalent state; second, trivalent titanium is finally reduced to metallic titanium.

Metallic titanium may be produced by electrolysis of potassium fluotitanate, K_2TiF_6, or sodium fluotitanate, Na_2TiF_6, in fused halide baths under argon cover. However, due to lack of protective atmosphere during the electrolysis, several experimenters (1, 2) failed to produce Ti by this method. For similar reasons (3) the formation of some titanium oxyfluoride compounds was observed while conducting electrolysis in open tubes.

Recently, positive results were obtained (4) on the production of Ti metal by electrolyzing, under an argon atmosphere, potassium fluotitanate K_2TiF_6 dissolved in NaCl; the outstanding industrial possibilities of this process have been shown.

The present authors (5) reported some of their results on the production of Ti by electrolysis of sodium and potassium fluotitanates in a mixture of fused sodium and potassium chlorides conducted in an argon atmosphere, and they have shown that this electrolysis lent itself very well to the study of the mechanism of the reaction involved in the production of metallic Ti.

In the present work, special attention has been paid to the determination of polarization voltages and of intermediary compounds appearing during electrolysis in order to find out more definitely by which steps the production of Ti occurred and also to verify if Ti was produced directly by electrolysis as a primary product or if it was the result of a secondary reaction between Ti compounds and Na formed as a primary deposit.

Experimental

Electrolysis was studied in graphite cells with ordinary or water cooled cathodes and also in U-shaped fused quartz cells using either a normal cathode or a rotating cathode with a dry salt injection system. Polarization voltage considered as the back emf of the over-all reaction was measured by the interruptor-commutator method using an electronic voltmeter.

Gases were analyzed in a mass spectrometer for chlorine and fluorine. The cathode products and the residual melt were submitted to a combined chemical, spectrographic, and x-ray analysis.

The electrolytic cell.—Fig. 1 represents a section through the furnace and the electrolytic graphite cell. The furnace has chromel wire heating elements with automatic temperature control. The graphite cell is the anode and is located in a closed gas-tight stainless steel cylinder. The central cathode is interchangeable. Argon gas is introduced through the top by means of an Inconel tube down to the crucible.

Fig. 2 shows a U-shaped tube used as a second cell; it is made of transparent fused quartz in order to follow the color change during the melt and the electrolysis. The electrodes are removable and both compartments of the U tube are flushed with a continuous flow of argon. Fig. 3 gives a detailed view of a similar cell with a rotating cathode and a dry salt injection system under argon atmosphere. In Fig. 4, more details are shown of the rotating cathode and the mercury seal and contact.

Results

The first experiments dealt with two series of electrolyses in which the fused bath mixtures consisted essentially of NaCl and KCl but differed by the addition either of potassium fluotitanate or sodium fluotitanate in the proportion of 20-30% as indicated in Tables I and II. These experiments were conducted in a graphite crucible maintained at 650°C or 700°C using a Mo cathode except in a few cases where it was replaced by a stainless steel water-cooled cathode.

In Series F, the voltage applied on the cell was between 3.80 and 4.5 v and the current between 9 and 15 amp. The polarization voltage measured between 2.60 and 2.80 v. The gas evolved was mainly chlorine containing but a trace of fluorine.

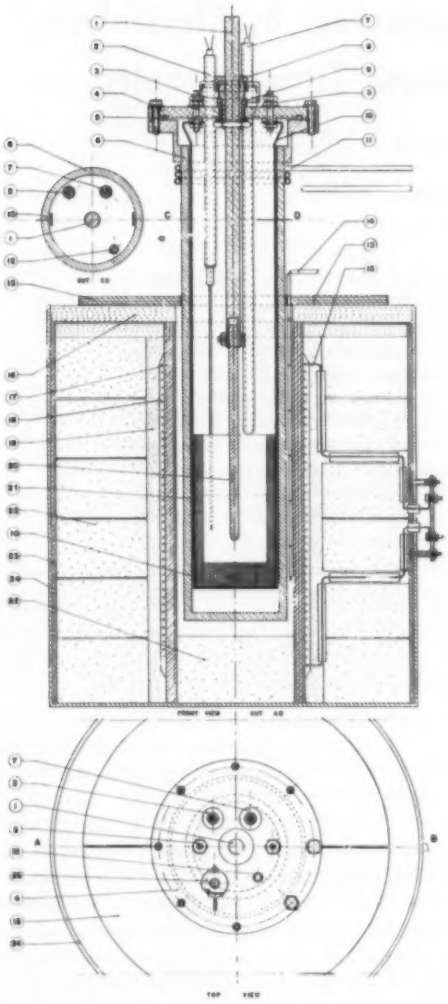

Fig. 1. Furnace and electrolytic cell. 1. cathode support; 2. Pt-PtRh thermocouple; 3. anode connections; 4. bolted lid (brass); 5. rubber seal; 6. stainless steel cylinder; 7. chromel-alumel thermocouple; 8. adjusting nut for electrode; 9. asbestos insulation; 10. stainless steel crucible support; 11. cooling spiral; 12. Argon inlet (stainless steel); 13. asbestos cover; 14. thermocouple for furnace control; 15. heating element (chromel); 16. alundum cement; 17. fused alumina tube; 18. refractory cement; 19. Sil-O-Cel; 20. stainless steel cathode; 21. graphite crucible; 22. refractory bricks; 23. asbestos; 24. furnace shell; 25. Argon outlet control valve.

In the second series, Series N, the applied voltage on the cell varied from 4.5 to 5.2 v with a current of 15-20 amp; polarization voltage was somewhat lower than in the first series, but it increased to 3.05 v when a water-cooled electrode was used. The gas evolved contained chlorine and appreciable amounts of fluorine in comparison with Series F.

Electrolytic Products

After cooling the melt, it was separated from the crucible as a cylindrical solid mass surrounding the cathode. When cut in half, it showed a section comprising two well-defined zones: (*a*) a spherical "nut" or ball around the cathode where metallic Ti crystals were embedded in a deep violet salt, and (*b*) a residual frozen melt of white salt with a light violet shade.

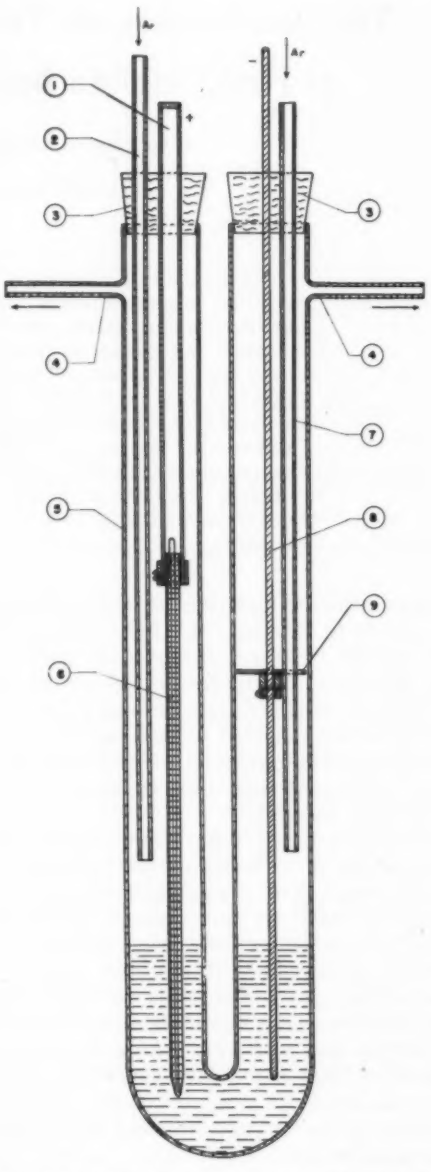

Fig. 2. U-tube cell with normal electrodes. 1. anode holder; 2. Argon inlet; 3. rubber stopper; 4. Argon outlet; 5. quartz U-shaped tube; 6. graphite anode; 7. Pyrex tube; 8. stainless steel cathode; 9. cathode guide.

After separating these two zones mechanically they were analyzed by physical and chemical methods.

The cathode "nut" proved to be Ti metal interlocked with a titanium fluoride compound which had never been described before in the literature. This deep violet compound was present invariably in all electrolyses mentioned above as it was established by x-ray diffraction.[1] It was isolated and analyzed spectrographically and chemically. Its formula was found to be K_2NaTiF_6 (compound A). K_2NaTiF_6 may

[1] Tracings have been deposited as Document 5134 with the ADI Auxiliary Publications Project, Photoduplication Service, Library of Congress, Washington 5, D. C. A copy may be secured by citing the Document number and by remitting $1.25 for a photoprint or for a 35-mm microfilm. Advance payment is required. Make check payable to: Chief, Photoduplication Service, Library of Congress.

Table I. Typical electrolyses of Series F

N°	Bath composition, g	Volts:cell	Amps:cell	Volts: polarization	Temp, °C	Amp-hr	Gas evolved	Analyses: Cathode* products	Analyses: Residual† melt
F3	NaCl —35.2 KCl —44.8 K_2TiF_6—20	3.75	8	2.82	660	10	Cl F (minor)	Ti K_2NaTiF_6	NaCl-KCl (major) NaF (minor) K_2NaTiF_6 (minor)
F14	NaCl —35.2 KCl —44.8 K_2TiF_6—20	4.40	15	2.85	690	17.5	Cl F (minor)	Ti K_2NaTiF_6	NaCl-KCl (major) NaF (minor) K_2NaTiF_6 (minor)

* NaCl-KCl and some NaF leached out with H_2O.
† No KCl or K_2TiF_6 and also no free TiF_3 or divalent titanium compounds could be detected.

be written 2KF, NaF, TiF_3 to indicate better that the K and Na contents are constantly in the ratio 2:1 and that the Ti is trivalent.

Compound A was also identified in the residual melt where it was present in smaller amounts, together with an excess of KCl, NaCl, and some NaF. It should be emphasized that no KF, nor TiF_3, nor divalent compounds could be detected; neither could any of the potassium and sodium fluotitanates added at the start of the electrolysis be detected.

Based on the spectrographic and chemical data alone, compound A could well have been a mixture of two other trivalent fluoride compounds, K_3TiF_6 (compound B) and Na_3TiF_6 (compound C), in the ratio 2:1.

Since compounds B and C are not described in the literature, it was necessary to synthesize them by electrolyzing two different melts which contained the tetravalent titanium fluoride compounds in the chloride salts and in which either solely sodium ions or solely potassium ions were present. The compositions of these melts are shown in Table III including also the conditions of the electrolysis of both types of melts. Although chlorine was evolved abundantly during the process, no fluorine could be detected with the mass spectrometer. Furthermore, in these two series of experiments, Ti was produced at the cathode interlocked with a dark violet salt. In the sodium bearing melt, this salt was identified by x-ray, spectrographic and chemical analysis as Na_3TiF_6 (compound C). In the potassium bearing melt it was identified as K_3TiF_6 (compound B).

Some important physical characteristics of the three new compounds A, B, and C are given in Table IV. From x-ray diagram tracings, it was found that compound A has a well-defined face-centered cubic lattice with a 8.374Å parameter and compounds B and C have a close to cubic structure distinctly different from compound A.[2]

Electrolysis with Water-Cooled Cathode

Another series of electrolysis was conducted in the graphite crucible using a water-cooled cathode. Operating conditions (Table V) were approximately the same as in the two series, mentioned previously, except for the total ampere-hours. Use of the cooled cathode produced a temperature gradient and made it possible to freeze out Na which was deposited as a primary product even at the very start of the electrolysis.

As expected with a cooled cathode, polarization voltage was higher than in the first series. Also, there was an excess of titanium salts in all the residual melts, indicating that Na was not formed at the end of the electrolysis on account of the exhaustion of titanium bearing raw materials in the electrolytic bath. If this had been the case, the polarization voltage would have shown a large increase and would have corresponded to the polarization voltage of NaCl which, for this low temperature, may be estimated at approximately 3.8 v.

As a blank run, a bath of the same composition as the above electrolytic melts was submitted to simple fusion without electrolysis and kept at 700°C for 5 hr. Traces of chlorine were evolved and appreciable amounts of K_2NaTiF_6 could be detected in the

[2] More details on the characteristics of these compounds will be published in a paper by Norman F. H. Bright, J. F. Rowland, and J. G. Wurm.

Table II. Typical electrolyses of Series N

N°	Bath composition, g	Volt: cell	Amp: cell	Volt: polarization	Temp, °C	Amp-hr	Gas evolved	Analyses: Cathode* products	Analyses: Residual† melt	Cathode
N2	NaCl — 87.75 KCl —111.9 Na_3TiF_6— 49.5	4.2	16.0	2.30	675	24	Cl F	Ti K_2NaTiF_6 unidentified minor	NaCl-KCl (major) NaF (minor) K_2NaTiF_6 (minor)	Mo wire
N7	NaCl — 87.75 KCl —111.90 Na_3TiF_6— 49.50	5.2	20.0	3.05 3.01	670	30	Cl F	Ti K_2NaTiF_6 unidentified minor (Na)	NaCl-KCl (major) NaF (minor) K_2NaTiF_6 (minor)	Stainless steel water-cooled

* NaCl; KCl; NaF; leached out with H_2O.
† No KF or Na_3TiF_6 also no free TiF_3 or divalent titanium compounds could be detected.

Table III. Typical electrolyses of Series S

N°	Bath composition, g	Graphite crucible as anode, stainless steel cathode						Analyses	
		Volt:cell	Amp:cell	Volt: polarization	Temp, °C	Amp-hr	Gas evolved	Cathode products	Residual melt
S1	NaCl —200 Na_2TiF_6— 50	4.3	20	2.60	820	20	Cl	Ti Na_3TiF_6 no Na_2TiF_6	NaCl (major) Na_3TiF_6 NaF (small minor)
S4	NaCl —200 K_2TiF_6— 50	5	25	2.87	780	25	Cl	Ti K_3TiF_6 K_2TiF_6 (minor)	KCl (major) K_3TiF_6 K_2TiF_6 (minor) KF (small minor)

melt. This proves that the reduction of the tetravalent titanium to the trivalent titanium in the complex fluoride starts as a chemical reduction by simple heating.

Fig. 5 is a photograph and matched drawing of a typical section through a spherical cathode nut; concentric zones are clearly visible showing compound A around the cathode with a well-defined zone of small Ti crystals and of larger crystals and also an external layer of compound A. At lower current density (5 amp/cm^2), the Ti crystals were of compact form as shown in Fig. 6, while at higher current density (10 amp/cm^2), they had a dendritic form (Fig. 7).

Current efficiency.—Typical current efficiencies obtained during electrolysis of K_2TiF_6 and Na_2TiF_6 in fused KCl-NaCl baths are given in Table VI.

Electrolysis in U-Shaped Tubes

With a U-shaped tube, it is possible to prevent recombination of cathode and anode products and to obtain more precise measurements of the polarization voltage.

In Tables VII and VIII are given the operating conditions used during the electrolysis in U-tubes. In the first series of electrolyses, bath composition and general conditions were approximately the same as in graphite cells with ordinary cathodes.

However, in the second of these series, only sodium and potassium chlorides were present at the start. This made is possible to measure polarization voltage when Na was produced under a given set of conditions and, also, to follow the polarization voltage when potassium fluotitanate K_2TiF_6 was injected subsequently in the cathode compartment already containing the electrodeposited metallic Na. The effect of rotating the cathode during these measurements was also ascertained.

Fig. 8 records the voltage applied in the cell and the corresponding amperage before and after injection of K_2TiF_6. The first curve shows that the current could not exceed 3 amp before injection due to the anode effect and to metallic sodium entering the melt; the resulting unstable condition was aggravated on attempting to raise the applied voltage

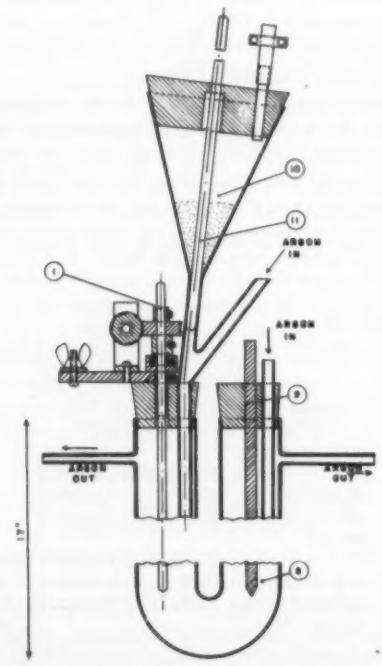

Fig. 3. Dry salt injection system

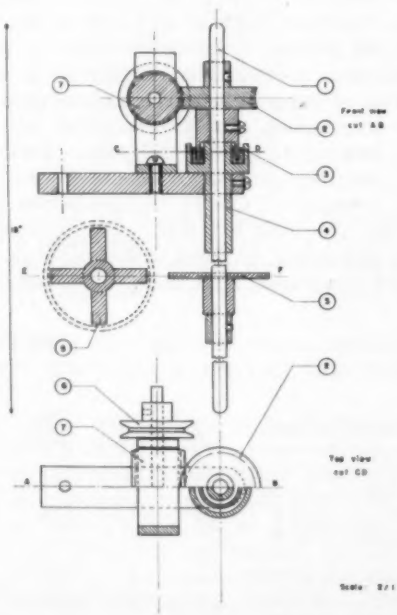

Fig. 4. Details of rotating electrode and mercury seal. 1. rotating electrode (stainless steel); 2. gear; 3. mercury container; 4. brass support; 5. cathode guide; 6. pulley; 7. worm gear; 8. U-shaped quartz tube; 9. graphite anode; 10. feeder (Pyrex); 11. glass stopper.

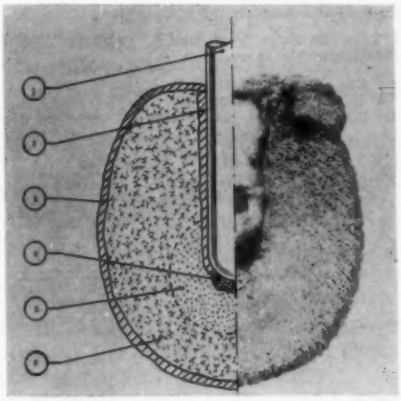

Fig. 5. Section through a cathode ball. 1. Water cooled stainless steel cathode; 2. and 3. layers of violet salt rich in K_2NaTiF_6 with some minor amounts of residual melt; 4. metallic Na embedded in residual melt; 5. fine Ti crystals with some K_2NaTiF_6 and residual melt; 6. large Ti crystals with small amounts of K_2NaTiF_6 and residual melt.

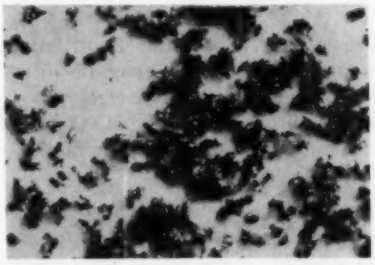

Fig. 6. Compact Ti crystals obtained with a current density at the cathode of 5 amp/cm².

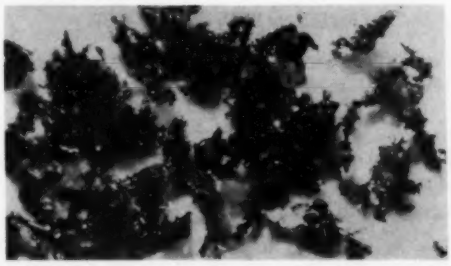

Fig. 7. Dendritic Ti crystals obtained with a current density at the cathode of 10 amp/cm².

whence the amperage dropped to a very low value. Immediately after injecting K_2TiF_6, the stability of the bath was improved considerably and the applied voltage and the corresponding current could be raised. At the same time, there was a sharp drop in the polarization voltage due to a secondary reaction between the Na present and the injected Ti bearing

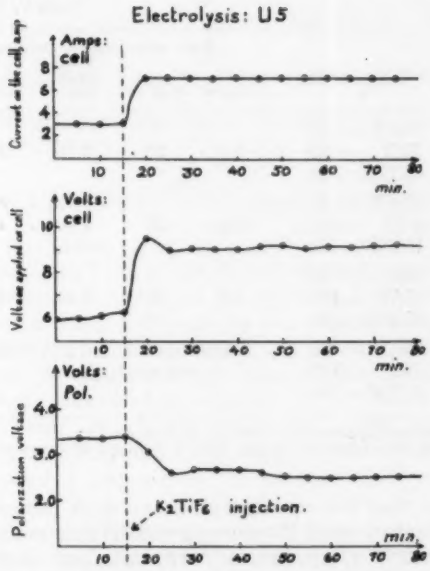

Fig. 8. Amperage and applied voltage on the cell and the corresponding polarization voltage before and after injection of K_2TiF_6 in a fused KCl-NaCl bath.

salts to produce metallic Ti as may be inferred from the constant value of 2.35 v which was reached by the polarization voltage. This voltage is close to the theoretical value calculated from the free energy change of the simplified reaction:

$$TiF_6 + 3NaCl \rightarrow Ti + 3NaF + 3/2\ Cl_2$$

which is 2.26 v at 680°C.

It should be emphasized that the melt turned violet immediately after the injection, indicating the formation of the trivalent fluoride compound at the very start much before the polarization voltage attained a constant value.

Interpretation of Results

Reaction in the Melt and Dissociation

The foregoing results show that in the early stage of melting and during electrolysis the following reaction takes place:

$$K_2TiF_6 + NaCl \overset{a}{\rightleftharpoons} K_2NaTiF_6 + 1/2\ Cl_2 \qquad (I)$$

The marked stability of the compound K_2NaTiF_6 points to a high heat of formation which favors reaction (I) in direction "a". Furthermore it may be seen in this reaction that the potassium fluotitanate must necessarily undergo ionization, that the radical (TiF_6) is carried along in the products and,

Table IV. Some physical characteristics of new compounds A,B,C

	Compound	Structure	Refractive indices	Cell-edge	Solubility in H_2O
A	K_2NaTiF_6	Face-centered cubic	1.408	8.374Å	Little soluble
B	K_2TiF_6	Close to cubic	(ω) 1.406 (e) < 1.406	—	More soluble in hot water with hydrolysis
C	Na_2TiF_6	Close to cubic	(ω) 1.387 (e) 1.382	—	Slightly soluble in hot water

Table V. Typical electrolyses of Series F

N°	Bath composition, g	With water cooled, stainless steel as cathode, graphite crucible as anode: Volt:cell	Amp:cell	Volt: polarization	Temp, °C	Amp-hr	Gas evolved	Cathode* products	Analyses: Residual† melt
F16	NaCl — 88 KCl —122 K_2TiF_6— 50	5.0	20	3.10	675	20	Cl F (minor)	Ti K_2NaTiF_6 (Na)	NaCl-KCl (major) NaF (minor) K_2NaTiF_6 (minor)
F17	NaCl — 88 KCl —122 K_2TiF_6— 50	6.0	30	3.15 3.40 (end)	660	30	Cl F (minor)	Ti K_2NaTiF_6 (Na)	NaCl-KCl (major) NaF (minor) K_2NaTiF_6 (minor)
F18	NaCl — 88 KCl —122 K_2TiF_6— 50	5.5	25	3.10	670	9	Cl F (minor)	Ti K_2NaTiF_6 (Na)	NaCl-KCl (major) NaF (minor) K_2NaTiF_6 (minor)
F19	NaCl — 88 KCl —122 K_2TiF_6— 50	Blank melt, fused at 700°C not electrolyzed					Cl No F	—	NaCl-KCl (major) K_2TiF_6 K_2NaTiF_6 (minor)

* NaCl-KCl, some NaF and Na leached out.
† No KF or K_2TiF_6, no free TiF_3 or divalent Ti compounds could be detected.

finally, that the tetravalent titanium is reduced to the trivalent state. However, from the data presented in Table V (Experiment F-19) and also in Table VII (Experiment U-3), it becomes evident that reaction (I) is slight in direction "a" when it is taking place by simple melting, but it will be greatly accelerated and rapidly completed by the passage of the current according to the equation:

$$K_2TiF_6 + NaCl \xrightarrow{e} K_2NaTiF_6 + 1/2\ Cl_2 \qquad (Ia)$$

It follows that K_2TiF_6 in the melt is not dissociated according to the equation:

$$K_2TiF_6 \rightleftharpoons 2K^+ + 2F^+ + TiF_4$$

since TiF_4, due to its high vapor pressure, would have showed up in the gaseous products. Apparently, this compound does not follow the same type of dissociation as cryolite (Na^+, F^-, and AlF_3). It follows therefore that the potassium fluotitanate dissociates as follows:

$$K_2TiF_6 \rightleftharpoons (TiF_6)^{--} + 2K^+ \qquad (II)$$
$$\Downarrow e$$
$$(TiF_6)^{---}$$

The dissociation of sodium fluotitanate Na_2TiF_6 follows a similar pattern as may be inferred from the products found after the electrolysis.

By analogy with K_2TiF_6 and Na_3TiF_6, dissociations of the trivalent titanium compounds may be written:

$$K_3TiF_6 \rightleftharpoons (TiF_6)^{---} + 3K^+ \qquad (III)$$

$$Na_3TiF_6 \rightleftharpoons (TiF_6)^{---} + 3Na^+ \qquad (IV)$$

$$K_2NaTiF_6 \rightleftharpoons (TiF_6)^{---} + Na^+ + 2K^+ \qquad (V)$$

That the possible alternative dissociation

$$M_2TiF_6 \rightleftharpoons TiF_3 + 3M^+ + 3F^-$$

does not take place is also confirmed by the absence of TiF_3 in the melt or in the gas evolved.

Mechanism of Electrolysis

First step.—Reduction of tetravalent to trivalent titanium.

(*A*) K_2TiF_6 in NaCl-KCl

Since metallic Na was found from the very start of the electrolysis it appears evident that the primary electrolytic reaction may be written

$$NaCl \rightarrow Na + 1/2\ Cl_2 \text{ (primary electrolytic reaction)} \qquad (VI)$$

followed by the secondary reaction

$$Na + K_2TiF_6 \rightarrow K_2NaTiF_6 \qquad (VII)$$

Table VI. Current efficiency

Electrolyses of NaCl—KCl—K_2TiF_6 (50 g)
Graphite crucible anode, stainless steel cathode

No.	Volt: cell	Amp: cell	Temp, °C	Cathode current densities, amp/cm²	Amp-hr	Current efficiency, %
F21	4.9	25	710	5.3	22.9	48.5
F22	5.1	30	680	6.3	27.5	41.3
F23	4.8	20	710	4.2	20	43.6
F24	4.85	25	700	5.3	22.9	47.2

Theoretical yield: 0.44 g Ti/amp-hr

Table VII. Typical electrolyses in U-shaped quartz tubes

Bath composition: NaCl—KCl—K_2TiF_6 (20%)
Cathode: stainless steel; anode: graphite

No.	Volt:cell	Amp:cell	Temp, °C	Polarization voltage
U3	7.0	7.0	680	2.40 2.50

Important observations before electrolysis: (a) color change of the melt: to violet; (b) significant amounts of chlorine evolved.

Table VIII. Typical electrolyses in U-shaped quartz tubes

Bath composition: NaCl--KCl, initial K_2TiF_6 injected after 15 min adding up to 20% of the total bath
Cathode: stainless steel; anode: graphite

No.	Cathode	Volt: cell	Amp: cell	Temp, °C	Polarization volt. before injection v	Polarization volt. after injection v
U2	Rotating	7.5	7	680	3.40	1.95-2.0
U3	No rotation	9.2	7	682	3.40	2.35

the latter is contributory to increasing the K_2NaTiF_6 formed by reaction (I) and predominantly (I*a*) and is the first step in the reduction of Ti.

The main features of the spherical cathode nut as illustrated in Fig. 5 may now find a logical explanation which at the same time brings further proof that the reactions written in (I), (I*a*) and (VII) actually take place at the same time. In fact, the outer concentric zone of the K_2NaTiF_6 violet salt is a visual proof that there is an advancing front of the trivalent compound formed to a large extent by reaction (I) and (I*a*) while, in the immediate vicinity of the cathode where Na tends to deposit before flowing down toward the end of the electrode, the K_2NaTiF_6 violet salt is formed nearly exclusively by way of reaction (VII).

(*B*) Na_2TiF_6 in NaCl-KCl

It should be noted that when Na_2TiF_6 instead of K_2TiF_6 is added to a NaCl-KCl bath the observed compound K_2NaTiF_6 formed during the electrolysis may possibly find its origin in the two different processes illustrated below.

First possibility

$$Na_2TiF_6 + 2KCl \overset{a}{\rightleftharpoons} K_2TiF_6 + NaCl \qquad \text{(VIII)}$$

b) $\Downarrow$ + NaCl

$K_2NaTiF_6 + 1/2\ Cl_2$

[as in (I) and also as in (VII)]

Although on thermodynamic basis, reaction (VIII) should be slight in direction (a), it is increased considerably by the formation (b) of the very stable compound K_2NaTiF_6.

Second possibility

The primary cell reaction (VI) $NaCl \rightarrow Na + 1/2\ Cl_2$ followed by the secondary reaction

$$Na_2TiF_6 + Na \rightarrow Na_3TiF_6 \qquad \text{(IX)}$$

However, this Na_3TiF_6 found as a free compound in the absence of potassium ions, as for instance in the electrolysis S_1, could not be detected in the presence of KCl. This indicates how strongly the following reaction takes place

$$Na_3TiF_6 + 2KCl \rightarrow K_2NaTiF_6 + 2NaCl \qquad \text{(X)}$$

(*C*) Na_2TiF_6 in NaCl and K_2TiF_6 in KCl

In the series S_3 of bath composition Na_2TiF_6 — NaCl the intermediary product Na_3TiF_6 was formed during the electrolysis by a reaction similar to (IX).

Furthermore, in series S_4 made by electrolyzing a bath of K_2TiF_6 in KCl, the intermediary product K_3TiF_6 similarly may be explained by a reaction of the same type as (IX).

$$K + K_2TiF_6 \rightarrow K_3TiF_6 \qquad \text{(XI)}$$

where K is the primary product of electrolysis in the absence of Na ions.

Second step.—Reduction of trivalent titanium to the metallic state.

The second step proceeds directly from the trivalent state to metallic Ti and may be explained by a series of two boundary mechanisms according to the following equations

$$3NaCl \overset{3e}{\rightarrow} 3Na + 3/2\ Cl_2 \qquad \text{(VI}a\text{)}$$

$$K_2NaTiF_6 + 3NaCl \overset{3e}{\rightarrow} Ti + 4NaF + 2KF \qquad \text{(XII)}$$

which may be written as an over-all electrolysis reaction as follows

$$K_2NaTiF_6 + 3NaCl \overset{3e}{\rightarrow} Ti + 4NaF + 2KF + 3/2\ Cl_2 \qquad \text{(XII}a\text{)}$$

Reaction (VI*a*) is the initial primary electrolytic reaction. In presence of the compound K_2NaTiF_6, it is immediately followed by the depolarization reaction (XII). This phenomenon in fact has been noticed and measured in particular in the U-tube cell with a delayed injection of K_2TiF_6. The use of a cooled cathode actually introduced a delay between reactions (VI*a*) and (XII) so that some metallic Na remained unreacted on the cathode after electrolysis.

In zone 5 of Fig. 5 Na diffuses more slowly in the partially cooled molten mass in the vicinity of the cathode and thus gives rise to finer Ti crystals according to reaction (XII). In zone 6 on the contrary, formation of dendritic crystals would result predominantly from the over-all electrolytic reaction (XII*a*). This difference between the size of the deposited Ti crystals was less marked when ordinary uncooled cathodes were used; in this latter case it appears that Ti was produced mostly under dendritic form by the over-all electrolytic reaction (XII*a*).

Another plausible intermediary step involving the reaction of trivalent into divalent titanium was discarded as of major occurrence since it would not be in agreement with the measured polarization voltages and, furthermore, would have given rise to divalent titanium compounds which could not be detected in the products.

Since appreciable quantities of KF were not found in the reaction products, it follows that the KF formed by equation (XII) reacts readily with the NaCl present in the bath as follows

$$KF + NaCl \rightarrow NaF + KCl \qquad \text{(XV)}$$

Hence the over-all cell reaction of this second step may be summarized by the following equation

$$2KF \cdot NaF \cdot TiF_3 + 5NaCl \overset{3e}{\rightarrow} Ti + 6NaF + 2KCl + 3/2Cl_2 \qquad \text{(XVI)}$$

The small amounts of fluorine detected in some of the experiments may be explained by traces of NaF participating in the primary reduction ($NaF \rightarrow Na + 1/2\ F_2$).

Conclusions

From the foregoing discussion, it may be concluded that the potassium and sodium trivalent titanium fluoride compound K_2NaTiF_6 or its parent compounds of the type M_3TiF_6 are always formed in the first stage of metallic Ti production upon electrolysis of fluotitanates in fused halide baths. The knowledge of the important part played by these trivalent fluoride compounds during electrolysis will lead to a better insight and a better control of the conditions

of Ti production and may possibly open the field to direct plating of Ti from baths containing these compounds, to refining and recovery processes using soluble impure Ti anodes.

Acknowledgment

The authors wish to express their indebtedness to the Defense Research Board of Canada for financial assistance. They also wish to thank Dr. J. Convey, Director, Dr. K. W. Downes and Dr. T. R. Ingraham, of the Bureau of Mines and Technical Surveys, Ottawa, for their continued interest and support. In addition appreciation is expressed to Dr. N. H. Bright from the above Bureau of Mines for his able collaboration in the crystal analysis of the new compounds.

REFERENCES

1. J. De Bussy, *Compt. rend.*, **36**, 540 (1853).
2. S. I. Sklyarenko and J. Lipkes, *Zhur. Priklad. Khim.*, **13**, 51 (1940).
3. P. Drossbach, *Z. Elektrochem.*, **57**, 548 (1953); **58**, 686 (1954); **59**, 512 (1955).
4. M. A. Steinberg, S. S. Carlton, M. E. Sibert, and E. Wainer, *This Journal*, **102**, 333 (1955).
5. Annual Reports of 1954 and 1955 to the Defense Research Board of Canada.

Manuscript received May 1, 1956. This paper was prepared for delivery before the San Francisco Meeting, April 29 to May 3, 1956 and is based on experimental work done by J. G. Wurm toward a Ph.D. degree at the Graduate School, Laval University.

Any discussion of this paper will appear in a Discussion Section to be published in the December 1957 JOURNAL.

Galvanic Cells for the Determination of the Standard Molar Free Energy of Formation of Metal Halides, Oxides, and Sulfides at Elevated Temperatures

Kalevi Kiukkola[1] and Carl Wagner

Department of Metallurgy, Massachusetts Institute of Technology, Cambridge, Massachusetts

ABSTRACT

The use of electromotive force measurements on galvanic cells for the determination of standard molar free energies of formation of halides, oxides, sulfides, and other compounds at elevated temperatures is surveyed. New potentialities and inherent limitations are shown. Formulas for the estimate of errors resulting from electronic conduction and from transference of the components of electrolytes between different activity levels are derived.

The standard free energy of formation of metal-nonmetal compounds may be obtained from: (*a*) standard heats of formation and standard molar entropies; (*b*) dissociation equilibria, e.g., $PdO(s) = Pd(s) + \frac{1}{2} O_2(g)$; (*c*) reduction equilibria, e.g., $PbS(s) + H_2(g) = Pb(l) + H_2S(g)$; and (*d*) emf measurements of galvanic cells.

The third method was widely used during the first three decades of this century. Nowadays the first method is favored by many authors after the precision of the determination of heats of formation has been increased, reliable standard entropy values at 25°C have become available, and the accuracy of the measurement of specific heats and heat contents at higher temperatures has been steadily improved. The first method is generally applicable. In contrast, the second method applies to very few compounds since in most cases dissociation pressures are much too low for reliable direct measurements. Likewise, the third method is confined to compounds for which the equilibrium ratio of the constituent molecules in the gas phase is not too extreme.

The fourth method has also been used for many years. Pertinent results have been obtained at room temperature and elevated temperatures as well. Although this method is not generally applicable, its usefulness seems to be underestimated. In what follows an attempt is made to show the potentialities of this method at elevated temperatures and some inherent limitations. For a comparison, cells involving aqueous electrolytes for measurements at room temperature are also considered but not discussed in detail.

Determination of standard molar free energies of formation at elevated temperatures is especially important in conjunction with metallurgical problems. Data deduced from emf data may supplement data obtained from reduction equilibria and other gas equilibria, e.g., $Cu_2S(s) + 2Cu_2O(s) = 6Cu(s) + SO_2(g)$.

The free energy change ΔF of a reaction is obtained from the emf E of a galvanic cell as

$$\Delta F = -nEF \qquad [1]$$

where n denotes the number of faradays to be passed across the cell in order to effect the reaction under consideration and F is the Faraday constant.

From Eq. [1] it follows that an uncertainty of 0.001 v = 1 mv in the emf corresponds to an uncertainty of 23 n cal in ΔF, i.e., 46 cal if $n = 2$. On the other hand, if the standard free energy change of a chemical reaction is obtained from gas equilibrium

[1] Present address: Ratakatu 5 B 18, Helsinki, Finland.

measurements by using the formula $\Delta F^\circ = -RT \ln K$, an uncertainty in the equilibrium constant of 1% corresponds to an uncertainty of 20 cal in ΔF° at 1000°K. In view of these figures an accuracy of the order of 1 mv in emf measurements may be considered as desirable and also as satisfactory in order to obtain significant data which supplement data deduced from gas equilibrium measurements, or may be used in order to predict gas equilibria.

Cells for the Determination of the Free Energy of Formation of Halides, Oxides, and Sulfides

Cells without Auxiliary Electrolyte

The standard free energy of formation of a compound A(X) may be obtained most directly from the emf of the cell

$$\text{A} \mid \text{A(X)} \mid \text{Pt, X} \qquad \text{(I)}$$

if the compound A(X) is a purely ionic conductor and if metal A, compound A(X), and nonmetal X are present as virtually pure phases at atmospheric pressure, i.e., in their standard states.

For convenience, the nonmetallic constituent may not be present in its standard state, e.g.,

$$\text{Ag(s)} \mid \text{AgI (s)} \mid \text{Pt, I}_2\ (p_{\text{I}_2} = 0.01\ \text{atm}), \text{N}_2\text{(g)} \qquad \text{(II)}$$

Then Eq. [1] gives the free energy of formation ΔF of AgI from silver and iodine vapor of partial pressure p_{I_2}. Therefrom the standard free energy of formation ΔF° is obtained by adding $\frac{1}{2} RT \ln p_{I_2}$.

From the emf of cells of type (I), standard free energies of formation at elevated temperatures have been obtained for silver halides (1-10), lead halides (1-3, 7-13), $CdCl_2$ (1, 9, 10), $ZnCl_2$ (1, 9, 11), and $MgCl_2$ (10, 14) in both the solid and the liquid state.

Solid compounds may exhibit electronic rather than ionic conduction. Therefore, the standard free energy of formation of compounds such as Cu_2O or Ag_2S cannot be obtained from emf measurements on cells of type (I). Even in the case of typical ionic conductors such as solid AgBr or AgI, electron hole conduction becomes appreciable at higher halogen partial pressures (15, 16), and therefore the relation between emf and ΔF stated in Eq. [1] is to be replaced by a more elaborate relation. If the compound A(X) exhibits only slight deviations from the ideal stoichiometric ratio, it has been derived that (17)

$$E = \frac{1}{z_X F}\int_{\bar{F}_X'}^{\bar{F}_X''} (t_A + t_X)\, d\bar{F}_X = \frac{1}{z_X F}\int_{\bar{F}_X'}^{\bar{F}_X''} (1 - t_e)\, d\bar{F}_X \qquad [2]$$

where t_A,t_X and t_e, respectively, are the transference numbers of metal A, nonmetal X, and electrons in compound A(X), z_X is the absolute value of the valence of nonmetal X and $\bar{F}_X'$ and $\bar{F}_X''$, respectively, are the partial molar free energies of nonmetal X on the left-hand and on the right-hand side of cell (I).

The free energy change $\Delta F_{A(X)}$ for the formation of compound A(X) in cell (I) for one mole of metal A of valence z_A is

$$\Delta F_{A(X)} = F_{A(X)}^\circ - F_A^\circ - (z_A/z_X)\bar{F}_X'' \qquad [3]$$

where $F_{A(X)}^\circ$ and F_A° are the standard molar free energies of compound A(X) and metal A, respectively.

The value of $\bar{F}_X'$ is given by the equilibrium condition between A, X, and A(X) on the left-hand side of cell (I),

$$F_A^\circ + (z_A/z_X)\bar{F}_X' = F_{A(X)}^\circ \qquad [4]$$

Upon combining Eqs. [3] and [4], it follows that

$$\bar{F}_X' = \bar{F}_X'' + (z_X/z_A)\Delta F_{A(X)} \qquad [5]$$

In view of Eq. [5], it follows from Eq. [2] that

$$\Delta F_{A(X)} = -z_A E F - \frac{z_A}{z_X}\int_{\bar{F}_X'}^{\bar{F}_X''} t_e\, d\bar{F}_X \qquad [6]$$

where the second term on the right-hand side is a correction term if the compound A(X) is mostly an ionic conductor, i.e., t_e is much smaller than unity.

In order to determine the value of t_e, the following methods may be considered.

(*A*) A significant contribution of electronic conduction is revealed by deviations from Faraday's law when an electrolysis is conducted. It is difficult, however, to determine small deviations from Faraday's law especially if the partial molar free energy of metal A or nonmetal X is to be varied.

(*B*) Another possibility is to measure the total conductivity of compound A(X) as a function of the partial pressure of metal A or nonmetal X (15, 18). If ionic conduction prevails, it is justifiable to assume that variations in the total conductivity are essentially due to *n*-type or *p*-type semiconduction since the mobilities of excess electrons or electron holes are much greater than the mobilities of ionic defects.

(*C*) Polarization measurements are especially profitable in order to determine very small contributions of electronic conduction (19, 20) and to ensure that the last term in Eq. [6] is negligible.

(*D*) For silver chloride the value of t_e has been calculated indirectly from the rate of the reaction between silver and chlorine (15). Therefrom the value of the integral in Eq. [6] for a cell involving the formation of silver chloride from chlorine of atmospheric pressure has been calculated to be 140 cal at 300°C. Since electron hole conduction in AgCl increases with increasing chlorine partial pressure, the error due to appreciable electron hole conduction may be minimized by applying a low halogen partial pressure. Eventually, free chlorine may be replaced by a mixture of hydrogen halide and hydrogen.

In the design of cells of type (I), care has to be exercised to minimize diffusion of nonmetal X to the left-hand electrode because otherwise there results a "mixed potential" (21-23) rather than an equilibrium potential due to cathodic reduction of nonmetal X and anodic dissolution of metal A at the left-hand electrode. In cells of type (I) involving solid A(X), the solid electrolyte must form a gas-tight seal between the two electrodes. Even under these conditions, continuous dissolution of metal A takes place by virtue of migration of ions and electrons in the solid compound as is known from in-

vestigations on reactions of metals with oxygen, sulfur, or halogen at elevated temperatures (17). A significant shift of the emf seems likely only if the distance between the two electrodes in cells of type (I) is less than 0.1 cm. If cells involving different thicknesses of the solid compound A(X) corresponding to different rates of the aforementioned side reaction show essentially the same emf, the effect of this side reaction can be regarded to be negligible.

In the case of a liquid compound A(X), separate electrode compartments warranting a minimum of convective mass transfer between the two compartments are needed. To prevent any transfer of nonmetal to the left-hand electrode in cell (I), Grube and Rau (7) have used glass as a solid intermediate electrolyte, e.g.,

$$\mathrm{Ag(s)\,|AgCl(l)\,|glass|AgCl(l)\,|graphite,\,Cl_2(g)} \quad \text{(III)}$$

The potential difference between liquid AgCl and glass on the left-hand side is supposed to cancel against that on the right-hand side. However, since silver chloride and glass have neither a cation nor an anion in common, the potential difference between liquid AgCl and glass is thermodynamically not well defined. Therefore, asymmetry potentials may occur. This may explain inconsistencies of the order of 0.01 v reported by Grube and Rau (7). The absence of asymmetry potentials may be checked by measuring the emf of symmetrical cells involving silver electrodes on both sides.

Cells Involving Aqueous Electrolytes

At room temperature the conductivity of most salts is inconveniently low. Therefore, cells involving aqueous electrolytes are used. If the compound A(X) is sufficiently soluble, an auxiliary electrolyte is, in principle, not needed. In general, however, an auxiliary electrolyte is used. The auxiliary electrolyte may have the anion in common with compound A(X). For instance, the cell

$$\mathrm{Ag|AgCl\ (s),\,HCl\ (aq)\,|HCl\ (aq)\,|Pt,\,Cl_2\ (g)} \quad \text{(IV)}$$

may be used to determine the standard free energy of formation of silver chloride (24). Under conditions where the composition of the electrolyte is virtually constant throughout cell (IV), the cell reaction for passing one faraday may be written as

$$\mathrm{Ag\ (s) + 1/2\ Cl_2(g) = AgCl\ (s)} \quad [7]$$

In addition, the amount of HCl in the left-hand compartment of cell (IV) decreases, and the amount of HCl in the right-hand compartment increases. Transfer of HCl from the left-hand to the right-hand compartment is immaterial for the free energy balance if the transfer takes place between solutions involving virtually equal activities.

If chlorine of atmospheric pressure is used, the activity of HCl on the right-hand side of cell (IV) is lowered by the formation of Cl_3^- ions and is increased by the hydrolysis of Cl_2. Thus, on passing current across cell (IV), not only silver chloride is formed according to Eq. [7] but also HCl is transferred between different activity levels. The difference in the HCl activity may be minimized by using low chlorine partial pressures (21) and extrapolating results to zero chlorine partial pressure. In this way, all uncertainties usually ascribed to liquid junction potentials may be eliminated.

This procedure becomes impractical in the case of iodides since the complex I_3^- is formed more readily than the complex Cl_3^-. Therefore, it is expedient to use an auxiliary electrolyte which has the cation in common with the compound whose free energy of formation is to be determined. As an example the cell (25)

$$\mathrm{Pb}\left|\begin{matrix}\mathrm{Pb(ClO_4)_2,}\\ \mathrm{HClO_4\ (aq)}\end{matrix}\right|\left|\begin{matrix}\mathrm{Pb(ClO_4)_2,\,HClO_4\ (aq),}\\ \mathrm{PbI_2(s),\,I_2\ (s)}\end{matrix}\right|\mathrm{Pt} \quad \text{(V)}$$

is cited.

On passing two faradays, the cell reaction is

$$\mathrm{Pb(s) + I_2\ (s) = PbI_2\ (s)} \quad [8]$$

since the solubilities of solid PbI_2 and I_2 in the electrolyte are sufficiently low so that there is no significant difference in composition between the left-hand and the right-hand electrolyte.

In cells of type (IV) involving an auxiliary electrolyte with the anion in common with compound A(X), formation of A(X) on passing current takes place at the left-hand electrode. Therefore, compound A(X) must be present in the left-hand compartment of cells of type (IV). If compound A(X) is only slightly soluble, presence of solid A(X) in the right-hand compartment is immaterial. If, however, the solubility of compound A(X) is appreciable, compound A(X) should be present in both compartments in order to ensure equal activities of the auxiliary electrolyte.

Conversely, in cells of type (V) involving an auxiliary electrolyte with the cation in common with compound A(X), formation of A(X) on passing current takes place at the right-hand electrode. Therefore, the electrolyte in the right-hand compartment of cells of type (V) must be saturated with compound A(X). Saturation of the left-hand compartment is immaterial if the solubility is low, but is necessary if the solubility is appreciable.

Cells with Auxiliary Electrolytes at Elevated Temperatures

If an auxiliary electrolyte is used as in cells (IV) and (V), not only the magnitude but also the nature of the conductivity of the compound A(X) is immaterial for the cell reaction. Therefore, cells involving auxiliary electrolytes are also profitable in order to determine the free energy of formation of halides, oxides, and sulfides at elevated temperatures. As an analogue to cell (IV), the cell

$$\mathrm{Al(s)}\left|\begin{matrix}\mathrm{KCl,\,NaCl\ (l),}\\ \mathrm{AlCl_3\ (s)}\end{matrix}\right|\left|\begin{matrix}\mathrm{KCl,\,NaCl\ (l),}\\ \mathrm{AlCl_3\ (s)}\end{matrix}\right|\mathrm{Pt,\,Cl_2(g)} \quad \text{(VI)}$$

has been investigated by Treadwell and Terebesi (26) between about 100° and 200°C. The cell reaction on passing three faradays is

$$\mathrm{Al(s) + 1.5\ Cl_2\ (g) = AlCl_3(s)} \quad [9]$$

Thus the emf of cell (VI) gives the free energy of formation of aluminum chloride.

In contradistinction to cell (IV), the electrolyte in cell (VI) must be saturated with solid $AlCl_3$ on both

sides in order to have a constant activity of the electrolyte because the solubility of $AlCl_3$ in the liquid electrolyte is substantial.

Hill and Porter (27) have investigated cells of type

$$Ni|NiO(s), \text{salt melt with CaO}|\text{salt melt with CaO}|Pt, O_2(g) \quad (VII)$$

Spurious results may have been caused by diffusion of oxygen to the left-hand electrode.

The compound A(X) whose free energy of formation is to be determined may not be stable in the presence of nonmetal of atmospheric pressure. This is true for FeO, CoO, and Cu_2O. In this case, the electrolyte in the right-hand compartment of cell (VII) cannot be saturated with compound A(X). If only the electrolyte in the left-hand compartment is saturated, there is necessarily a difference in the activity of the components of the electrolyte between the left-hand and the right-hand compartment. Thus the cell reaction involves not only formation of compound A(X) but also transfer of electrolyte between different activity levels. A simple evaluation of emf measurements is possible only if the solubility of compound A(X) in the electrolyte is sufficiently low, and therefore, the activity difference between the electrolyte with and without saturation with compound A(X) is negligible. To overcome this restriction, Treadwell (28) has used porcelain as an intermediate solid electrolyte in determining the standard free energy of formation of Cu_2O, CoO, NiO, and other oxides. As an example, we quote the cell

$$Cu\ (s)|Cu_2O\ (s), \text{borate melt}|\text{porcelain}|Ag\ (l), O_2\ (g) \quad (VIII)$$

which involves the cell reaction

$$2Cu\ (s) + 1/2\ O_2\ (g) = Cu_2O\ (s) \qquad [10]$$

on passing two faradays if oxygen ions alone carry the current in porcelain used as an intermediate electrolyte.

To ensure a low solubility of compound A(X), use of a solid auxiliary electrolyte may be considered, e.g.,

$$Cu\ (s), Cu_2O(s)|(ZrO_2 + CaO)|Pt, O_2\ (g) \quad (IX)$$

Since the current in a solid solution of CaO in ZrO_2 is carried essentially by oxygen ions (18), the virtual cell reaction on passing two faradays is that in Eq. [10].

Cell (IX) has not been investigated so far. Oxygen must be prevented from diffusing to the left-hand electrode since otherwise a mixed potential rather than an equilibrium potential would prevail. To this end, gas-tight crucibles consisting of the solid electrolyte are needed. Since such crucibles are not easy to make, measurements on cell (IX) do not seem recommendable. Instead, cell (XXI) has been investigated (*see* below).

As an example for a cell where the compound A(X) and the electrolyte have the cation in common, the cell

$$Mg\ (l)\left|\begin{matrix}MgF_2\ (s),\\ MgO\ (s)\end{matrix}\right|\left|\begin{matrix}MgF_2\ (s),\\ MgO\ (s)\end{matrix}\right|Pt, O_2(g) \quad (X)$$

is cited. Cell (X) has been investigated by Treadwell, Ammann, and Zürrer (14) between 637° and 727°C. Regardless of the nature of the migrating ions in solid MgF_2, the cell reaction on passing two faradays is

$$Mg\ (l) + 1/2\ O_2\ (g) = MgO\ (s) \qquad [11]$$

Thus the emf of cell (X) gives the standard free energy of formation of solid MgO.

Another example is the cell

$$Ag(s)|AgI(s)|Ag_2S(s), S(l), Pt \quad (XI)$$

with solid AgI as electrolyte involving migration of silver ions. The virtual cell reaction on passing two faradays is

$$2Ag(s) + S(l) = Ag_2S(s) \qquad [12]$$

The emf of cell (XI) has been measured by Reinhold (29) and by Kiukkola and Wagner (18). Therefrom the standard molar free energy of formation of Ag_2S has been deduced. Analogous investigations have been made with Ag_2Se (18, 29).

In cells involving liquid electrolytes, diffusion of nonmetal to the metal electrode must be prevented. To this end, an intermediate solid electrolyte analogous to that in cell (III) may be used. In order to obtain the standard free energy of formation of Al_2O_3, Treadwell and Terebesi (30) have investigated the cell

$$Al(l)\left|\begin{matrix}Na_3AlF_6(l),\\ Al_2O_3(s)\end{matrix}\right|\text{porcelain}\left|\begin{matrix}Na_3AlF_6(l),\\ Al_2O_3(s)\end{matrix}\right|Pt, O_2(g) \quad (XII)$$

Cells for Determination of the Standard Free Energy Change of Displacement Reactions

The foregoing measurements may be supplemented by investigations on cells involving metal displacement reactions,

$$(1/z_A)\ A + (1/z_B)\ B(X) = (1/z_A)A(X) + (1/z_B)\ B \qquad [13]$$

where z_A and z_B, respectively, denote the valences of metals A and B in the compounds A(X) and B(X). The standard free energy change of reaction [13] formulated for one equivalent is equal to the difference of the standard free energies of formation of the metal compounds A(X) and B(X) per equivalent. Consequently, if one of the latter values is known, the other value may be calculated readily from the difference which in turn may be obtained from the emf value of an appropriate cell.

Cells without Auxiliary Electrolyte

In some cases, it is possible to design cells without any auxiliary electrolyte, e.g. (2, 3, 31-33)

$$Pb(s)|PbCl_2(s)|AgCl(s)|Ag(s) \quad (XIII)$$

Since chlorine ions migrate in $PbCl_2$ and silver ions in AgCl, the virtual cell reaction on passing two faradays across cell (XIII) is

$$Pb(s) + 2AgCl(s) = 2Ag(s) + PbCl_2(s) \qquad [14]$$

Cell (XIII) is a so-called Daniell-type cell. In general, investigations on such cells have been made with molten salts, e.g. (1, 7, 10, 32, 34-39)

$$Pb(l)|PbCl_2(l)|AgCl(l)|Ag(s) \qquad (XIV)$$

In view of the liquid junction, the virtual cell reaction also involves transfer of $PbCl_2$ and AgCl between different activity levels. Thus the emf of cell (XIV) does not give directly the standard free energy change of displacement reaction [14].

To derive a general formula, consider the cell

$$A|A(X)|B(X)|B \qquad (XV)$$

in which the composition of the salt melt is supposed to be a continuous single-valued function of distance x from the left-hand electrode at $x = 0$ up to $x = L$ at the right-hand electrode. The transference numbers of the cations, t_A and t_B, may be defined by assigning a value of zero to the transference number of the anion. Thus the value of t_A in pure A(X) is equal to unity by definition, and the same is true for t_B in pure B(X).

On passing electrical current across cell (XV), A-ions enter the melt of pure A(X), A-ions and B-ions are transferred in the salt melt in the x-direction, and B-ions are discharged at the right-hand electrode. Then it follows from the free energy balance for one faraday that

$$(1/z_A)[\overline{F}_{A\text{-ion}}\ (x = 0) - F_A^\circ] + (1/z_A)\int_0^L t_A\ (\partial\overline{F}_{A\text{-ion}}/\partial x)\,dx + (1/z_B)\int_0^L t_B\ (\partial\overline{F}_{B\text{-ion}}/\partial x)\,dx + (1/z_B)[-\overline{F}_{B\text{-ion}}\ (x = L) + F_B^\circ] = -EF \qquad [15]$$

Using the general relations

$$(1/z_A)\overline{F}_{A\text{-ion}} + (1/z_X)\overline{F}_{X\text{-ion}} = (1/z_A)\overline{F}_{A(X)} \qquad [16]$$

$$(1/z_B)\overline{F}_{B\text{-ion}} + (1/z_X)\overline{F}_{X\text{-ion}} = (1/z_B)\overline{F}_{B(X)} \qquad [17]$$

one may eliminate the partial molar free energies of the ions from Eq. [15] and obtains

$$[(1/z_A)\ (F_{A(X)}^\circ - F_A^\circ) - (1/z_B)\ (F_{B(X)}^\circ - F_B^\circ)] + \int_0^L (t_A/z_A)\,(\partial\overline{F}_{A(X)}/\partial x)\,dx + \int_0^L (t_B/z_B)\,(\partial\overline{F}_{B(X)}/\partial x)\,dx = -EF \qquad [18]$$

where the expression in brackets is equal to the standard free energy change ΔF° of the displacement reaction formulated in Eq. [13].

The derivatives of $\overline{F}_{A(X)}$ and $\overline{F}_{B(X)}$ are interrelated by the Gibbs-Duhem equation

$$N_{A(X)}\,d\overline{F}_{A(X)} + N_{B(X)}\,d\overline{F}_{B(X)} = 0 \qquad [19]$$

where $N_{A(X)}$ and $N_{B(X)}$ are the mole fractions of A(X) and B(X), respectively. Substituting Eq. [19] and transposing integrals to the right-hand side of Eq. [18],

$$\Delta F^\circ = -EF - \int_0^L \left[\frac{t_B}{z_B N_{B(X)}} - \frac{t_A}{z_A N_{A(X)}}\right] N_{B(X)}\,\frac{\partial F_{B(X)}}{\partial x}\,dx \qquad [20]$$

Finally, the relation

$$F_{B(X)} = F_{B(X)}^\circ + RT \ln N_{B(X)}\,\gamma_{B(X)} \qquad [21]$$

may be introduced where $\gamma_{B(X)}$ is the activity coefficient of B(X) in the binary melt A(X)—B(X). Substitution of Eq. [21] in Eq. [20] yields

$$\Delta F^\circ = -EF + \Delta F^* \qquad [22]$$

where

$$\Delta F^* = -RT\int_0^L \left[\frac{t_B}{z_B N_{B(X)}} - \frac{t_A}{z_A N_{A(X)}}\right]\left(1 + \frac{\partial \ln \gamma_{B(X)}}{\partial \ln N_{B(X)}}\right) dN_{B(X)} \qquad [23]$$

If the mobilities of A-ions and B-ions are equal and independent of the composition of the salt melt, the expression in brackets under the integral vanishes and thus the emf of cell (XV) gives directly ΔF°. In general, equal mobilities of A-ions and B-ions cannot be expected and, therefore, the integral in Eq. [23] does not vanish. If the mobilities of the ions in the melt A(X)-B(X) are of the same order of magnitude, deviations from Raoult's law are not excessive, and $z_A = z_B$, then the absolute value of ΔF^* is of the order of or less than RT/z_A, i.e., 1000 cal at 1000°K for $z_A = z_B = 2$.

The value of ΔF° for the displacement reaction in Eq. [13] can be obtained rigorously as the product of the Faraday constant and the difference E' of the emf values of cells of type (I) involving the formation of compounds A(X) and B(X) as virtual cell reactions. Upon substituting $\Delta F^\circ = -E'F$ in Eq. [22], it follows that

$$(E - E')F = \Delta F^* \qquad [24]$$

As far as experimental values are available (7, 10, 34-39), it has been found that the absolute value of the difference $E - E'$ is, in general, of the order of or less than 0.03 v and, therefore, ΔF^* is of the order of or less than 700 cal in accord with the above estimate based on Eq. [23]. If this result is generalized, the error may be estimated when the emf of a cell of type (XV) has been measured and the value ΔF° of the displacement reaction in Eq. [13] is calculated approximately from Eq. [22] under neglect of the term ΔF^*. Greater discrepancies reported by Lorenz and Velde (10) for cells involving magnesium seem to be due to errors resulting from mixed potentials in view of the high reactivity of magnesium.

As a rule, measurements on Daniell-type cells are not recommended for a thermodynamic evaluation since reliable transference numbers are not available. Schwarz (40) has pointed out that it may be more appropriate to calculate transference numbers from emf measurements rather than to measure these values directly with the aid of the Hittorf method.

In cell (XIII) both compounds A(X) and B(X) show predominantly ionic conduction. This is not a necessary condition. The virtual cell reaction is also represented by Eq. [13] if only the compound of the less noble metal is an ionic conductor. A hypothetical cell is

$$Zr|ZrO_2\ (+\ CaO)|Ni, NiO \qquad (XVI)$$

where solid ZrO_2 is doped with CaO in order to ensure ionic conduction and the right-hand electrode is a tablet consisting of an intimate mixture of nickel and nickel oxide. Thus the virtual cell reaction on passing four faradays would be

$$Zr\,(s) + 2NiO\,(s) = ZrO_2\,(s) + 2Ni\,(s) \quad [25]$$

It is doubtful, however, whether zirconia doped with CaO is still an ionic conductor under highly reducing conditions corresponding to the coexistence of zirconium metal and zirconia.

Cells Involving Aqueous Electrolytes

If the compound of the less noble metal of the pair A-B is considerably more soluble than the compound of the more noble metal, a cell without auxiliary electrolyte may be investigated, e.g.,

$$Pb|PbCl_2(s), aq|PbCl_2(s), AgCl(s), aq|Ag \quad (XVII)$$

with reaction [14] as the virtual cell reaction.

In order to minimize the difference in composition of the electrolyte, an auxiliary electrolyte which has the anion in common with compounds A(X) and B(X) may be used, e.g.,

$$Pb|0.1M\ KCl, PbCl_2(s)|\ 0.1M\ KCl, PbCl_2(s), AgCl(s)|Ag \quad (XVIII)$$

It is also possible to use a soluble salt of the less noble metal of the pair A-B as auxiliary electrolyte, e.g.,

$$Pb\left|\begin{matrix}0.1M\ Pb(ClO_4)_2,\\ PbCl_2(s)\end{matrix}\right|\left|\begin{matrix}0.1M\ Pb(ClO_4)_2,\\ PbCl_2(s), AgCl(s)\end{matrix}\right|Ag \quad (XIX)$$

Instead of displacement reaction [13] involving two metals A and B and their compounds, also consider displacement reactions involving hydrogen instead of metal A, e.g.,

$$1/2\,H_2(g) + AgCl(s) = HCl(aq) + Ag(s) \quad [26]$$

for which the free energy change may be obtained from the emf of the cell

$$Pt, H_2(g)|0.1M\ HCl|0.1M\ HCl, AgCl(s)|Ag \quad (XX)$$

In the presence of water, most halides are not stable as anhydrous salts. Therefore, pertinent results have been obtained for AgCl, HgCl, and $PbCl_2$ but not for other chlorides such as $CdCl_2$ or $ZnCl_2$. For the latter salts, however, values are obtainable from emf measurements on cells of type (I) at elevated temperatures without presence of water as has been reported above.

Similarly, reactions involving metal oxides and sulfides have been investigated (41-46). For various reasons, however, the applicability of emf measurements is limited. Reasons for lack of accuracy in some cases needs further clarification.

Cells Involving Auxiliary Electrolytes at Elevated Temperatures

If both compounds A(X) and B(X) exhibit electronic conduction, cells of type (XV) or (XVI) must be replaced by cells involving an auxiliary electrolyte. In the first place, an auxiliary electrolyte may be used which has the anion in common with compounds A(X) and B(X), e.g.,

$$Fe, FeO|ZrO_2\ (+\ CaO)|Cu, Cu_2O \quad (XXI)$$

with a solid solution of CaO in ZrO_2 involving anionic conduction. Measurements on cells of types (XXI) have been used in order to calculate the standard molar free energy of formation of Cu_2O, NiO, and CoO between about 800° and 1100°C (18).

A liquid electrolyte may also be used, e.g.,

$$Cu(s)|Cu_2S(s), Na_2S(l)|Na_2S(l)|\ Na_2S(l), Ag_2S(s)|Ag(s) \quad (XXII)$$

where the left-hand compartment contains a Na_2S melt saturated with solid Cu_2S and the right-hand compartment contains liquid Na_2S saturated with solid Ag_2S. If the solubilities of Cu_2S and Ag_2S in molten Na_2S are sufficiently low, the virtual cell reaction on passing two faradays may be formulated as

$$2Cu(s) + Ag_2S(s) = 2Ag(s) + Cu_2S(s) \quad [27]$$

under neglect of transfer of Na_2S between different compartments of cell (XXII).

Under conditions involving an appreciable solubility of Cu_2S and Ag_2S in molten Na_2S, the virtual cell reaction also involves transfer of Na_2S between different activity levels and, therefore, the emf of cell (XXII) does not give directly the standard free energy change of displacement reaction [27].

To derive a general formula, consider the cell

$$A|A(X), C(X)|C(X)|C(X), B(X)|B \quad (XXIII)$$

where the auxiliary electrolyte is liquid C(X). The left-hand compartment and the right-hand compartment of cell (XXIII) are supposed to be saturated with solid A(X) and B(X), respectively. The composition of the liquid phase is assumed to be a single-valued function of distance x from the left-hand electrode at $x = 0$.

In essence, cell (XXIII) consists of two half cells, one extending from $x = 0$ to $x = L_1$ and the other one extending from $x = L_1$ to $x = L_2$ where L_1 is the coordinate of a plane within the middle compartment containing pure C(X), and L_2 is the coordinate of the right-hand electrode.

On passing current across cell (XXIII), A-ions are formed at the left-hand electrode, and A-ions and C-ions are transferred in the x direction. On the right-hand side of cell (XXIII), B-ions and C-ions are transferred in the x-direction, and B-ions are reduced to metal B.

From the free energy balance for one faraday it follows that

$$(1/z_A)[\overline{F}_{A\text{-ion}}\ (x = 0) - F_A^\circ] + (1/z_A)\int_0^{L_1} t_A\,(\partial\,\overline{F}_{A\text{-ion}}/\partial\,x)\,dx + (1/z_C)\int_0^{L_1} t_C\,(\partial\,\overline{F}_{C\text{-ion}}/\partial\,x)\,dx + (1/z_B)\int_{L_1}^{L_2} t_B\,(\partial\,\overline{F}_{B\text{-ion}}/\partial\,x)\,dx$$

$$+ (1/z_C) \int_{L_1}^{L_2} t_C \, (\partial \bar{F}_{C\text{-ion}}/\partial x) \, dx$$

$$+ (1/z_B) \, [\bar{F}_{B\text{-ion}} \, (x = L_2) + F_B^\circ] = -EF \qquad [28]$$

Using Eqs. [16] and [17] and an analogous equation for C(X), one may eliminate the partial molar free energies of the ions from Eq. [28] and obtains

$$[(1/z_A) \, (F_{A(X)}^\circ - F_A^\circ - (1/z_B) \, (F_{B(X)}^\circ - F_B^\circ)]$$

$$+ \int_0^{L_1} (t_A/z_A) \, (\partial \bar{F}_{A(X)}/\partial x) \, dx$$

$$+ \int_0^{L_1} (t_C/z_C) \, (\partial \bar{F}_{C(X)}/\partial x) \, dx$$

$$+ \int_{L_1}^{L_2} (t_B/z_B) \, (\partial \bar{F}_{B(X)}/\partial x) \, dx$$

$$+ \int_{L_1}^{L_2} (t_C/z_C) \, (\partial \bar{F}_{C(X)}/\partial x) \, dx = -EF \qquad [29]$$

For the two binary systems A(X)–C(X) and B(X)–C(X) the Gibbs-Duhem equations read

$$N_{A(X)} \, d\bar{F}_{A(X)} + N_{C(X)} \, d\bar{F}_{C(X)} = 0 \qquad [30]$$

$$N_{B(X)} \, d\bar{F}_{B(X)} + N_{C(X)} \, d\bar{F}_{C(X)} = 0 \qquad [31]$$

Substituting Eqs. [30] and [31] in Eq. [29] and recalling that the expression in brackets in Eq. [29] is equal to the standard free energy change ΔF° of the displacement reaction formulated in Eq. [13], one obtains

$$\Delta F^\circ = EF$$

$$- \int_0^{L_1} \left[\frac{t_A}{z_A N_{A(X)}} - \frac{t_C}{z_C N_{C(X)}} \right] N_{A(X)} \frac{\partial \bar{F}_{A(X)}}{\partial x} \, dx$$

$$- \int_{L_1}^{L_2} \left[\frac{t_B}{z_B N_{B(X)}} - \frac{t_C}{z_C N_{C(X)}} \right] N_{B(X)} \frac{\partial \bar{F}_{B(X)}}{\partial x} \, dx \qquad [32]$$

For solubilities of A(X) and B(X) lower than 10 mole %, the relations for dilute solutions

$$d\bar{F}_{A(X)} = RT \, d \ln N_{A(X)} \qquad [33a]$$

$$d\bar{F}_{B(X)} = RT \, d \ln N_{B(X)} \qquad [33b]$$

may be used as fair approximations.

Writing Eq. [32] for ΔF° in the general form in Eq. [22], one finds from Eqs. [32], [33a], and [33b] that the additional term ΔF^* resulting from the contribution of transference effects is

$$\Delta F^* = - RT \int_0^{N_{A(X),\,sat}} \left[\frac{t_C}{z_C N_{C(X)}} - \frac{t_A}{z_A N_{A(X)}} \right] dN_{A(X)}$$

$$+ RT \int_0^{N_{B(X),\,sat}} \left[\frac{t_C}{z_C N_{C(X)}} - \frac{t_B}{z_B N_{B(X)}} \right] dN_{B(X)} \qquad [34]$$

where $N_{A(X),\,sat}$ and $N_{B(X),\,sat}$ are the mole fractions of A(X) and B(X) in the auxiliary liquid electrolyte saturated with solid A(X) and B(X), respectively.

For a numerical evaluation, we assume equal valences of the cations

$$z_A = z_B = z_C \qquad [35]$$

Moreover, for an estimate of the order of magnitude, we assume a negligible mobility of the anions and denote the ratio of the mobility of cations A and B to that of C by f_A and f_B. Thus

$$u_A = f_A u_C; \; u_B = f_B u_C; \; u_X = 0 \qquad [36]$$

Hence in mixtures of the binary system A(X)-C(X)

$$t_A = \frac{f_A N_{A(X)}}{1 + (f_A - 1) N_{A(X)}} \qquad [37]$$

$$t_C = \frac{1 - N_{A(X)}}{1 + (f_A - 1) N_{A(X)}} \qquad [38]$$

and in mixtures of the binary systems B(X)-C(X)

$$t_B = \frac{f_B N_{B(X)}}{1 + (f_B - 1) N_{B(X)}} \qquad [39]$$

$$t_C = \frac{1 - N_{B(X)}}{1 + (f_B - 1) N_{B(X)}} \qquad [40]$$

Upon substitution of Eqs. [35] to [40] in Eq. [34], it follows that

$$\Delta F^* = (RT/z_A) \ln[1 + (f_A - 1) N_{A(X),\,sat}] - (RT/z_A) \ln[1 + (f_B - 1) N_{B(X),\,sat}] \qquad [41]$$

or approximately,

$$\Delta F^* \cong (RT/z_A) \, (f_A - 1) N_{A(X),\,sat} - (RT/z_A) \, (f_B - 1) N_{B(X),\,sat}$$
$$\text{if } z_A = z_B = z_C, \; N_{A(X)} \ll 1, \; N_{B(X)} \ll 1 \qquad [42]$$

According to Eq. [42] the value of ΔF^* is determined by two terms which are proportional to the solubilities of compounds A(X) and B(X) in the auxiliary electrolyte C(X) and moreover proportional to the difference between the mobilities of ions A and C and ions B and C, respectively.

As an illustrative example, it is assumed that $z_A = z_B = z_C = 1$, $f_A = 2$, $f_B = 1$, $N_{A(X),\,sat} = 0.01$, and $T = 1000°K$ whereupon ΔF^* is found to be equal to 20 cal. For most purposes, such a low value is negligible but the term ΔF^* may be significant if one of the compounds A(X) or B(X) has a higher solubility in the auxiliary electrolyte C(X).

The foregoing considerations also apply to galvanic cells involving solid electrolytes. Cell (XXI) represents a particularly simple case, since the auxiliary electrolyte (ZrO_2 + CaO) is essentially an anion conductor due to the presence of anion vacancies (47, 48). If none of the cations Zr^{4+}, Ca^{2+}, Ni^{2+}, and Cu^+ has a mobility comparable to that of oxygen ions, passage of current does not result in transfer of one of the oxide components between different activity levels in the electrolyte. Thus the virtual cell reaction is given by the general Eq. [13] regardless of the magnitude of the solubility of the oxides at the electrodes in the auxiliary electrolyte (ZrO_2 + CaO).

Another cell involving a liquid auxiliary electrolyte is the cell

$$\mathrm{Ni(s)}\,\left|\begin{matrix}\text{borate melt,}\\ \mathrm{NiO(s)}\end{matrix}\right|\,\begin{matrix}\text{borate}\\ \text{melt}\end{matrix}\,\left|\begin{matrix}\text{borate melt,}\\ \mathrm{Cu_2O(s)}\end{matrix}\right|\,\mathrm{Cu(s)} \qquad \text{(XXIV)}$$

The virtual cell reaction on passing two faradays is

$$2\mathrm{Ni(s)} + \mathrm{Cu_2O(s)} = 2\mathrm{Cu(s)} + \mathrm{NiO(s)} \qquad [43]$$

if the solubilities of NiO and Cu_2O in the borate melt are sufficiently low so that the difference in composition of the electrolyte on the left-hand and the right-hand side of the cell can be disregarded.

A calculation of the term ΔF^* accounting for transference effects in the general Eq. [22] is more involved than for cell (XXIII) since the auxiliary electrolyte involves two components, Na_2O and B_2O_3. On the left-hand side of cell (XXIV) there is, therefore, a liquid junction potential for the ternary system $NiO\text{-}Na_2O\text{-}B_2O_3$. Thus the emf of cell (XXIV) is not completely defined by the composition of the terminal solutions next to the electrodes but also depends on the trajectory in the Gibbs triangle $NiO\text{-}Na_2O\text{-}B_2O_3$ for the transition from the electrolyte next to the left-hand electrode to the electrolyte in the middle compartment, and likewise on the trajectory in the Gibbs triangle $Cu_2O\text{-}Na_2O\text{-}B_2O_3$ for the transition from the electrolyte in the middle compartment to the electrolyte next to the right-hand electrode. This is essentially the same situation found in ternary aqueous solutions where a liquid junction potential may correspond to the Planck formula, to the Henderson formula, or other formulas, depending on the experimental conditions provided for establishing a liquid junction (49).

In addition, one may consider auxiliary electrolytes which have the cation in common with the compound of the less noble metal of the pair A-B, e.g., (18)

$$\mathrm{Pb(s)}\,|\,\mathrm{PbCl_2(s)}\,|\,\mathrm{PbS(s)}, \mathrm{Ag_2S(s)}, \mathrm{Ag(s)} \qquad \text{(XXV)}$$

where $PbCl_2$ shows predominantly ionic conduction and the right-hand electrode is an intimate mixture of PbS, Ag_2S, and Ag. Thus the virtual cell reaction on passing two faradays is

$$\mathrm{Pb(s)} + \mathrm{Ag_2S(s)} = 2\mathrm{Ag(s)} + \mathrm{PbS(s)} \qquad [44]$$

Treadwell, Ammann, and Zürrer (14) have investigated cells analogous to cell (XXV) in order to determine the free energy change of the reaction

$$3\mathrm{MgO} + 2\mathrm{Al} = \mathrm{Al_2O_3} + 3\mathrm{Mg} \qquad [45]$$

but the formation of the spinel phase $MgAl_2O_4$ may interfere with the main reaction.

Similarly, displacement reactions between compounds of metal A with different nonmetals may be investigated, e.g.,

$$\mathrm{PbI_2(s)} + \mathrm{Cl_2(g)} = \mathrm{PbCl_2(s)} + \mathrm{I_2(g)} \qquad [46]$$

Appropriate cells may be devised by using the same principles as for metal displacement reactions. In general, cells of this type do not seem recommendable since use of gas electrodes is inconvenient.

Conclusions

In the foregoing sections, different types of galvanic cells have been listed. A careful selection of the most promising type is necessary because the relation between emf and ΔF stated in Eq. [1] never holds rigorously, but is an approximation. The most important deviations are due to the following reasons.

1. Electronic conduction may occur in addition to ionic conduction. A more elaborate relation between E and ΔF has been stated in Eq. [6] for cells of type (I). Similar equations may be derived for other types of cells. By and large, interference due to electronic conduction is more serious with solid than with liquid electrolytes.

2. In view of mutual solubility, reactants and reaction products may not be present in their standard states. If the solubilities are known, correction terms may be estimated in order to obtain standard free energy changes. Reference is made to recent calculations for Cu_2S (50).

3. If the solubility of reactants and reaction products in solid or liquid electrolytes is not negligible, the virtual cell reaction also involves transfer of the components of the electrolyte between different activity levels which have to be considered in the thermodynamic evaluation, e.g., Eq. [22]. A rigorous evaluation requires numerical values of the transference numbers as a function of the composition of the electrolyte. Unfortunately, these values are difficult to obtain.

As a rule, solubilities in solid electrolytes are lower than in liquid electrolytes. Cells involving solid electrolytes have, therefore, some merits in comparison to cells involving liquid electrolytes, but it must be ascertained that the error resulting from electronic conduction is sufficiently low when a solid electrolyte is used.

This survey has been used as a basis for the selection of cells which were considered to be particularly promising for the determination of standard molar free energies of formation of metallurgically important compounds at elevated temperatures.

In a separate paper (18) results of emf measurements on galvanic cells involving solid electrolytes are presented. Therefrom the standard molar free energies of formation of CoO, NiO, Cu_2O, Ag_2S, Ag_2Se, PbS, and several phases of the system Ag-Te have been deduced. Experimental investigations have been made exclusively with solid electrolytes in order to show new potential uses, but further investigations on cells involving liquid electrolytes are likewise desirable. To obtain reliable results, it will be necessary to determine solubilities of the reactants and reaction products in liquid electrolytes for an estimate of the contribution of transference effects with the help of formulas derived above.

Emf measurements may be considered especially for the investigation of compounds which are difficult to reduce by means of hydrogen or carbon monoxide and, therefore, do not lend themselves readily for gas equilibrium investigations. Treadwell and his associates (14, 26, 30) have shown the usefulness of emf measurements in the case of magnesium

oxide, aluminum oxide, and aluminum chloride. Adaption of emf measurements to thermodynamic investigations on titanium and zirconium compounds may be possible. Use of emf measurements for thermodynamic investigations on the system uranium-oxygen has been discussed in a separate report (51).

Manuscript received August 9, 1956. The paper is based on a thesis submitted by Kalevi Kiukkola in partial fulfillment of the requirements for the D.Sc. degree, Massachusetts Institute of Technology. Work was done under Contract AT(30-1)-1002 with the U.S.A.E.C.

Any discussion of this paper will appear in a Discussion Section to be published in the December 1957 JOURNAL.

REFERENCES

1. R. Lorenz, Die Elektrolyse geschmolzener Salze, Vol. 3, Knapp, Halle (1906).
2. M. Katayama, *Z. physik. Chem.*, **61**, 566 (1908).
3. H. Reinhold, *Z. anorg. u. allgem. Chem.*, **171**, 181 (1928).
4. E. J. Salstrom and J. H. Hildebrand, *J. Am. Chem. Soc.*, **52**, 4650 (1930).
5. E. J. Salstrom, *ibid.*, **55**, 4426 (1936).
6. E. J. Salstrom, *ibid.*, **56**, 1272 (1934); E. J. Salstrom, T. J. Kew, and T. M. Powell, *ibid.*, **58**, 1848 (1936).
7. G. Grube and E. A. Rau, *Z. Elektrochem.*, **40**, 352 (1934).
8. U. Croatto and C. Bruno, *Ricerca Sci.*, **17**, 1998 (1947).
9. R. Lorenz and M. G. Fox, *Z. physik. Chem.*, **63**, 109, 121 (1908).
10. R. Lorenz and H. Velde, *Z. anorg. u. allgem. Chem.*, **183**, 81 (1929).
11. J. H. Hildebrand and A. Wachter, *J. Am. Chem. Soc.*, **52**, 4655 (1930).
12. J. H. Hildebrand and G. C. Ruhle, *ibid.*, **49**, 722 (1927).
13. E. J. Salstrom and J. H. Hildebrand, *ibid.*, **52**, 4641, 4650 (1930).
14. W. D. Treadwell, A. Ammann, and Th. Zürrer, *Helv. Chim. Acta*, **19**, 1255 (1936).
15. C. Wagner, *Z. physik. Chem.*, **B32**, 447 (1936).
16. W. Jost and K. Weiss, *Z. physik. Chem. N. F.*, **2**, 112 (1954).
17. C. Wagner, *Z. physik. Chem.*, **B21**, 25 (1933).
18. K. Kiukkola and C. Wagner, *J. Electrochem. Soc.*, to be published.
19. C. Wagner, *Z. Elektrochem.*, **60**, 4 (1956); Proc. Internat. Committee of Electrochemical Thermodynamics and Kinetics, 1956.
20. J. B. Wagner and C. Wagner, *J. Chem. Phys.*, June 1957.
21. C. Wagner and W. Traud, *Z. Elektrochem.*, **44**, 391 (1938).
22. K. Nagel, *ibid.*, **44**, 637 (1938); E. Lange and K. Nagel, *ibid.*, **44**, 792, 856 (1938).
23. I. M. Kolthoff and C. S. Miller, *J. Am. Chem. Soc.*, **62**, 2171 (1940).
24. L. Wolff, *Z. Elektrochem.*, **20**, 19 (1914).
25. R. H. Gerke, *J. Am. Chem. Soc.*, **44**, 1684 (1922).
26. W. D. Treadwell and L. Terebesi, *Helv. Chim. Acta*, **18**, 103 (1935).
27. D. G. Hill and R. Porter, AEC Report Contract AT-(40-1)-1526, Sept. 15, 1953.
28. W. D. Treadwell, *Z. Elektrochem.*, **22**, 414 (1916).
29. H. Reinhold, *ibid.*, **40**, 361 (1934).
30. W. D. Treadwell and L. Terebesi, *Helv. Chim. Acta*, **16**, 922 (1933).
31. F. Haber and S. Tolloczko, *Z. anorg. Chem.*, **41**, 407 (1904).
32. B. A. Rose, G. J. Davis, and H. J. T. Ellingham, *Disc. Faraday Soc.*, **4**, 154 (1948).
33. A. Sator, *Compt. rend.*, **234**, 2283 (1952).
34. R. Suchy, *Z. anorg. Chem.*, **27**, 152 (1901).
35. G. Tammann, *Z. anorg. u. allgem. Chem.*, **133**, 267 (1924).
36. L. Holub, F. Neubert, and F. Sauerwald, *Z. physik. Chem.*, **A174**, 161 (1935).
37. R. Lorenz, *ibid.*, **130**, 39 (1927).
38. R. Lorenz and F. Michael, *ibid.*, **A137**, 1 (1928).
39. F. Oppenheimer, *Z. anorg. u. allgem. Chem.*, **189**, 297 (1930).
40. K. E. Schwarz, *Z. Elektrochem.*, **45**, 740 (1939); **47**, 144 (1941).
41. D. F. Smith and H. K. Woods, *J. Am. Chem. Soc.*, **45**, 2632 (1923).
42. C. G. Maier, G. S. Parks, and C. T. Anderson, *ibid.*, **48**, 2564 (1926).
43. C. G. Maier, *ibid.*, **51**, 194 (1929).
44. A. A. Noyes and E. S. Freed, *ibid.*, **42**, 476 (1920).
45. I. A. Makolkin, *Zhur. Fiz. Khim.*, **16**, 13, 18 (1942).
46. J. R. Coates, A. G. Cole, E. L. Gray, and N. D. Faux, *J. Am. Chem. Soc.*, **73**, 707 (1951).
47. C. Wagner, *Naturwissenschaften*, **31**, 265 (1943).
48. F. Hund, *Z. physik. Chem.*, **199**, 142 (1952).
49. D. A. MacInnes, The Principles of Electrochemistry, pp. 226 ff., Reinhold Publishing Corp., New York (1939).
50. J. B. Wagner and C. Wagner, *This Journal*, 1957.
51. C. Wagner, "Thermodynamics of the System Uranium-Oxygen", AEC Report WAPD-144, July 23, 1955.

Technical Notes

Growth of Silicon Crystals by a Vapor Phase Pyrolytic Deposition Method

R. C. Sangster,[1] E. F. Maverick, and M. L. Croutch

Research and Development Department, Semiconductor Division,

Hughes Aircraft Company, Culver City, California

A study has been made of the feasibility of growing Si crystals by the reaction of gaseous $SiBr_4$ with H_2 at the surfaces of hot Si seed filaments (1). The immediate objective has been to produce deposits of a purity and a crystal perfection sufficient for semiconductor device purposes. An ultimate objective has been the deposition of arbitrary, complex, *p-n* junction structures by control of the types and amounts of impurities deliberately introduced into the process gas stream. This is a partial report covering the more interesting observations and results.

$SiBr_4$ has been produced by reaction of Br_2 with hot Si (2) and has been purified by fractional distillation and chromatographic adsorption techniques. The product normally used was spectrographically pure according to Harvey's semiquantitative method (3).

The deposition reaction has been assumed to be

$$2H_2(g) + SiBr_4(g) = Si(s) + 4HBr(g)$$

Computations based on data in the literature (4) give for this reaction $\Delta H^\circ = 50.4 \pm 1.2$ kcal/mole in the range 0°-1500°C, and indicate that ΔF° is favorable above about 1000°C. This reaction has been studied in the apparatus shown in Fig. 1.

Description of Apparatus

Purified H_2 and He—clean, dry and oxygen-free—are supplied to the deposition apparatus of Fig. 1 from other equipment not shown. He is used to flush the apparatus before and after the runs. During the runs, part of the purified H_2 is bubbled through the boiling $SiBr_4$ in the "pot." The resulting H_2-$SiBr_4$ mixture is stripped down to a known concentration in the thermostated "stripping condenser." The remaining, make-up H_2 is added to the gas emerging from the condenser to produce the desired reaction mixture. This mixture passes through a glass tube system, heated to prevent condensation, into the reaction tube. The gas passes first over a hot (1100°-1300°C) Ta impurity-scavenging filament and then over the Si filament. The effluent gases then enter more apparatus not shown here and are disposed of.

The Si filaments are 0.02-0.06 in. (0.5-1.5 mm) thick, 0.05-0.10 in. (1.25-2.5 mm) wide, and 1.5-2.5 in. (3.7-6.2 mm) long. They are mounted on the power leads by Ni and Ta wire loops anchored to the ends of the filaments by bundles of tightly wound, fine Ta wire. Glass-to-metal seals are used for the two central power leads. The two end power leads consist of heavy tungsten wires sliding in close-fitting capillary tubes. Bits of "Tackiwax" provide a flexible seal between the wires and the capillaries. Spring tension applied to the tungsten leads keeps the filaments taut. The filament power supplies each consist of a Variac, a rheostat, and an ammeter, in series. The rheostat is necessary in the case of the Si filaments because of the negative resistance characteristics of Si. The useful filament temperature range is 1100°-1350°C. Below 1100°C the reaction yield drops off rapidly. Above 1350°C difficulties due to the alloying of Si and Ta are encountered.

The filament temperatures can be measured optically with a precision of ±10°-20°C. The precision of setting and determining the H_2 flow rates is ±2.5%, and the $SiBr_4$ concentration ±10%.

Semi-Empirical Analysis of the Deposition Process

Basic phenomena.—The basic phenomena determining the physical nature of the deposit seem to be

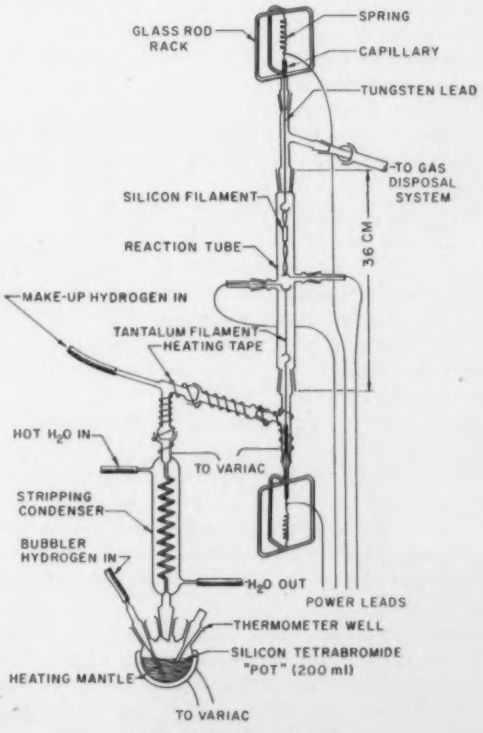

Fig. 1. Deposition apparatus

[1] Present address: Texas Instruments Incorporated, 6000 Lemmon Avenue, Dallas, Texas.

the following: (*a*) competitive nucleation rates for oriented and disoriented growth; (*b*) mobility of the atoms on the surface of the deposit; (*c*) rate of deposition of the Si; and (*d*) turbulence and inhomogeneity of the process gas at the surface of the filament.

Nucleation for disoriented growth obviously must be suppressed when monocrystalline deposits are desired. The mobility of the atoms on the surface of the deposit should be such that an atom can get to a normal surface lattice site before the next layer of atoms is deposited, but not so high that many can be attracted to regions of incipient disoriented or dendritic growth. The deposition rate should be such that atoms are supplied as rapidly as the growing crystal can accept them, but not so fast that nucleation for polycrystalline growth is favored, or so slow that the atoms have a chance to migrate very far before the next layer is put down. The turbulence of the process gas must be high enough to insure reasonably thorough contact with the filament surfaces, but not so high as to lead to pronounced inhomogeneity near the surfaces; such inhomogeneity can produce local areas of either high or low deposition rate and can otherwise favor disoriented or nonuniform growth.

Effects of process variables.—Proper pretreatment of the Si seed surface is necessary if oriented growth is to be obtained. Chemical etching is desirable for producing a superficially clean surface, but all such techniques apparently leave an oxide film which must be destroyed before deposition is begun. For this purpose the only successful technique that has been found is preheating in a stream of pure H_2 for 30-60 min at 1275°C.

The purity of the $SiBr_4$ affects directly the chemical purity and therefore the electrical properties of the deposit; equally important, however, is the fact that some impurities can make it impossible to obtain monocrystalline deposits. Moreover, even when clean, dry, oxygen-free H_2 and highly purified $SiBr_4$ are used, it is still necessary to use a hot Ta scavenging filament for further purification of the gas.

The thermodynamic effects of the filament temperature are, of course, basic to the entire process. In addition, temperature affects the physical nature of the deposit through its influence on the rates of nucleation and on the mobility of the atoms on the surface of the deposit. Nucleation for disoriented growth is favored by the higher temperatures; the mobility of the atoms is increased.

The effects of changes in the $SiBr_4$ concentration are caused primarily by changes in the rate at which the Si is deposited. The accompanying variation in the total amount of Si which happens to be deposited in a given run is important only secondarily. In general, dendrite formation is suppressed and deposit uniformity favored by the higher $SiBr_4$ concentrations.

Longer running times lead to the deposition of more material, other conditions being equal. Whenever the total amount of the deposit increases, characteristic changes occur. The deposits become thicker; dendrites, if present, grow larger; the smaller dendrites are crowded out by the larger; and there are more opportunities in general for disoriented growth.

The most important effects of the process gas flow rate are due to the turbulence and inhomogeneity of the gas phase. The higher the flow rate, the greater the turbulence, and the more dendritic the deposit. However, with the composition of the gas phase held constant, the higher flow rates also involve higher Si deposition rates, and this tends to counteract some of the effects of the increased turbulence.

In the case of the reaction chamber diameter, turbulence is again the important factor. The larger diameters lead to greater effective turbulence at the filament surface. This is in direct contrast to the normal expectation that a constant volume flow rate and a larger diameter will yield a less turbulent flow. The thermal convection effects existing in the deposition chamber complicate much of the reasoning about turbulence.

With regard to position on the filament, the deposits on the lower portions of the filaments are cooler, thicker, and usually more impure than those higher up.

Results

Deposits of Si on Si seed filaments have been produced with properties adequate for experimental device purposes (*see* Fig. 2 and 3). Both metallographic sectioning and x-ray diffraction techniques show that the best deposits have the same orientation as the base filaments. There are only faint indications of the junctions between the seeds and the deposits, and there is relatively little indication of lineage structure. The deposited Si is normally *n*-type, with a resistivity in the range 1-100 ohm-cm, as computed from the results of two-point probe measurements on the filament before and after deposition. The existence of *p-n* junctions between *n*-type deposits and *p*-type seeds makes it possible to apply Gudmundsen's (1) micro-optical probe technique to measure the minority carrier lifetimes. The

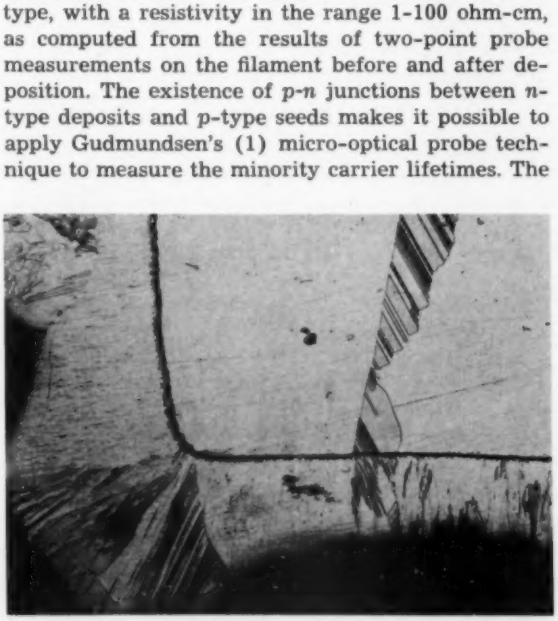

Fig. 2. Part of a metallographic cross section of the first filament produced with a reasonably uniform, oriented deposit. The deposit is about 0.010 in. (0.25 mm) thick at the lower right. The area toward the upper right represents part of the original seed. Several characteristic structures are present: a layer of inclusions at the seed-deposit interface, propagation of seed structures into the deposit, and lineage and polycrystalline regions in the deposit proper.

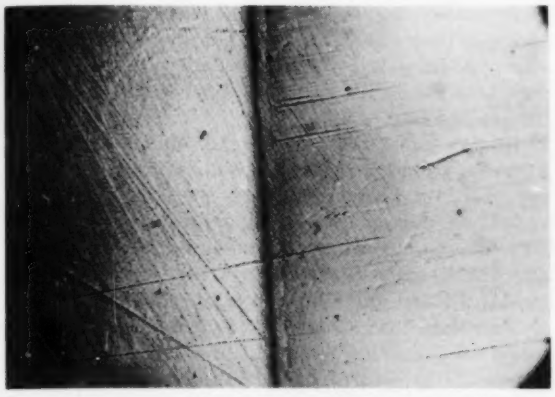

Fig. 3. Part of a metallographic section of a very good filament. The seed is at the left, the deposit at the right. The total width of the picture corresponds to about 0.003 in. (0.075 mm). Most of the apparent imperfections are surface scratches and grain.

lifetimes found for the deposits range from 0.1 to 1 μsec.

Optimum conditions for the formation of these deposits involve $SiBr_4$ concentrations in the range 0.6-1.0 mole %, total H_2 flow rates of about 1.5 l/min, and filament temperatures in the range 1100°-1200°C, when a reaction chamber with a 25 mm inner diameter is used. Under these conditions 0.005-0.010 in. (0.125-0.25 mm) of Si/hr is deposited.

Deposits can also be obtained on both Si and Ta filaments in the form of dendrites which have large, well-formed, pyramidal endcaps, with face edges 0.01-0.02 in. (0.25-0.5 mm) long. Individual dendrites of this sort might be useful in some point-contact devices. Optimum reaction conditions for the formation of this type of deposit are a $SiBr_4$ concentration of about 0.3 mole %, a total H_2 flow rate of 1-1.5 l/min, and a filament temperature of 1275°C, with a reaction tube having a 25 mm inner diameter.

Above approximately 1100°C, about 40% of the input $SiBr_4$ reacts to deposit Si, with no apparent dependence on the temperature and with relatively little on the other reaction conditions, within the ranges covered. There appears to be a maximum in the rate of deposition vs. concentration curve at about 0.6-0.7 mole % $SiBr_4$.

Acknowledgments

The authors wish to acknowledge the aid of the many individuals in these laboratories who helped with the different specialized phases of this work. This project was part of Contracts No. DA-36-039 SC-42574 and DA-36-039 SC-56755 with the United States Army Signal Corps. The authors are grateful to the Signal Corps for permission to publish.

Manuscript received May 2, 1956.

Any discussion of this paper will appear in a Discussion Section to be published in the December 1957 JOURNAL.

REFERENCES

1. Final Report No. SC-14A-F, "Silicon Transistor," Signal Corps Contract No. DA-36-039 SC-42574, Hughes Aircraft Co., Culver City, California (October, 1953); Final Report No. SC-14-F, "Silicon Transistor," Signal Corps Contract No. DA-36-039 SC-56755, Hughes Aircraft Co., Culver City, California (December, 1954).
2. J. W. Mellor, "A Comprehensive Treatise on Inorganic and Theoretical Chemistry," Vol. VI., pp. 977-978, Longmans, Green and Co., New York (1925).
3. C. E. Harvey, "A Method of Semi-Quantitative Spectrographic Analysis," Applied Research Laboratories, Glendale, Calif. (1947).
4. F. D. Rossini, D. D. Wagman, W. H. Evans, S. Levine, and I. Jaffe, *U. S. Natl. Bur. Standards Circ. 500* (1952); K. K. Kelley, *U. S. Bur. Mines Bull.*, **476**, 241 (1949); *ibid.*, **477**, 147 (1950); O. Kubaschewski and E. Ll. Evans, "Metallurgical Thermochemistry," Butterworth-Springfield, London (1951); L. L. Quill, Editor, "The Chemistry and Metallurgy of Miscellaneous Materials," NNES IV-19B, McGraw-Hill Book Co., Inc., New York (1950).

Notes on Hydrogen Overvoltage

I. Maximum Concentration of Atomic Hydrogen on the Surface of a Working Cathode

Hugh W. Salzberg

College of the City of New York, New York, New York

and

Sigmund Schuldiner

Naval Research Laboratory, Washington, D. C.

Several recent papers (1-3) have expressed the idea that the rate of direct combination of hydrogen atoms on a cathode surface is too slow to support currents of more than 10^{-1} amp/cm^2. In consequence, removal of atomic hydrogen from the surface would have to occur by an alternative mechanism, specifically the electrochemical combination of an adsorbed atom and a hydronium ion. However, calculations indicate that the rate of direct atomic combination is great enough to support extremely high current densities. These calculations and some conclusions drawn from them appear below.

The rate of combination of hydrogen atoms on a surface may be expressed as follows

$$r = K\,(kT/h)\,H^2\,(f^*/F^2_H)\exp -\Delta H_o/RT \qquad (I)$$

where r is the number of combinations/cm²/sec, (kT/h) is the Eyring frequency factor, H is the number of hydrogen atoms/cm² of surface, f^* is the partition function of the activated complex, f_H is the partition function of the hydrogen atom, ΔH_o is the heat of activation at 0°K, and K is the transmission coefficient. The dimensions of $f^*/f^2_H \exp -\Delta H_o/RT$ are cm²-molecule/atom² and the term is equal to $\exp -G^*/RT = K = H^*/H^2$, where G^* is the free energy of activation and H^* refers to the activated complex.

Values for the partition function depend on the mobility of the atoms, i.e., for immobile atoms there are no rotational or translational contributions. Since vibrational partition functions are of the order of unity at room temperature, the ratio of partition functions in this case is approximately unity.

For mobile hydrogen atoms, as in a two-dimensional monatomic gas, the partition functions include translational terms only since these mobile hydrogen atoms have 2 degrees of translation freedom and no modes of rotational or vibrational freedom. Therefore (5)

$$f_H = 2\,\pi\,mkt/h^2$$

where m is the mass of a hydrogen atom.

The activated complex has two degrees of translational freedom and only one mode of rotation, since the other rotational mode of this linear molecule would be normal to the surface. The normal mode of vibrational freedom of this diatomic molecule is replaced by translation in the coordinate of decomposition. Therefore

$$f^* = (4\,\pi\,mkt/h^2)\,(4\,\pi^2\,kt\,\sigma^2\,m/h^2)^{1/2}$$

σ is the distance between centers of the atoms in the activated state, here taken as 0.74×10^{-8} cm. Therefore, in the case of a mobile atom the ratio of partition functions is equal to $2\sigma h/(mkt)^{1/2}$. The over-all equations can then be expressed as

$$r_{mobile} = (kT/h)\,\sigma\,H^2\,[h/(mkt)^{1/2}] \exp -\Delta H_o/RT$$
$$= H^2\,\sigma\,(kT/m)^{1/2} \exp -\Delta H_o/RT \qquad (IIa)$$

The term $H^2\,\sigma\,(kT/h)^{1/2}$ is equal to the collision number, as it should be.

$$r_{immobile} = (kT/h)\,H^2\,(S/2L) \exp -\Delta H_o/RT \qquad (IIb)$$

where S is the number of adjacent sites per atom (either 2 or 4), and L is the number of sites/cm² (about 10^{15}). The factor $(S/2L)$ is necessary since only adjacent atoms can combine.

Inserting the correct numerical values into the first terms on the right hand sides of (IIa) and (IIb) gives

$$r_{mobile} = 1 \times 10^{-8}\,H^2 \exp -\Delta H_o/RT$$
$$r_{immobile} = 3 \times 10^{-8}\,H^2 \exp -\Delta H_o/RT$$

Surprisingly enough it seems to make little difference in the numerical calculation whether the hydrogens are considered mobile or immobile. However, since immobility seems more probable, it is assumed that the rate is $3 \times 10^{-8}\,H^2 \exp -\Delta H_o/RT$.

To obtain the values of ΔH_o, it is assumed that this will be equal to ΔH, the experimental activation energy. ΔH_o is less than ΔH by only 300 cal in the case of a mobile layer and 600 cal in the case of an immobile layer.

ΔH has been determined only for Pt, since for cathodes at which combination is not rate-determining there is no obvious way of determining the activation energy for a nonrate-determining step. It was found to be about 2 kcal/mole (3). Estimates have been made (1-4) to the effect that on other metals the activation energy for combination should be even less than 2 kcal/mole. These estimates are based on the ideas that: (*a*) the combination rate is essentially a surface radical reaction and should be very rapid; (*b*) the more tightly the atom is held to the surface the lower the energy of the initial state and therefore the higher the energy of activation should be. Pt has a very high heat of adsorption of H. For other metals with lower heats of adsorption, the energy of activation for combination should be less than that on Pt.

Also, on a theoretical basis [(5) p. 214], the specific rate constant for the homogeneous gas phase combination of hydrogen atoms has been estimated to be given by the expression

$$k = k' \times 2.98 \times 10^{14} \text{ cc mole}^{-1} \text{ sec}^{-1}$$

where k' is the transfer coefficient. The free energy of activation calculated from this is less than 1 kcal/mole. The entropy of activation at a standard state of 1 mole/cc is estimated by the same source to be 5.3 e.u. The energy of activation would therefore be about 2½ kcal/mole or less for the gas phase reaction. Normally the heterogeneous reaction would be expected to have a lower activation energy, or at the most only a slightly higher value. Therefore the value of ΔH is taken as being about 3 kcal or less with an upper limit of 6 kcal. This is three times that determined for Pt and more than twice the estimated value for the gas phase reaction.

Numerical Calculations

This provides all the information needed to calculate the rate at any surface coverage and the surface coverage at any given combination rate. Expressing the specific rate in terms of current density by multiplying by $2F/N$, i.e., two electrons per combination, gives

$$i_{comb.} = 6 \times 10^{-21}\,H^2 \exp -\Delta H_o/RT \qquad (III)$$

If the surface is saturated with hydrogen atoms, H is 10^{15}. The following combination currents result for indicated values of ΔH:

i (amp/cm²)	ΔH (kcal/mole)
10^6	0
6×10^4	3
2×10^4	6
50	10

Even with the extremely high value of activation energy of 10 kcal/mole, the calculated combination rate is 50 amp when the surface is saturated.

To determine the surface concentration at any particular current density, it is necessary to relate

the rate of direct combination to the over-all current density.

If the rate-determining step is direct combination, the over-all rate is the combination rate. However, if the electrochemical mechanism is the rate-determining step, it must be at least 100 times as fast as the direct combination. Consequently, direct combination is at most one one-hundredth of the observed current density and the maximum concentration of atomic hydrogen is that which supports this fraction of the over-all current density. If the discharge is the rate-determining step, maximum coverage may be obtained by assuming a minimum rate of removal which will equal the current.

From these considerations, for the various rate-determining mechanisms the combination rate at any observed over-all current can be calculated, and from this a maximum value of the surface concentration of hydrogen can be obtained using Eq. (III). Table I shows values of hydrogen atom concentration, expressed as the fraction of the total surface covered, at a current density of 1 amp/cm^2.

From Table I it can be seen that only 2% of the surface would be covered at a current density of 1 amp/cm^2 even if the activation energy were 10 kcal, which is five times that of the observed value for combination on Pt.

Table I

Rate-determining step	ΔH = 3 Kcal	6 Kcal	10 Kcal
Slow combination	$10^{-0.8}$	$10^{-4.6}$	$10^{-1.7}$
Slow discharge	$10^{-0.8}$	$10^{-4.6}$	$10^{-1.7}$
Electrochemical combination	$10^{-7.8}$	$10^{-5.6}$	$10^{-2.7}$

Conclusions

In the case of the combination of hydrogen atoms on a cathode surface, the frequency factor is independent of the mobility of the adsorbed hydrogen.

The surface of a working cathode is only sparsely covered with hydrogen atoms even at high current densities.

The electrochemical mechanism may be rate determining but not because the combination rate is too slow to support the current.

Reduction of cations at a cathode would not seem to be due to the action of adsorbed hydrogen atoms but would take place at the metal surface, i.e., such reduction is electrochemical, not chemical.

The action of depolarizers, such as KNO_2 in the study of dissolution of metals in acids (6), seems to be something other than removal of hydrogen atoms from the surface.

Manuscript received March 12, 1956.

Any discussion of this paper will appear in a Discussion Section to be published in the December 1957 JOURNAL.

REFERENCES

1. P. Parsons and J. O'M. Bockris, *Trans. Faraday Soc.*, **47**, 920 (1951).
2. J. O'M. Bockris and A. M. Azzam, *ibid.*, **48**, 145 (1952).
3. J. O'M. Bockris and E. C. Potter, *This Journal*, **99**, 169 (1952).
4. K. J. Laidler, Private communication.
5. S. T. Glasstone, K. J. Laidler, and H. Eyring, "Theory of Rate Processes", McGraw-Hill Book Co., Inc., New York (1950).
6. M. B. Abramson and C. V. King, *J. Am. Chem. Soc.*, **61**, 2290 (1939).

Electrical Conduction in Silicon Carbide

G. H. Fetterley

Norton Company, Chippawa, Ontario, Canada

ABSTRACT

Commercial SiC is a semiconductor that can be prepared as predominantly *n*- or *p*-type at will. The body conductivity is linear and determines the behavior of SiC heating elements, which are usually made from *n*-type. The interfacial conductivity is much lower, nonlinear, and is exploited in lightning arresters, which are made from *p*-type. While the electrical behavior of this material is poorly understood in detail, the broad outlines are summarized in terms of semiconductor theory.

SiC is manufactured and used on a large scale as an abrasive and refractory, and is a familiar material to workers in the electrothermic industries. More interesting from a theoretical point of view and of more recent development are its applications as an electrical conductor. In the following, the two basic types of electrical application are described, followed by a discussion of the attempts to explain the observed phenomena. The objective is to present a survey for the nonspecialist and a guide to the widely scattered literature on this subject.

Crystal Structure

When SiC is formed at a temperature of 2000°C or lower, it has a cubic structure. This modification has been designated beta silicon carbide. It has been prepared only in very small crystals, and the bulk properties have not been reported to any extent in the literature. Attempts to hot press or sinter the crystals to form a coherent body cause a transformation to the alpha form, which is the ordinary SiC of commerce.

Alpha silicon carbide occurs in a number of hexagonal and rhombohedral crystal types, which have been investigated extensively by Thibault (1), Ramsdell (2), and Lundqvist (3). A review of the literature on crystal structure has been compiled by Harman and Mixer (4).

Since it has been impossible to isolate specimens of the various types of alpha silicon carbide the relationship, if any, between crystal form and electrical properties has not been clarified. Therefore, this approach is not considered further here. The remainder of the text deals for the most part with the usual alpha type, and essentially without consideration of the various crystal habits described by Thibault, Ramsdell, and Lundqvist.

Commercial Silicon Carbide

Transparent crystals of SiC, colorless or pale yellow to greenish, occur as occasional isolated pockets in commercial ingots. This material is of no importance commercially. In spite of the attractive appearance of the crystals, chemical analysis shows that impurities are still present to the extent of possibly 0.3%.

Green SiC is available commercially in moderate quantities, and is used in the manufacture of certain grades of grinding wheels and in heating elements. It has been shown to conduct electricity principally by flow of electrons, and is classed as an *n*-type or electron excess semiconductor.

So-called gray SiC is the standard abrasive and refractory material, and is the type usually encountered under the name silicon carbide and various trade names. The color of individual crystals varies widely through dark green, blue, various shades of dark gray, and black. Electrical properties are quite variable, but charge is transferred principally by flow of holes, and this material is classed rather loosely as a *p*-type or electron defect semiconductor.

Gray SiC may be called black if it is unusually dark in color. However, this designation usually means a material to which alumina has been added to produce strong electron defect conduction. This material is used to make nonlinear resistors of various kinds, ranging in size from automatic volume controls the size of a dime to large lightning arresters several feet high.

While the nomenclature described above has grown up with the industry and is serviceable within its limitations, it has been shown by Kendall (5) that the color and mechanism of conduction can be made independent of each other to a considerable degree by special techniques of preparation. In general, Kendall's light colored crystals were *n*-type, but black ones could be made either *n*-or *p*-type at will. The above classification should therefore be regarded only as a useful guide to currently available commercial products.

Table I. Chemical analysis of commercial silicon carbides, in per cent

	Colorless	Green	Gray	Black
SiC	99.7	99.0	98.7	98.7
Free C	0.11	0.30	0.20	0.20
Free SiO_2	0.02	0.00	0.75	0.71
Al	<0.05	0.05	0.20	0.30
Fe	<0.05	<0.05	<0.05	<0.05
Ca	<0.03	<0.03	0.03	0.03
Mg	<0.05	<0.05	<0.05	<0.05

The various types of commercial SiC do not differ very much in chemical analysis. The most obvious difference is in the aluminum content. The colorless material is purer but still far short of the purity required for basic research on electrical conduction. Table I shows typical analyses for samples of SiC that have undergone a severe acid treatment to remove surface contamination.

Silicon Carbide Heating Elements

When granular SiC is pressed or rammed with a temporary bond and subsequently fired at 2000°-2500°C, the individual grains sinter together to form a strong, refractory and somewhat porous body. When suitably processed, this body is a fairly good electrical conductor, having a specific resistance of about 0.1 ohm-cm at 1000°C and not more than about 0.2 ohm-cm at room temperature. It can be exposed to oxidizing conditions at temperatures as high as 1400°C for several thousand hours without serious loss in strength or change in electrical resistance. Since the individual grains are welded together at points of contact, the electrical properties are determined by the body conductivity of the crystals. Current is proportional to voltage, and conduction is linear by definition. Simple, rugged heating elements made of sintered SiC have been available for many years, both in Europe and North America, under various trade names.

While heating elements can be made from any of the commercially available types of SiC, the green n-type is used ordinarily. The electrical characteristics are more uniform than those of the black type, the change in resistance with temperature is smaller, and the temperature coefficient of resistance is positive in the usual operating range.

The commercial development of SiC heating elements in this country during the last thirty years has involved two complementary and concurrent mechanisms: (*a*) a steady improvement in physical properties, both in mechanical ruggedness and resistance to deterioration in service, and (*b*) a gradual education of industrial consumers to the advantages of this method of heating, and the development of practical electric kilns.

An important feature of the modern SiC heating element is the so-called "cold end". Integral end sections of the elements are impregnated with silicon on other materials to make them highly conducting. Since the end sections are strong mechanically and the same diameter as the central heating section, the element is easily mounted and replaced, and little electrical energy is wasted outside the heating zone of the kiln.

SiC heating elements were originally used only in laboratory furnaces and in small kilns for high grade ceramic ware, but are now being used in many industries such as the currently booming ceramic dielectric industry. At least two large abrasive plants in the United States use electric kilns for firing grinding wheels.

Mann (6) recently published a discussion of SiC heating elements as used in Europe, largely from the point of view of operating economics. The art of making such heating elements has received little attention in the scientific and industrial literature, and is best studied from patents. It has been impossible to prepare a list of patents for inclusion in the bibliography of this review.

Silicon Carbide Nonlinear Resistors

SiC nonlinear resistors operate by entirely different mechanism from heating elements and are prepared in a different way. For this purpose black (p-type) SiC is used to form a column of discrete grains, which is made into a monolith by adding a ceramic bond and firing in a kiln. The temperature must be high enough to mature the bond, but much too low to sinter the grains together. Contacts are added to the ends with a metal spray. A body made in this way has the following characteristics: (*A*) It can conduct at very high current densities for short periods of time without damage. As much as 3000 amp/in.^{2} can be carried for a few microseconds. (*B*) Most of the voltage drop across the resistor occurs at the interfaces between the grains. Ohm's law becomes completely invalid and an approximate empirical relationship is used

$$V = KI^n \qquad (I)$$

where V is the voltage drop, K is a constant depending on the geometry of the body and the manufacturing process, I is current, and n is an empirically determined exponent. For small resistors that are used at current densities measured in milliamperes per square inch, n ranges between 0.20 and 0.35. At current densities of hundreds of amperes per square inch, as found in lightning arrester applications, n may be as low as 0.1.

SiC nonlinear resistors lend themselves readily to use in lightning arresters, since the current passed increases very rapidly with increasing voltage. They have a pronounced valving action and do not allow high voltages to be built up across them. In a typical installation, a SiC nonlinear resistor and a series of air gaps are connected in series from the line to ground. A sudden increase in voltage, such as is caused by a lightning discharge, breaks down the gap and a large current flows to ground, limiting the peak voltage on the line to a safe value. As soon as the line voltage returns to normal, the resistor reduces the current to such a low value that the arc across the gaps goes out.

Such lightning arresters were first used about 1908, when two patents were issued. Since that time development has been continuous and there are now at least five large manufacturers of SiC lightning arresters in this country. Recently, small nonlinear

SiC resistors, down to a watt or two in rating, have become increasingly available for use as surge suppressors, automatic volume controls, and for many applications in electronic equipment.

An outstanding paper on SiC nonlinear resistors was published in 1946 by Ashworth, Needham, and Sillars (7). This review is recommended as a basic text on the subject. Teszner *et al.* (8) have made an extensive investigation of the effect of the bond on the properties of lightning arrester blocks. An excellent article on lightning arresters was published by Roth (9) in 1954. Thien-Chi and Vergnolle (10) and Zückler (11) have published papers of general interest recently. The literature noted above is essentially practical in outlook. More theoretical papers are listed below.

Pure Silicon Carbide

The past ten years have seen tremendous advances in the basic theory of semiconductors. Such advances are possible only when a large commercial demand, either actual or potential, is coupled with adequate materials and facilities for research. The need for microwave rectifiers, followed by the discovery of transistor action, and the pressure for miniaturization of electronic components provided the impetus. In addition the most promising materials, Ge and Si, melt at readily attainable temperatures and can be prepared in extremely high purity. While SiC might potentially be equally useful as a semiconductor as Ge and Si, work on this material has been greatly hampered by the lack of specimens of high or even accurately known purity. SiC cannot be melted, sublimes with partial decomposition at about 2600°C, and its formation temperature under the usual conditions of manufacture is well above 2000°C. Under such handicaps it is not remarkable that this compound has not yet been made to the purity levels (impurities measured in parts per 10^6) required for basic research on semiconductors. In spite of these difficulties, three research groups have succeeded in recent years in preparing SiC of purity greatly exceeding that of the commercial material.

In 1931 Moers (12) reported the preparation of pure SiC by passing a gaseous mixture of hydrogen, silicon tetrachloride, and toluene over a filament heated to a temperature of at least 2200°C. Small, transparent yellow crystals grew on the filament. They were found by x-ray analysis to be of the cubic or beta modification, and were reported to be nonconducting, although no very serious attempt seems to have been made to measure their conductivity.

In 1947 Kendall and Yeo (13) described a development of the same process, and in 1953 Kendall (14) reported a further refinement of the technique. Using a carbon filament at 2100°-2200°C, and the mixture of gases noted above, he was successful in producing small, transparent yellow crystals of beta silicon carbide. Kendall and Yeo reported a readily measurable conductivity for all of their specimens, and noted that the deposited crystals conducted better than commercially prepared crystals. This may have resulted from the fact that their crystals were the beta modification, while the commercial crystals were almost certainly the alpha type. The few observations that have been made indicate that beta silicon carbide is probably a better conductor than the alpha type. Data available are not sufficient to show whether this apparent difference in conductivity is consistent.

Kendall determined the sign of the thermoelectric coefficient at room temperature and concluded that all yellow crystals were *n*-type. Black crystals could be made at temperatures below 2000°C and were usually found to be *n*-type, although commercial black SiC is *p*-type.

In 1955 Lely (15) reported a new approach to the problem of making the pure compound. By heating a SiC crucible from the outside to a temperature of 2500°-2600°C, he produced sublimed crystals for which he claimed a content of total impurities as low as 10^{-5} at. %. This figure represents a long step toward the purity required for research on semiconductors and probably exceeds anything done previously. The crystals were hexagonal, as would be expected in this temperature range, and the best ones were colorless and transparent. While Lely did not report conductivity figures, he apparently calculated the purity of 10^{-4} at. % from such measurements. If so, he must have obtained some crystals that were very low in conductivity.

Since atomic bonding in SiC is almost purely covalent, and since intrinsic conduction does not become significant below 1600°-1700°C, it is reasonable to expect that the pure compound is colorless, transparent, and substantially nonconducting at all ordinary temperatures. All the reported work supports this conclusion, in that the above array of properties is approached more and more closely as the purity increases. Therefore, it is assumed that the general nature of the pure compound is established, and that any explanation of the observed electrical properties of the commercial material must be based on the effects of various impurities that it contains.

Mechanism of Linear Conduction

The bare fact of electrical conduction by SiC is readily explained by the presence of impurities, especially those trivalent and pentavalent atoms that can occupy normal lattice sites. In general, a trivalent atom provides at its lattice site one less valence electron than is necessary to produce the four covalent bonds of the perfect SiC lattice. The missing electron acts as a hole that conducts very much as a positive electron would, with possibly a lower mobility. The only trivalent atom used commercially for this purpose is that of Al. Lundqvist (3) reported that the presence of Al favors the formation of the so-called type III modification of the hexagonal structure, but the resulting correlation between electrical properties and crystal type is probably coincidental.

A pentavalent atom provides at a lattice site one more than the number of electrons required for the normal covalent bonds. The excess electron is loosely bound and is easily raised to an energy level at which it can migrate through the lattice under

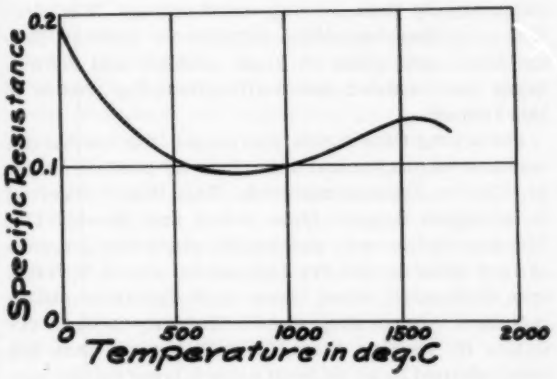

Fig. 1. Specific resistance in ohm-cm as a function of temperature for a typical SiC heating element.

the influence of an applied field. This phenomenon constitutes n-type conduction by definition.

It is instructive to examine a typical curve of specific resistance vs. temperature for a commercial SiC heating element (Fig. 1). The temperature scale has been divided rather arbitrarily into low, medium, and high ranges, respectively. In the low temperature region, the density of conducting electrons increases progressively with rising temperature as more and more electrons are released by thermal excitation from imperfect covalent bonds. These imperfect bonds occur at lattice sites occupied by atoms other than Si and C, or possibly where there is a local deficiency of C. The resistivity falls with increasing temperature, as is usually the case with semiconductors. In the medium temperature range, most of the available bonds have been broken and the number of conducting electrons changes little with temperature. In this range the thermal vibration of the lattice plays the leading role. Since this vibration interferes with the migration of conduction electrons, resistivity rises with increasing temperature. The conduction is essentially metallic, except for the low density of electrons as compared with typical metals. At about 1600°-1700°C, intrinsic conduction becomes significant as electrons are released from the normal covalent bonds, and the resistivity falls steeply with increasing temperature.

The "metallic" conduction range is of the greatest importance commercially, since the positive temperature coefficient of resistance confers a large degree of temperature stability on an electrically heated kiln. Heating elements made from gray SiC tend to have a higher initial resistance than those made from green SiC, and the range of negative temperature coefficient tends to extend over the metallic range and frequently to obscure it completely. This is probably the principal reason for the choice of green SiC as the raw material for commercial heating elements.

Theoretically it is possible for SiC containing nothing but Si and C to act as an impurity semiconductor as long as there are points in the crystal where the compound is at least locally nonstoichiometric. The existence of nonstoichiometric SiC has often been conjectured but never proved. The departure from stoichiometric proportions that would be necessary to explain the observed electrical effects is very much less than can be detected by chemical analysis, and there seems little likelihood that the question will ever be settled in this way. Lely (15) states rather positively that there is no evidence of any kind for the existence of nonstoichiometric SiC. He attributes the green color and conductivity to the presence of 0.0001-0.001% of pentavalent nitrogen, which would produce n-type conductivity as observed. Lely used a furnace with a protective atmosphere, and added various volatile halides to the gas to control the composition of the product. He found that Al and B additions promote p-type conductivity and that N and P cause n-type.

Kendall (14) produced SiC by deposition from the gas phase as noted earlier. By changing the Si/C ratio in the gases entering the furnace he was able to produce n- or p-type material at will, from which he concluded that he was obtaining a slight departure from stoichiometric proportions. If his starting materials were pure, his conclusion seems inescapable.

Summarizing the data, it seems likely that nonstoichiometric but otherwise pure SiC can be prepared under special conditions. The commercially important green variety seems to be an n-type semiconductor containing pentavalent nitrogen atoms on normal lattice sites. The ordinary gray SiC contains so many impurities that it may never be possible to explain its properties except in a qualitative way. As might be expected, it is quite variable electrically, and this variability extends down to individual crystals, where p-n junctions are not uncommon although the material is predominantly p-type. While black electrical grade SiC is also a comparatively impure product, the deliberate addition of Al swamps out the effect of the other impurities and results in stable and consistent p-type conductivity.

Mechanism of Nonlinear Conduction

In nonlinear SiC resistors the bulk resistivity of the crystals has no significant influence, since practically the entire voltage drop occurs at the interfaces between grains. Eq. (I) is sufficiently accurate for most purposes, but closer examination shows that n changes with current density if the latter is allowed to vary over a sufficiently large range.

In 1944 Kendall (16) reported measurements of voltage vs. current for single contacts between metal and SiC and between crystals of SiC. In the experiment most pertinent to the present discussion, he worked with a single contact between a green crystal and a black one. The range of current was from 10^{-10} to about 10^{-4} amp. Log-log voltage-current plots were approximately linear (n constant) over a current range of several powers of ten, but were far from linear when considered in their entirety. One of Kendall's curves is reproduced in Fig. 2. This example illustrates the fact that current flow between grains of SiC is a complicated phenomenon, and different mechanisms may be expected to play the leading role at different current densities.

Since the theory is controversial, it is well to examine first the empirical observations. To this end it

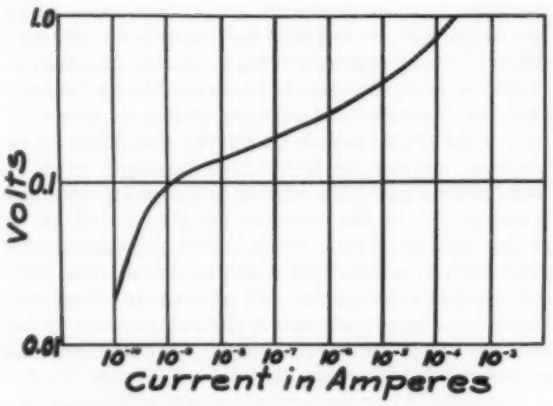

Fig. 2. Volt-ampere characteristic curve for a single contact between grains of SiC.

is convenient to speak of low, medium, and high current ranges.

In the low current range, current is proportional to voltage. Both Braun and Busch (17) and Kendall (16) made measurements in this range, and Kendall showed that for his particular crystals it extended up to a current density of about 10^{-9} amp/contact. The conclusion is clear that grain contacts conduct linearly at sufficiently low current densities.

The medium current range extends to 10^{-4}-10^{-3} amp/contact. In this range n of Eq. (I) is constant. The value of n is different for different specimens of SiC, but is within the range 0.20-0.35. The medium range of current densities is characterized by the fact that conduction is clearly nonlinear, and independent of secondary thermal effects caused by the dissipation of electrical energy at the contacts.

The high current range extends up to a current density at which the contacts suffer permanent damage from excessive heating, of the order of 0.1-1.0 amp/contact. This range is characterized by strong thermal effects, as shown by the appearance of a hysteresis loop in the voltage vs. current plot. Because of the thermal effects, it becomes difficult to attach a clear meaning to n, but the apparent value decreases to about 0.1. This low value of n is advantageous in lightning arrester applications, since it means that the nonlinear resistor has a pronounced "safety valve" action, and strongly resists any influence that tends to build up a high voltage across it.

With the above facts in mind, an attempt will be made to set up a model by which the various phenomena can be understood. Experience in this field has shown that a statement made today is likely to be proved wrong tomorrow. With this reservation in mind, it is still possible to trace some sort of logical path through the maze of experiment and argument that has grown up about this subject.

The basic fact to be explained is that the resistance of a single contact is much too high to arise from the known fairly low resistivity of the bulk material. This is true even if the true area of contact is a small fraction of the apparent area, leading to a so-called constriction resistance. Further, this contact resistance is nonlinear, the current changing much more rapidly than the impressed voltage. It is clear that a voltage-sensitive barrier to current flow exists at each grain to grain contact, and controversy has centered essentially about the nature of this barrier.

For a long time it was considered that the barrier was a solid mechanical one, made up predominantly of silica or siliceous materials. This theory received its strongest support from Braun and Busch (17). The assumption was reasonable, since the presence of such films on SiC crystals can be shown by electron diffraction. Also, some manufacturers obtain increased voltage drop and nonlinearity in their resistors by making them from SiC grain that has been calcined in air to form a silica layer on the surface. In addition, bonded lightning arrester blocks have a high initial resistance and must be "formed" by subjecting them to repeated high current surges. Forming greatly reduces and also stabilizes the resistance. There is little doubt that forming breaks down films of siliceous bond that infiltrate between the grains in the manufacturing process.

However, in 1949, Jones, Scott, and Sillars (18) and Mitchell and Sillars (19) showed clearly that the high and nonlinear contact resistance remained undiminished when all surface films were very carefully and completely removed. Surfaces for which the residual film, if any, was certainly less than 3Å thick were almost indistinguishable electrically from ones on which silica had been evaporated to a thickness of 90Å.

Since the barrier is a fairly good insulator at low field strengths, it can be made to act as the dielectric in a capacitor by firing a thin layer of silver on the surface. This experiment was carried out at the Norton Co. and capacitance was found to increase with increasing voltage. Assuming an effective dielectric constant of 10 for the barrier, its apparent thickness remained constant at 500Å up to 0.5 v, but decreased rapidly with increasing voltage and reached a value of 40Å at 2.0 v. A much more elaborate experiment of the same general type was reported by Mitchell and Sillars (19).

Since it has been shown that a mechanical film is not necessary to produce the observed effects, and that the apparent barrier thickness can be changed over a range of ten to one by changes in field strength, the mechanical film theory has become untenable. Meanwhile, research on transistors has provided plausible models of charge distribution that predict, at least qualitatively, the observed effects. The present consensus is that the barrier results from the distribution of space charge in the SiC lattice within a few angstroms of the surface. Further discussion of this phenomenon would exceed the scope of this article. Williams (20) has written a theoretical survey of the problem, and it can be followed in detail in the excellent series of papers by the research staff of Metropolitan-Vickers in England (5, 7, 13, 14, 16, 18, 19, 21).

Conclusions

While electrical uses of SiC have assumed industrial importance in recent years, the art has greatly exceeded the science. Research on SiC has been

hampered by an almost total lack of specimens of high or even known purity. Two methods have been developed to make the pure compound, and this problem is no longer insurmountable. The linear body resistance, and especially the nonlinear contact resistance, are both exploited commercially, but still present unsolved problems to the theoretician. Much excellent experimentation has been reported, especially in England, and a theoretical solution is probably attainable by the use of quantum mechanics. An attempt has been made to list the principal papers that should be read by those who would like to become conversant with the work that has been done in this field.

Manuscript received October 29, 1956. This paper was prepared for delivery before the Cleveland Meeting, Sept. 30 to Oct. 4, 1956.

Any discussion of this paper will appear in a Discussion Section to be published in the December 1957 JOURNAL.

REFERENCES

1. N. W. Thibault, *Am. Mineralogist*, **29**, 249 (1944); **29**, 327 (1944); **31**, 512 (1946); **33**, 588 (1948).
2. L. S. Ramsdell, *ibid.*, **32**, 64 (1947).
3. Dick Lundqvist, *Acta Chem. Scand.*, **2**, 177 (1948).
4. C. G. Harman and W. G. Mixer, Jr., U. S. A.E.C. Rpt. BMI 748, June 3, 1952.
5. J. T. Kendall, *J. Chem. Phys.*, **21**, 821 (1953).
6. F. J. Mann, *Elektrizitätswirtschaft*, **54**, 871 (1955).
7. F. Ashworth, W. Needham, and R. W. Sillars, *J. Inst. Elect. Engrs. (London)*, **93**, Part 1, 385 (1946).
8. S. Teszner, P. Seguin, and J. Millet, *Annales des Télécommunications*, **8**, 271 (1953).
9. A. W. Roth, *Elektrotech. u. Maschinenbau*, **71**, 107 (1954).
10. N. Thien-Chi and J. Vergnolle, *L'Onde Électrique*, **35**, 336, 222 (1955).
11. K. Zückler, *Z. angew. Phys.*, **8**, 34 (1956).
12. K. Moers, *Z. anorg. u. allgem. Chem.*, **198**, 243 (1931).
13. J. T. Kendall and D. Yeo, *Proc. Intern. Congr. Pure & Appl. Chem.*, **11**, 167 (1947).
14. J. T. Kendall, *J. Chem. Phys.*, **21**, 821 (1953).
15. J. A. Lely, *Ber. deut. keram. Ges.*, **32**, 229 (1955).
16. J. T. Kendall, *Proc. Phys. Soc. London*, **56**, 123 (1944).
17. A. Braun and G. Busch, *Helv. Phys. Acta*, **15**, 571 (1942).
18. T. K. Jones, R. A. Scott, and R. W. Sillars, *Proc. Phys. Soc. London*, **62**, 333 (1949).
19. E. W. J. Mitchell and R. W. Sillars, *ibid.*, **62**, 509 (1949).
20. M. O. Williams, *Automatic Telephone and Electric J., British*, **10**, 144 (1954).
21. R. Stratton, *Proc. Phys. Soc., London*, **68**, 746 (1955).

FUTURE MEETINGS OF
The Electrochemical Society

Washington, D. C., May 12, 13, 14, 15, and 16, 1957

Headquarters at the Statler Hotel

Sessions will be scheduled on

Electric Insulation, Electronics (including Luminescence, Semiconductors, Thermionic Cathodes, Instrumentation, and Screen Applications), Electrothermics and Metallurgy, Industrial Electrolytics, and Theoretical Electrochemistry (including a special symposium on electrolytes)

★ ★ ★

Buffalo, October 6, 7, 8, 9, and 10, 1957

Headquarters at the Statler Hotel

Sessions will be scheduled on

Batteries, Corrosion, Electrodeposition (symposium on "Metal Powders"), Electrodeposition—Corrosion (Joint Symposium on "Corrosion of Electrodeposited Metals"), Electronics (Semiconductors), Electro-Organics, Electro-Organics—Theoretical Electrochemistry (Joint Symposium), and Electrothermics and Metallurgy

★ ★ ★

New York, April 27, 28, 29, 30, and May 1, 1958

Headquarters at the Statler Hotel

★ ★ ★

Ottawa, September 28, 29, 30, October 1, and 2, 1958

Headquarters at the Chateau Laurier

★ ★ ★

Papers are now being solicited for the meeting to be held in Buffalo, N. Y. Triplicate copies of each abstract (*not exceeding 75 words in length*) are due at the Secretary's Office, 216 West 102nd St., New York 25, N. Y., *not later than June 1, 1957* in order to be included in the program. *Please indicate on abstract for which Division's symposium the paper is to be scheduled.* Complete manuscripts should be sent in triplicate to the Managing Editor of the JOURNAL at the same address.

Current Affairs

News Notes in the Electrochemical Field

New Patron Member

Westinghouse Electric Corp., Pittsburgh, Pa., recently became a Patron Member of The Electrochemical Society.

International Symposium on Passivity

The Electrochemical Society, the Bunsen Gesellschaft, and the Faraday Society are jointly sponsoring discussions on the subject of passivity in metals to be held near Darmstadt, Germany, during the week of September 2-7, 1957. This is probably the first international symposium on this subject since a similar meeting was arranged by the Faraday Society in 1914.

The program calls for invited and submitted papers from representatives of many countries including the United States, Canada, Germany, England, Switzerland, Italy, France, Japan, and Russia. Papers and discussion will appear in a special issue of the *Z. Elektrochem.*

Members of the committee arranging the Symposium are Professor K. F. Bonhoeffer, representing the Bunsen Gesellschaft, Dr. T. P. Hoar, representing the Faraday Society, and Professor H. H. Uhlig, representing The Electrochemical Society. Accommodations at the meeting are limited, but it is hoped that a few places can be kept open for active research workers in the field of passivity who feel that they would benefit by attending the discussions.

Inquiries in the United States should be addressed to Professor H. H. Uhlig, 8-202 Massachusetts Institute of Technology, Cambridge 39, Mass.

A.C.S.—E.C.S. Northwest Regional Meeting

The Pacific Northwest Section of The Electrochemical Society and the Northwest Region local section of the American Chemical Society are jointly sponsoring a meeting to be held in Spokane, Wash., June 13 and 14, 1957, at the Davenport Hotel. Chairman of The Electrochemical Society Program is Dr. G. H. Kissin, Dept. of Metallurgical Research, Kaiser Aluminum & Chemical Corp., Spokane, Wash.

Divisional sessions in organic chemistry, biochemistry, analytical chemistry, physical chemistry, and inorganic radiochemistry will be held under the sponsorship of the A.C.S. In addition, special symposia dealing with chemical educational programs, industrial cost estimation, and technical advances in the food industry will be held.

Eleventh Battery Research and Development Conference

The Eleventh Annual Battery Research and Development Conference will be held on Wednesday and Thursday, May 22 and 23, 1957, at the Berkeley-Carteret Hotel, Asbury Park, N. J.

The Conference will feature presentations on newly developed primary and secondary batteries and will be highlighted by a discussion of nuclear and solar energy devices. Dr. Farrington Daniels of the University of Wisconsin will be the luncheon speaker on May 23.

New E.C.S. Headquarters

Effective June 1, 1957, the national headquarters office of The Electrochemical Society will be located at 1860 Broadway, New York, N. Y. After that date, all communications should be sent to the above address. Until then, mail should be sent to 216 West 102nd St., New York 25, N. Y.

American Potash Sodium Chlorate Plant

American Potash & Chemical Corp. has announced plans to construct a $5,000,000 chemical manufacturing plant at Aberdeen, Miss., for the production of sodium chlorate.

Construction will start immediately at a 586-acre site on the Tombigbee River seven miles outside of Aberdeen, with completion scheduled for mid-1958. Initial production at the Aberdeen plant will be at the rate of 15,000 tons of sodium chlorate per year, with provisions for possible future expansion into other chemical fields.

The new facility marks AP&CC's first venture east of the Mississippi River for the manufacture of its Trona electrochemicals. When the plant is in production, it is believed AP&CC will be the largest producer of sodium chlorate in the western hemisphere.

Union Carbide to Build Nuclear Research Center in Sterling Forest

Plans for the construction of a nuclear research center in Sterling Forest, N. Y., were announced recently by Union Carbide and Carbon Corp. The Sterling Forest region is located in the southern part of Orange County, N. Y., approximately 40 miles from New York City.

The major facilities on the site will include: a five megawatt pool-type reactor, a radioactive materials laboratory, an ores and engineering laboratory, and a building for allied research operations and administrative functions. The Research Center will be operated jointly by Union Carbide Nuclear Co. and Union Carbide Ore Co., two of the corporation's divisions. It will serve as the focal point for nuclear research activity within Union Carbide.

Graham, Crowley & Associates Changes Name

Dr. A. K. Graham, President, has announced that effective March 31, 1957 the corporate name Graham, Savage & Associates, Inc. supersedes the former Graham, Crowley & Associates, Inc.

Frank K. Savage, who has been Vice-President of the firm since 1948, becomes a member of the Board of Directors. He is President and owner of Savage-Rowe Plating Co., Kalamazoo. This company's facilities include the pilot plant activity of Graham, Savage & Associates, Inc. and, to integrate Graham, Savage

and Savage-Rowe interest as particularly related to electrochemical research and development, Dr. Graham is Vice-President of Savage-Rowe Plating Co.

"Research—Key to Progress"

The role of scientific research in the national economy has been documented in a motion picture produced by Armour Research Foundation of Illinois Institute of Technology, Chicago.

Presented as a public service, the 15-min, 16 mm color film titled "Research—Key to Progress," traces the rise and contributions of research, particularly by independent industrial research organizations such as Armour Research Foundation. It is available for showing by colleges, professional societies, civic organizations, and other groups. Arrangements for showing it can be made by writing to the Public Relations Dept., Armour Research Foundation of Illinois Institute of Technology, 10 W. 35th St., Chicago 16, Ill.

Division News

Electrodeposition Division Symposia

The Electrodeposition Division is planning two symposia for the 1957 fall meeting of the Society in Buffalo, to be held October 6-10.

Dr. Cloyd Snavely, Battelle Memorial Institute, Columbus, Ohio, is arranging for a series of papers on "Metal Powders," covering the production, use, and properties of electrolytic powders.

"Corrosion of Electrodeposited Metals" is being organized by Dr. F. A. Lowenheim, Metal & Thermit Corp., P. O. Box 471, Rahway, N. J., and Dr. Harry Copson, International Nickel Co., P. O. Box U, Bergen Point Station, Bayonne, N. J., as a joint symposium with the Corrosion Division.

Authors who wish to present papers on either or both subjects are invited to contact the respective chairmen promptly. Abstracts (*not exceeding 75 words in length*) must be submitted to the Society Headquarters Office *not later than June 1, 1957.*

Electro-Organic—Theoretical Electrochemistry Symposium

A joint symposium sponsored by the Electro-Organic and the Theoretical Electrochemistry Divisions is to be held at the Buffalo Meeting of The Electrochemical Society, October 6-10, 1957. Among the topics selected for discussion are:

(*A*) Mechanism of organic reactions at electrodes.

(*B*) Mass transport in organic electrochemical systems.

(*C*) Polarization, adsorption, and double layer theory in organic systems.

(*D*) Round table—subject to be announced.

The program is to include invited and contributed papers. All abstracts of papers should be submitted in triplicate to the Secretary's Office, 216 W. 102nd St., New York 25, N. Y., *not later than June 1, 1957.*

Extended Abstracts Booklets

The Electronics Division will again publish an "Enlarged Abstracts" booklet for the Spring 1957 convention of the Society at Washington. The booklet will have 1000-word abstracts of the papers to be presented before the Electronics Division in its symposia on

Luminescence
Semiconductors
Instrumentation
Thermionic Cathodes
Screen Application

The abstracts will contain pertinent information and experimental data given in the papers, and will provide these details before publication, thus aiding workers in the field. The abstracts will be "printed but not published."

The booklet was to be available by about April 15; the price is $2.00.

Copies of the 1956 "Enlarged Abstracts" booklet of the San Francisco Meeting are still available at $2.00 per copy.

Checks should be made payable to: Electronics Division, The Electrochemical Society.

Orders should be sent to:
Martin F. Quaely
c/o Westinghouse Electric Corp.
Research Dept., Lamp Div.
Bloomfield, N. J.

★ ★ ★

The Theoretical Electrochemistry Division is making available extended abstracts of the symposium sponsored by the Division and the National Science Foundation on the Structure of Electrolytic Solutions (Electrolytes), as well as the two general symposia, for the Spring 1957 Washington Meeting.

Copies of the booklet can be obtained, at $3.00 each, from:
Dr. Ralph Roberts
3308 Camalier Drive
Washington 15, D. C.

Copies of the extended abstracts booklet of the 1956 San Francisco Meeting are still available at $2.00 each.

Electro-Organic Symposia

Papers are being solicited for presentation at the ECS Meeting to be held in Buffalo, October 6-10, 1957. The major topics to be presented are:

(*A*) Electrochemical methods in organic analysis.

(*B*) Electrolytic oxidation or reduction in organic synthesis.

(*C*) Organic polarography.

(*D*) Arc electrolysis.

(*E*) Mechanism of the Kolbe reaction.

(*F*) Anodic substitution reactions.

All abstracts of papers (*not exceeding 75 words in length*) should be submitted in triplicate to the Secretary's Office, 216 W. 102nd St., New York 25, N. Y., *not later than June 1, 1957.*

M. J. Allen, *Secretary-Treasurer*

Electrothermics and Metallurgy Division

The Nominating Committee (J. H. Brennan, Chairman, A. T. Hinckley, and B. L. Bailey) has proposed the following nominees for officers of the Electrothermics and Metallurgy Division for the coming term:

Chairman—A. U. Seybolt, 861 Charles St., Scotia, N. Y.

Vice-Chairman—G. M. Butler, Carborundum Co., Niagara Falls, N. Y.

Vice-Chairman—E. M. Sherwood, Battelle Memorial Institute, Columbus, Ohio

Secretary-Treasurer—J. H. Westbrook, General Electric Co., Schenectady, N. Y.

Members-at-Large—W. E. Kuhn, L. H. Juel, L. A. Stoyell, and M. A. Steinberg

Each nominee has given assurance of his willingness to serve if elected.

Additional nominations may be made from the floor. The election will be held at the business meeting of the Division during the Spring Meeting of the Society in Washington, D. C.

Theoretical Electrochemistry Division

The Nominating Committee (Norman Hackerman, Chairman, H. H. Uhlig, and Ernest Yeager) has selected the following nominees for

officers of the Theoretical Division for the coming term:

Chairman—Paul Delahay, Louisiana State University, Baton Rouge, La.

Vice-Chairman—Charles Tobias, University of California, Berkeley, Calif.

Secretary-Treasurer—Ralph Roberts, 3308 Camalier Drive, Washington, D. C.

Members-at-Large on Executive Committee—J. O'M. Bockris and Sigmund Schuldiner

Each nominee has given assurance of his willingness to serve if elected.

The election will be held at the business meeting of the Theoretical Division, May 16, during the Spring Meeting of the Society in Washington, D. C.

Battery Life Symposium Papers

The life of lead-acid batteries was discussed at the 1956 Cleveland Meeting in a symposium sponsored by the Battery Division. A booklet, "Life Testing of Automobile Batteries and Related Subjects," has been prepared containing the complete text and illustrations along with a summary of the discussion which followed.

This booklet can be obtained by sending $2.00 to E. J. Ritchie, Secretary, Battery Division, Eagle Picher Co., Joplin, Mo.

Papers included in this 96-page booklet are:

"Appearance of Battery Components at the End of Life Under Laboratory Test" by B. Agruss.

"Effect of Normal Car Service on the Intermediate and Final Periods of Lead Storage Battery Performance" by D. Haskell.

"The Correlation of Laboratory Life Tests with Automotive Service Tests of Lead-Acid Batteries" by J. F. Schaefer.

"The Effect of Temperature on the Cycling Life of Lead-Acid Storage Batteries" by J. F. Macholl and A. G. Koch.

"The Effect of Arsenic and Silver in Grid Alloy on Storage Battery Life in Field Tests and Fleet Service" by Howard Stoertz.

"Pulse Maintaining of Storage Batteries" by J. B. Godshalk.

"Positive Post Corrosion in Lead-Acid Cells" by Otto H. Bauer.

Section News

Chicago Section

On its Corrosion Night in January the Chicago Section presented Dr. Andrew Dravnieks, Head of the Corrosion Section of the Engineering Research Lab., Standard Oil Co. (Indiana). The subject of the talk was "Corrosion and Corrosion Research in the Oil Refining Industry." Dr. Dravnieks briefly described the laboratories of the Standard Oil Co. and the Corrosion Lab. specifically. He pointed out the peculiar task of the oil companies, namely making noncorrosive products from corrosive crudes.

A good portion of the problems of the refinery are concerned with high temperature corrosion (above 400°F) by sulfur compounds in the crude. He showed that the corrosivity of the crude was proportional to its sulfur content. On steel, iron sulfide scale formed and, to mitigate this, chromium was added to the steel. In recent times, the newer processes for obtaining higher octane numbers cause hydrogen attack in spite of the chromium content of the steels, hence refineries are using 18-8 chrome nickel steels. The growth of sulfide scales follows linear, parabolic, and sigmoid curves.

The low temperature corrosion problems are those of condensed water in the crudes. Inhibitors are usually amines. Dr. Dravnieks showed the results of an economic study to determine the best inhibitor for this problem. The effectiveness of the inhibitor was studied using a conductometric test, in which the depth of the attack is measured by the increase in resistance of a ribbon-like specimen.

At the Chicago Section's February meeting the featured speaker was Dr. Arthur Fleisher, Research Director, Nickel-Cadmium Battery Corp., who spoke on the subject "Nickel-Cadmium Batteries." He pointed out that some of the original sintered batteries developed by I. G. Farben were captured during the war. Their performance and rechargeability at low temperatures were found attractive by the U. S. Although they are more expensive initially, they compare economically on other bases with lead cells. The speaker showed many applications of the nickel-cadmium battery, such as starters for emergency telephone generators, street light relays, and other emergency power sources.

The discharge reactions are the oxidation of cadmium and reduction of the nickelic ion. The construction and method of assembly were demonstrated with the aid of samples and slides. Dr. Fleisher then described a very interesting, completely sealed cell which apparently is feasible with nickel-cadmium.

William H. Colner, *Secretary*

Midland Section

The first technical meeting of the year was held on February 5 at the Dow Chemical Co. Auditorium in Midland, Mich.

Charles H. Clark of the Power Sources Branch of the Signal Corps Engineering Lab., Fort Monmouth, N. J., spoke on "Communications Type Batteries for Military Use."

Mr. Clark described three types of primary cells: (*a*) the zinc-carbon-manganese dioxide, Leclanché Cell, (*b*) the zinc-mercuric oxide cell, and (*c*) the magnesium-carbon-manganese dioxide cell. He traced the history of each type of cell illustrating the factors involved in improving the capacity, shelf life, and other properties of the batteries.

The need for military batteries to operate over a broad temperature range was stressed, the lowest temperatures of the Arctic being in the neighborhood of —65°F, and the highest in the tropics 115°F. The magnesium battery has been found to have excellent tropical storage (113°F) properties, but the Signal Corps is continually striving to find better low temperature batteries.

Now that the trend is to smaller batteries, the zinc-mercuric oxide cell and the magnesium cell will be playing more of a part in the battery field in the future.

P. F. George, *Secretary-Treasurer*

Ontario-Quebec Section

The first meeting of the 1956-57 season was held in the afternoon of November 16 at McGill University in Montreal. The speakers were Mr. R. M. O. Maunsell, Vice-President and Technical Director, Electric Reduction Co. of Canada, Ltd., Toronto, and Mr. W. E. Schwabe, Development Labs., Niagara Falls, N. Y. Dr. Peter Ensio acted as technical chairman.

Mr. Maunsell's paper entitled "Production of Phosphorus" outlined the early history of the production of phosphorus and the development of the present method of making this element, with particular details of the latest types of electric furnaces employed and the energy distribution in the furnaces. Raw material requirements for producing phosphorus were discussed. Modern

methods for the production of phosphoric acid, sodium phosphate, and other products of phosphorus to meet the demands of the Canadian market were also considered.

Mr. Schwabe addressed the meeting on the "Fundamental Principles of the Electric Arc." He pointed out that the influence of thermic, magnetic, and convection conditions on the arc in the electric furnace are only qualitatively understood. Open arcs of steel furnaces display a very erratic behavior during melt-down, whereas submerged arcs in most cases are smooth. The investigation of some factors of erraticity of open arcs by means of motion pictures was discussed. The geometry of the electrode tip, arc length, and thermoionization were found to be the most important parameters. The power or heat release in an arc was given by the condition of the circuit such as arc voltage, current, and power factor. Mr. Schwabe used slides and motion pictures to show typical conditions of the electric furnace arcs.

H. A. Timm, *Secretary*

Washington-Baltimore Section

The Section held its February meeting at the National Bureau of Standards.

Mr. George G. Harman spoke on an investigation which he conducted as an associate of the National Bureau of Standards and the University of Maryland. His topic was "High Frequency Induced Electroluminescence." He gave a short review of three possible mechanisms of electroluminescence. Apparatus and techniques for measuring electroluminescence at excitation frequencies of up to 400 megacycles were described. The "avalanche breakdown" mechanism was given as the basis for explaining the electroluminescence properties of $BaTiO_3$, $SrTiO_3$, and TiO_2. Mr. Harman said that the high fields obtained in the electrode-crystal interface region were due to a saturated dielectric layer such as that described by Kanzig.

Dr. S. Schuldiner of the Naval Research Lab. talked on "Hydrogen Producing Reactions on Alpha and Beta Palladium." He discussed the mechanisms of hydrogen-producing reactions which occur on cathodically polarized noble metals.

Gwendolyn B. Wood, *Secretary*

New Members

In March 1957 the following were approved for membership in The Electrochemical Society by the Admissions Committee:

By action of the Board of Directors of the Society, all prospective members must include first year's dues with their applications for membership.

Also, please note that, if sponsors sign the application form itself, processing can be expedited considerably.

Active Member Sponsored by a Sustaining Member

Martin E. Kagan, Yardney Electric Corp., 40-50 Leonard St., New York 3, N. Y. (Battery)

Active Members

John N. Agar, University of Cambridge; Mail add: Flat 6, "Southacre," Latham Rd., Cambridge, England (Corrosion, Theoretical Electrochemistry)

Douglas R. Allenson, National Carbon Co.; Mail add: 5830 Woolman Court, #51, Parma 30, Ohio (Battery)

Ralph T. Angstadt, Electric Storage Battery Co.; Mail add: 4542 Manayunk Ave., Philadelphia 28, Pa. (Battery)

Avak Avakian, Sylvania Electric Products Inc., Woburn, Mass. (Electronics)

Ralph A. Bacon, Dow Chemical Co.; Mail add: 502 State St., Midland, Mich. (Corrosion)

Austin H. Beebe, Jr., Federal-Mogul-Bower Bearings, Inc.; Mail add: P.O. Box 377, Ann Arbor, Mich. (Electrodeposition)

Thomas J. Butler, U. S. Steel Research Lab.; Mail add: 114 Elmwood St., Monroeville, Pa. (Corrosion)

Charles R. Campana, Spectranome Plating Co., Inc.; Mail add: 2459 De Voe Terrace, New York 68, N. Y. (Electrodeposition, Theoretical Electrochemistry)

Paul R. Carter, Applied Research Lab., U. S. Steel Corp., Monroeville, Pa. (Corrosion)

Arthur J. Catotti, Capacitor Dept., General Electric Co., Hudson Falls, N. Y. (Electric Insulation)

John W. Cleland, Oak Ridge National Lab., Union Carbide Nuclear Co., Bldg. 3025, Oak Ridge, Tenn. (Electronics)

Howard L. Craig, Jr., Reynolds Metals Co.; Mail add: 5019 W. Seminary Ave., Richmond 27, Va. (Corrosion)

Paul F. Derr, Westvaco Chlor-Alkali Div.; Mail add: 220 Bird Court, South Charleston 3, W. Va. (Industrial Electrolytic)

Arthur B. Eilbeck, Nife, Inc.; Mail add: 100 Fremont Ave., Park Ridge, N. J. (Battery)

Christopher J. B. Fincham, National Research Corp.; Mail add: Apt. 23, 60 The Fenway, Boston 15, Mass. (Electrothermics & Metallurgy, Theoretical Electrochemistry)

William H. Fischer, General Electric Co.; Mail add: 20 Jay St., Schenectady 5, N. Y. (Corrosion, Electric Insulation)

Harvey L. Goering, Battelle Memorial Institute, 505 King Ave., Columbus 1, Ohio (Electronics)

Mitchell J. Halle, Sylvania Electric Products Inc.; Mail add: 26 Woodcrest Dr., Wakefield, Mass. (Electronics)

Herman N. Hammer, Hill Cross Co., Inc.; Mail add: 94 Vivian Ave., Emerson, N. J. (Electrodeposition)

Leland F. Hunt, Kaiser Aluminum & Chemical Corp.; Mail add: 2 Hidden Valley Rd., Lafayette, Calif. (Industrial Electrolytic)

Bernard Jacobs, Sperry Semiconductor Div., Sperry Rand Corp., Wilson Ave., So. Norwalk, Conn. (Electronics)

Jack G. Jeffries, Aluminum Co. of Canada, Ltd.; Mail add: 233 Gay Lussac St., Arvida, Que., Canada (Industrial Electrolytic)

Howard R. Karas, Globe-Union Inc.; Mail add: 5730 M. Bay Ridge Ave., Milwaukee 17, Wis. (Battery, Theoretical Electrochemistry)

Kenneth L. Keating, Semiconductor Products Div., Motorola Inc., 5005 E. McDowell Rd., Phoenix, Ariz. (Electronics)

Sara J. Ketcham, Aeronautical Materials Lab.; Mail add: Alden Park Manor, Philadelphia 44, Pa. (Corrosion, Electrodeposition, Theoretical Electrochemistry)

Otto J. Klingenmaier, Kersman Equipment Co.; Mail add: 853 Second St., N. W., Grand Rapids 4, Mich. (Electrodeposition)

James L. Kroon, Dow Chemical Co.; Mail add: 714 E. Ashman, Midland, Mich. (Industrial Electrolytic, Theoretical Electrochemistry)

San-Mei Ku, Sylvania Electric Products Inc.; Mail add: 20-65 Crescent St., Apt. 2B, Long Island City 5, N. Y. (Electronics)

Jack Lowen, Lincoln Labs., M.I.T.; Mail add: 98 Wayne Rd., Needham 94, Mass. (Corrosion, Electrodeposition, Electronics, Theoretical Electrochemistry)

Ulrich F. Marx, Wilmot Breeden Labs., Umberslade Park, Hockley Heath, Solihull, Warwicks, England (Electrodeposition)

William E. Moffitt, National Carbon Co.; Mail add: 1673 Wright Ave., Apt. 4, Rocky River, Ohio (Battery)

Donald Mohler, General Electric Co.; Mail add: Kaydeross Ave., Saratoga Springs, N. Y. (Electric Insulation)

Roger Parsons, Dept. of Chemistry, The University, Bristol 8, England (Theoretical Electrochemistry)

Donald K. Pattilloch, Electro Chem Fiber Seal Corp. and Sun Chemical Co.; Mail add: 110 East End Ave., New York 28, N. Y. (Electric Insulation, Electrodeposition, Electronics, Electro-Organic)

Paul G. Pohl, Chemi-Graphic Inc.; Mail add: 72 Lower Beverly Hills, West Springfield, Mass. (Corrosion, Electrodeposition)

Anders J. Ringb Om, Dept. of Chemistry, Abo Akademi (Swedish University of Finland), Abo, Finland (Theoretical Electrochemistry)

Bernard J. Rothlein, Sperry Semiconductor Div., Sperry Rand Corp., Wilson Ave., So. Norwalk, Conn. (Electronics)

Lincoln R. Samelson, Lake Publishing Co., 718 Western Ave., Lake Forest, Ill. (Electric Insulation)

Baldwin Sawyer, Sawyer Research Products, Inc., 35400 Lakeland Blvd., Eastlake, Ohio (Electronics)

Milton L. Selker, Clevite Research Center; Mail add: 3175 Morley Rd., Shaker Heights 22, Ohio (Electrodeposition)

Norman R. Thielke, National Carbon Co.; Mail add: 4601 Georgette Ave., North Olmsted, Ohio (Electronics)

Helmut E. Thierfelder, C & D Batteries, Inc.; Mail add: 9526 Clark St., Philadelphia 15, Pa. (Battery)

Roger C. Tittel, Cummins Engine Co., Inc., Columbus, Ind. (Electrodeposition)

Fritz Todt, Bundesanstalt fur Materialprufung; Mail add: Berlin-Wannsee, Tristanstr. 28, Germany (Corrosion, Electrodeposition, Electronics)

Loerwood C. Wasson, A. O. Smith Corp., Milwaukee 1, Wis. (Corrosion)

Robert C. Weast, Case Institute of Technology; Mail add: 10900 Euclid Ave., Cleveland 6, Ohio (Corrosion)

Reinstatements to Active Membership

Joseph B. Kushner, Joseph B. Kushner Electroplating School; Mail add: 115 Broad St., Stroudsburg, Pa. (Electrodeposition)

Ralph H. Lee, J. Holland & Sons, Inc.; Mail add: 3314 Giles Place, New York 63, N. Y. (Electrodeposition, Theoretical Electrochemistry)

Transfers from Student Associate to Active Membership

Milton B. Clark, National Carbon Co.; Mail add: 8078 Royal Haven Dr., Cleveland 33, Ohio (Theoretical Electrochemistry)

Robert C. Griffis, General Electric Co., 1331 Chardon Rd., Euclid, Ohio (Electrothermics & Metallurgy, Industrial Electrolytic)

John W. Winslow, Jr., U. S. Naval Radiological Defense Lab.; Mail add: 2125 Paradise Dr., Tiburon, Calif. (Electric Insulation)

Student Associate Members

Alfred E. Hoover, University of Michigan; Mail add: 2107 Jackson Ave., Ann Arbor, Mich. (Theoretical Electrochemistry)

Yemmanur Jayachandra, Indian Institute of Science, E-28 Hostels, Bangalore 3, India (Industrial Electrolytic)

Gadamsetty Venkateswarlu, Indian Institute of Science, Hostel F-2, Bangalore 3, South India

Transfers from Student Associate to Associate Membership

Aleksandrs Martinsons, University of Michigan; Mail add: 513½ E. William, Ann Arbor, Mich. (Theoretical Electrochemistry)

Harold E. Munns, Diamond Alkali Research Center, P.O. Box 348, Painesville, Ohio (Electrodeposition)

Deceased Reported During February 1957

Erwin F. Lowry, Salem, Mass.

Book Reviews

Electrochemistry. Principles and Applications, by Edmund C. Potter. Published by the Macmillan Co., New York; Cleaver-Hume Press Ltd., London, 1957. xii + 418 pages, $10.00.

The first eight chapters of this book deal with: laws of electrolysis, coulometry, conductance and transport, ionic equilibria, reversible potentials, reference cells, irreversible electrode processes, electric double layer and electrokinetic phenomena, electrochemical measurements in analysis. Chapters 9 and 10 are on the theory and practical aspects of metallic corrosion. Chapters 12-17 deal with technical processes: first cathodic, then anodic electrolytic processes; primary and secondary cells of commercial importance, and a concluding section on fuel cells.

The author states as his aim: to fill the need for a concise, introductory text showing how basic principles relate to the diverse applications of electrochemistry, reflecting modern interpretations of electrolytic processes, and suitable for the technological student or the specialist electro-

Manuscripts and Abstracts for Fall Meeting

Papers are now being solicited for the Fall Meeting of the Society, to be held at the Statler Hotel in Buffalo, N. Y., October 6, 7, 8, 9, and 10, 1957. Technical Sessions will be scheduled on Batteries, Corrosion, Electrodeposition (symposium on "Metal Powders"), Electrodeposition—Corrosion (Joint Symposium on "Corrosion of Electrodeposited Metals"), Electronics (Semiconductors), Electro-Organics—Theoretical Electrochemistry (Joint Symposium), and Electrothermics and Metallurgy.

To be considered for this meeting, triplicate copies of abstracts (*not to exceed 75 words in length*) must be received at Society Headquarters, 216 West 102nd St., New York 25, N. Y., *not later than June 1, 1957. Please indicate on abstract for which Division's symposium the paper is to be scheduled.* Complete manuscripts should be sent in triplicate to the Managing Editor of the JOURNAL at the same address.

* * *

The Spring 1958 Meeting will be held in New York City, April 27, 28, 29, 30, and May 1, 1958, at the Statler Hotel. Sessions will be announced in a later issue.

chemist. This aim has been achieved admirably. The book reads smoothly, is full of informative material, for the most part is accurate, up to date, and written from a thoroughly modern viewpoint. It is evident that the author is well aware of recent developments in theory and practice.

There are only a few oversights of proofreading; for examples, *see* Eq. 8, p. 50; second line from bottom, p. 50; coordinates of figures, pp. 161, 167.

No book, of course, is perfect. Since this one, in spite of the word "introductory" used above, is not at the elementary level, it is possibly unfortunate that the author did not treat some of the theoretical topics more completely. At least, it would be useful to have specific references to literature where details can be found (only a general bibliography is given, at the end of the book). In some cases, the author leaves a false impression: *see* Fig. 12, p. 41, and the statement, p. 43 "As we have seen, the basis of the Debye-Hückel-Onsager theory is the complete dissociation of strong electrolytes with segregation of ions into clusters." The treatment of cells without transference could well be extended, calculation of activities illustrated, evaluation given of the reliability of standard potentials from various sources. On p. 153, the implication that really pure H_2SO_4 would show no "residual current" is misleading.

The treatment of potentials, Chapter 4, illustrates the wide divergence of thought concerning reversible cells, and the need for authoritative clarification in this field. The heading is "Reversible Electrode Potentials," but the treatment is essentially of cell or reaction potentials, with what is now the customary confusion about the role of interfacial Galvani potentials. The author says "Thus, practical measurements always yield the *difference* between two metal-solution electrode potential differences (but see a refinement of this statement below." The refinement, of course, does not help much. Also, the discussion of "null" electrodes, while of interest in itself, does not contribute much to the subject in general.

C. V. King

Vacuum Deposition of Thin Films by L. Holland. Published by John Wiley & Sons, Inc., New York, 1956. xix + 541 pages, + 25 full-page plates. $10.00.

The deposition of thin films by high vacuum techniques is still very much of an art based on a multitude of empirical and inadequately tested 'trial and error' procedures. Furthermore, these procedures have not been at all well communicated. As a result, their repeated and time-consuming rediscovery has become the custom among an ever-increasing number of users of thin films.

It is, therefore, a most welcome event to find this well-written, thorough, up-to-date book by Holland. While it will be extremely valuable to the many newcomers in this field, it will perhaps be most appreciated by those of us who have had to learn the "hard way." Not only does the text present details of the various techniques, but it also provides a critical comparison and evaluation of these techniques based on the author's own extensive experimental studies.

The book is divided into 16 chapters, six of which deal with the equipment used and methods of preparing films: Vacuum Evaporation; Degassing of Plastic Materials in Vacuo; Durability of Vacuum Deposited Layers and Surface Cleaning Apparatus; Vapour Sources; Evaporation Techniques for a Range of Metals and Alloys; Cathodic Sputtering. The remaining chapters are concerned with the formation, structure, and properties of the films and with their practical applications, thus: optical interference; metallized resistors; capacitors; crystal oscillator electrodes; surface replicas; metal oxide conductors; decorative films on plastics, etc.

The text contains an overwhelming amount of practical information. Especially to be mentioned are the numerous and valuable summary tables, for example: Vacuum Properties of Several Plastics; Water Absorption on Plastic Materials; Techniques and Refractory Support Materials for Evaporating Metals; Resin-Solvent Compatibility Chart; Protective Lacquer Coatings; and the Appendix "Deposition Characteristics and Refractive Indices of a Range of Inorganic Compounds."

The detailed discussions of prevention of pump oil contamination; of chemical, ionic, and electron bombardment cleaning; of evaporation of alloys; of 'flash' evaporation; of the crystalline growth of films; of evaporated coatings on plastics; of oxide films all supply a long standing void in our information concerning these subjects.

Nor has the scientific approach to the subject been overlooked. Thus, Chapter 5 presents a theoretical approach to the "Emission Characteristics of Vapour Sources and Film Thickness Distribution" and then compares such theoretical results with the distribution actually obtained using "practical" vapor sources. The subjects of gas ballasting; physical properties of thin films; interference films are given such theoretical treatment as is currently possible.

A bibliography of 557 references, referred to by number in the text but also indexed by authors, is a most valuable feature of the book. It is amply illustrated with line drawings and a number of photo-plates.

It is the opinion of this reviewer that Holland's book is a most important and valuable addition to the field of high vacuum technology and that its clear presentation will stimulate the application of high vacua methods to many current problems.

Joseph Greenspan

Precision Electrical Measurements, Proceedings of an International Symposium held at the National Physical Lab., Teddington, Middlesex, England, in December 1954. Published by Philosophical Library, Inc., New York, 1956. About 250 pages, $12.00.

The 26 papers included in this volume have as their theme the techniques of precise measurement of certain electrical quantities. The Proceedings are divided into five parts, dealing successively with techniques applicable to electrical fields and dielectrics, magnetic fields and associated materials, electrotechnical measurements, high voltage measurement, and impulse testing.

In the section on capacitance and dielectrics, measurements from 0.05 cps up to microwave frequencies are described. A full description of instrumentation and practical difficulties is given in most cases. The section on magnetic fields includes studies over a broad range of frequencies, but most of the papers are of a general nature. The last three sections will be of particular interest to designers of transformers and others concerned with high voltages.

Summaries of the discussions are attached to each part. The volume is liberally illustrated and the photographic stencils used to reproduce the papers seem satisfactory.

B. R. Sundheim

pH Measurements by Victor Gold. Published by Methuen & Co., Ltd., London; John Wiley & Sons, Inc., New York, 1956. 125 pages, $2.25.

An excellent little monograph for those who still think of pH in terms of $-\log C_{H^+}$ or $-\log a_{H^+}$; emphasizes the fact that the modern definition of pH is an operational one. The theory is examined in detail to show

why this must be so. The accepted British and American standards are presented, with clear discussion of the theoretical and practical reasons for their choice, and of their validity.

C. V. King

Announcements from Publishers

Arcs in Inert Atmospheres and Vacuum. Edited by W. E. Kuhn. Published by John Wiley & Sons, Inc., New York; Chapman & Hall, Ltd., London, 1956. viii + 188 pages, $7.50.

Papers presented at a Symposium of the Electrothermics and Metallurgy Division of The Electrochemical Society in San Francisco, May 1956.

Fundamental Properties of Metal-Ceramics Mixtures at High Temperatures, Alfred University, for Office of Naval Research, Jan. 1955. Report PB 121413,* 103 pages, $2.75.

Corrosion Preventive Additives, 2 reports, prepared by E. J. Schwoegler and L. U. Berman, Armour Research Foundation, for Wright Air Development Center. **Part 2**—PB 121113,* March 1954, 168 pages, $4.25. **Part 3**—PB 121108,* Dec. 1954, 65 pages, $1.75.

Calculated Efficiencies of NaI Crystals, E. A. Wolicki, R. Jastrow, and F. Brooks, Naval Research Lab., Oct. 1956. Report PB 121419,* 40 pages, $1.00.

Elementary Quantitative Analysis; Theory and Practice by W. J. Blaedel and V. W. Meloche. Published by Row, Peterson and Co., Evanston, Ill. 832 pages.

Alkaline Storage Batteries: The Self-Discharge of the Positively Charged Nickel Oxide Electrode. Part 2—Potential as a Function of Time on Open Circuit and as a Function of the Active Oxygen on the Nickel Oxide Plates, R. C. Pitman and G. W. Work, Naval Research Lab., Oct. 1956. Report PB 121483,* 17 pages, 50 cents.

Chain Reactions by F. S. Dainton. Published by Methuen & Co., Ltd., London; John Wiley & Sons, Inc., New York, 1956. xv + 183 pages, $2.90.

Surface Treatments of Low Alloy Steels, Sam Tour, Sam Tour and Co., Inc., for Wright Air Development Center, Nov. 1954. Manual PB 121507,* $5.00.

A compilation of information and data on surface treatments for low alloy steels for corrosion and oxidation resistance includes general descriptions of coating techniques, analyses of temperature ranges to which each technique is applicable, cost and life limitations, possibilities of treatment of assemblies, and formability and weldability methods for materials treated before assembly.

Survey of the Literature on Antioxidants and Anticorrosion Additives for Lubricants at Elevated Temperatures, J. W. Cole, Jr., A. Burger, and A. F. Benton, University of Virginia, for Wright Air Development Center, May 1954. Report PB 121726,* 830 pages, $10.00.

This bibliography of 2500 items was compiled from a survey of literature between 1916 and 1952 on high temperature oxidation and corrosion inhibitors for synthetic and natural lubricating oils.

Ellipsometry: 1—General and Theoretical Considerations; 2—Application to the Fundamental Examination of Adhesion, R. L. Patrick, D. A. Ross, and W. A. Vaughn, Quantum, Inc., for Wright Air Development Center, March 1956. Report PB 121663,* 44 pages, $1.25.

New fields of investigation in the biological, chemical, and physical sciences have been opened up by the ability to measure films in terms of their molecular thickness. A simple, versatile tool for determining these thicknesses is the ellipsometer, or polarizing spectrometer. Precise determinations to a few Angstroms are possible.

* Order from Office of Technical Services, U. S. Dept. of Commerce, Washington 25, D. C.

Phase Diagrams for Ceramists by Ernest M. Levin, Howard F. McMurdie, and F. P. Hall. Edited and published by The American Ceramic Society, Inc., Columbus, Ohio, 1956. 286 pages, $10.00.

Materials and Processing in Manufacturing by E. Paul Degarmo. Published by the Macmillan Co., New York, 1957. x + 755 pages, $8.50.

High Temperature—A Tool for the Future. Proceedings of a Symposium sponsored by Stanford Research Institute, June 1956. Published by the Institute. 218 pages, $5.00.

Les Principes de l'Electrophorese by René Audubert and Serge de Mende. Published by Presses Universitaires de France, 108 Boulevard Saint-Germain, Paris VI°, 204 pages, 1,500 French francs.

The volume is devcted to the study of the fundamental laws governing electrophoresis. Like electrophoresis in liquid phase, *electrophoresis on paper* is a direct application of the fundamental principles of electrochemistry. This book expounds the principal results obtained in the various spheres in which it is used, particularly *in human pathology.*

Proceedings of the Sixth Meeting of the International Committee for Electrochemical Thermodynamics and Kinetics (C.I.T.C.E.). Published by Butterworths Scientific Publications, London, 1955. xvi + 567 pages, 84s. (about $12.00).

An Encyclopedia of the Iron and Steel Industry. Compiled by A. K. Osborne. Published by Philosophical Library, Inc., New York, 1956. xi + 558 pages, $25.00.

Electronic Computers. Edited by T. E. Ival. Published by Philosoph-

December 1957 Discussion Section

A Discussion Section, covering papers published in the January—June 1957 JOURNALS, is scheduled for publication in the December 1957 issue. Any discussion which did not reach the Editor in time for inclusion in the June 1957 Discussion Section will be included in the December 1957 issue.

Those who plan to contribute remarks for this Discussion Section should submit their comments or questions in triplicate to the Managing Editor of the JOURNAL, 216 W. 102 St., New York 25, N. Y., *not later than September 1, 1957.* All discussion will be forwarded to the author, or authors, for reply before being printed in the JOURNAL.

ical Library, Inc., New York, 1956. viii + 167 pages, $10.00.

Organo-Metallic Compounds by G. E. Coates. Published by Methuen & Co., Ltd., London; John Wiley & Sons, Inc., New York, 1956. viii + 197 pages, $2.50.

A review of compounds with metal-carbon bonds only; 434 literature references.

Transactions of the Institute of Metal Finishing, Vol. XXXI, 1955. Proceedings of the 4th International Conference on Electrodeposition and Metal Finishing, London, April 1954. Published by the Institute. £3.10.

Salt and Water, Power and People. A Short History of Hooker Electrochemical Co. by Robert E. Thomas. Published by the Hooker Electrochemical Co., Niagara Falls, N. Y., 1955. 109 pages.

College Chemistry by Linus Pauling. Published by W. H. Freeman & Co., San Francisco. 2nd Edition, 1955. xii + 685 pages, $6.00.

Meetings of Other Organizations

May 20-22—National Association of Corrosion Engineers, Northeast Regional Meeting, Syracuse, N. Y.

May 22-24—American Institute of Chemists, Annual Meeting, Sheraton-Mayflower Hotel, Akron, Ohio.

June 9-12—American Institute of Chemical Engineers, Regional Meeting, Olympic Hotel, Seattle, Wash.

June 17-21—American Society for Engineering Education, Annual Meeting, Cornell University, Ithaca, N. Y.

June 20-22—American Physical Society, Regional Meeting, Notre Dame, Ind.

Sept. 8-13—American Chemical Society, National Meeting, New York, N. Y.

Sept. 15-18—American Institute of Chemical Engineers, Regional Meeting, Lord Baltimore Hotel, Baltimore, Md.

Advertisers' Index

American Potash & Chemical Corporation 118C
Bell Telephone Laboratories, Inc. 108C
Dow Chemical Company..... 110C
Enthone, Incorporated ..... Cover 4
Great Lakes Carbon Corporation ..... Cover 2
National Carbon Company..... 118C
E. H. Sargent & Company..... 107C
Stackpole Carbon Company..... 106C

Employment Situation

Please address replies to box shown, c/o The Electrochemical Society, Inc., 216 W. 102nd St., New York 25, N. Y.

Position Wanted

Chemist, 15 years' creative and responsible work in metal finishing, corrosion, with experience in the continuous anodizing and dyeing of aluminum, seeks position in or near Metropolitan New York. *Reply to Box 361.*

Opening for ELECTROCHEMIST

Interested In Development Work in aqueous and fused salt electrolysis, including all aspects of cell operation

A program is being established in a new laboratory devoted to these fields of investigation, and contacts will be had with Management, Research, Sales, Production, and Customer organizations.

The man we want should be well grounded in theoretical and applied electrochemistry and preferably should have had one or more years experience in the electrolysis of alkali halides and metal compounds. Emphasis will be placed on the commercial application of the work.

This is a challenging opportunity to establish yourself with a Development program in electrolysis where the future is practically unlimited.

Please submit full details of qualifications to:

NATIONAL CARBON COMPANY

Division of Union Carbide Corporation • Development Laboratory
3825 Highland Avenue, Niagara Falls, New York—Attention: Dr. N. J. Johnson

RESEARCH AND DEVELOPMENT

Research program requires experienced electrochemists to work in electrolytic process development. Excellent laboratory facilities located twenty miles East of Los Angeles.

GROUP LEADER

Electrochemical engineer, three to four years experience desired. The man we are seeking need not be acting in this capacity at the present time, but desires more responsibility based on successful performance in electrochemical research and process development.

ELECTROCHEMIST

Position open in electrochemical process development. Degree in chemistry or chemical engineering with two to three years experience required. Salary commensurate with experience.

Send resume to: Personnel Manager

American Potash & Chemical Corporation

3030 W. 6th St., Los Angeles, Calif.

The Electrochemical Society

INSTRUCTIONS TO AUTHORS OF PAPERS

Address all correspondence to the Editor, JOURNAL OF THE ELECTROCHEMICAL SOCIETY, 216 W. 102nd St., New York 25, N. Y. *After June 1* please address to 1860 Broadway, New York, N. Y.

FORM

Manuscripts submitted for publication should be in triplicate to expedite review. They should be typewritten, double-spaced, with 2½-4 cm (1-1½ in.) margins.

Title should be brief, followed by the author's name and his business or university connection.

Abstract of about 100 words should state the scope of the paper and give a brief summary of results.

ILLUSTRATIONS

Drawings will be reduced to column width, 8 cm (3⅛ in.), and after reduction should have lettering at least 0.15 cm (1/16 in.) high. Original drawings in India ink on tracing cloth or white paper are preferred. Curves may be drawn on coordinate paper only if the paper is ruled in blue. All lettering must be of lettering-guide quality. See sample drawing on reverse page.

Photographs must be glossy prints and mounted flat.

Captions for all figures must be included on a separate sheet. Captions and figure numbers should not appear in the body of the figure.

General—Figures should be used only when necessary. Omit drawings or photographs of familiar equipment. Figures from other publications are to be used only when the publication is not readily available, and should always be accompanied with written permission for reprinting.

REFERENCES

Literature and patent references should be listed at the end of the paper on a separate sheet, in the order in which they are cited. They should be given in the style adopted by *Chemical Abstracts*. For example:

R. Freas, *Trans. Electrochem. Soc.*, **40**, 109 (1921).

H. T. S. Britton, "Hydrogen Ions," Vol. **1**, p. 309, D. Van Nostrand Co., New York (1943).

H. F. Weiss (To Wood Conversion Co.), U. S. Pat. 1,695,445, Dec. 18, 1928.

UNITS OF MEASUREMENT

Metric units should be used throughout but, where desirable, English units may be given in parentheses.

Corrosion rates in the metric system should preferably be expressed as milligrams per square decimeter per day (mdd), and in the English system as inches penetration per year (ipy).

As regards algebraic signs of potentials, the standard electrode potential for $Zn \rightarrow Zn^{++} + 2e$ is negative; for $Cu \rightarrow Cu^{++} + 2e$, positive.

ABBREVIATIONS

Abbreviations should conform with the American Standards Association's list of "Abbreviations for Scientific and Engineering Terms."

GENERAL

Authors should be as brief as is consistent with clarity, and must omit all material which can be regarded as familiar to specialists in the particular field.

The use of proprietary names, trade-marks, and trade names should be avoided if possible. If used, these should be capitalized so that the owner's legal rights are not jeopardized.

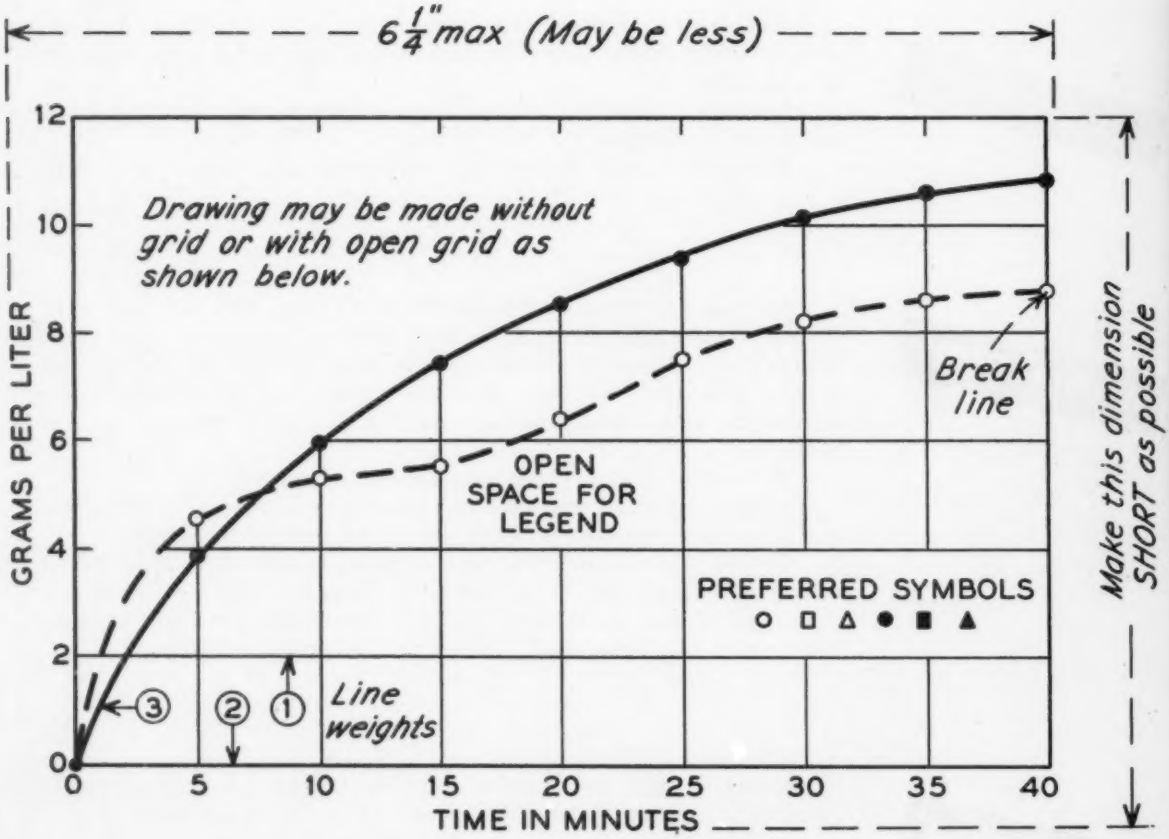

Remarks: Line weight ② is used for borders and zero lines. When several curves are shown, each may be numbered and described in the caption. Lettering is approx. 1/8".

SAMPLE CURVE DRAWING FOR REDUCTION TO $\frac{1}{2}$ SIZE